

PCT COOPERATION TREATY

PCT

NOTIFICATION OF ELECTION

(PCT Rule 61.2)

From the INTERNATIONAL BUREAU

To:

Commissioner
 US Department of Commerce
 United States Patent and Trademark
 Office, PCT
 2011 South Clark Place Room
 CP2/5C24
 Arlington, VA 22202
 ETATS-UNIS D'AMERIQUE
 in its capacity as elected Office

Date of mailing (day/month/year) 15 June 2001 (15.06.01)	
International application No. PCT/US00/08943	Applicant's or agent's file reference 1797.020PC02
International filing date (day/month/year) 05 April 2000 (05.04.00)	Priority date (day/month/year) 10 September 1999 (10.09.99)
Applicant ANLAGE, Steven, Mark et al	

1. The designated Office is hereby notified of its election made:

☒ in the demand filed with the International Preliminary Examining Authority on:
 09 April 2001 (09.04.01)

☐ in a notice effecting later election filed with the International Bureau on:

2. The election ☒ was
☐ was not

made before the expiration of 19 months from the priority date or, where Rule 32 applies, within the time limit under Rule 32.2(b).

The International Bureau of WIPO 34, chemin des Colombettes 1211 Geneva 20, Switzerland Facsimile No.: (41-22) 740.14.35	Authorized officer R. Raissi Telephone No.: (41-22) 338.83.38
---	---

REC'D 07 DEC 2001

PO

PCT

INTERNATIONAL PRELIMINARY EXAMINATION REPORT

(PCT Article 36 and Rule 70)

14

Applicant's or agent's file reference 1797.020PC02	FOR FURTHER ACTION See Notification of Transmittal of International Preliminary Examination Report (Form PCT/IPEA/416)	
International application No. PCT/US00/08943	International filing date (day/month/year) 05/04/2000	Priority date (day/month/year) 10/09/1999
International Patent Classification (IPC) or national classification and IPC G01R27/26		
Applicant UNIVERSITY OF MARYLAND et al.		

1. This international preliminary examination report has been prepared by this International Preliminary Examining Authority and is transmitted to the applicant according to Article 36.


2. This REPORT consists of a total of 6 sheets, including this cover sheet.

- ☒ This report is also accompanied by ANNEXES, i.e. sheets of the description, claims and/or drawings which have been amended and are the basis for this report and/or sheets containing rectifications made before this Authority (see Rule 70.16 and Section 607 of the Administrative Instructions under the PCT).

These annexes consist of a total of 45 sheets.

3. This report contains indications relating to the following items:

- I ☒ Basis of the report
- II ☐ Priority
- III ☒ Non-establishment of opinion with regard to novelty, inventive step and industrial applicability
- IV ☒ Lack of unity of invention
- V ☒ Reasoned statement under Article 35(2) with regard to novelty, inventive step or industrial applicability; citations and explanations supporting such statement
- VI ☐ Certain documents cited
- VII ☒ Certain defects in the international application
- VIII ☐ Certain observations on the international application

Date of submission of the demand 09/04/2001	Date of completion of this report 05.12.2001
Name and mailing address of the international preliminary examining authority:  European Patent Office D-80298 Munich Tel. +49 89 2399 - 0 Tx: 523656 epmu d Fax: +49 89 2399 - 4465	Authorized officer Rath, R Telephone No. +49 89 2399 8950





**INTERNATIONAL PRELIMINARY
EXAMINATION REPORT**

International application No. PCT/US00/08943

I. Basis of the report

1. With regard to the **elements** of the international application (*Replacement sheets which have been furnished to the receiving Office in response to an invitation under Article 14 are referred to in this report as "originally filed" and are not annexed to this report since they do not contain amendments (Rules 70.16 and 70.17)*):

Description, pages:

1-30 as received on 12/11/2001 with letter of 09/11/2001

Claims, No.:

1-29 as received on 12/11/2001 with letter of 09/11/2001

Drawings, sheets:

1/19-19/19 as originally filed

2. With regard to the **language**, all the elements marked above were available or furnished to this Authority in the language in which the international application was filed, unless otherwise indicated under this item.

These elements were available or furnished to this Authority in the following language: , which is:

- ☐ the language of a translation furnished for the purposes of the international search (under Rule 23.1(b)).
☐ the language of publication of the international application (under Rule 48.3(b)).
☐ the language of a translation furnished for the purposes of international preliminary examination (under Rule 55.2 and/or 55.3).

3. With regard to any **nucleotide and/or amino acid sequence** disclosed in the international application, the international preliminary examination was carried out on the basis of the sequence listing:

- ☐ contained in the international application in written form.
☐ filed together with the international application in computer readable form.
☐ furnished subsequently to this Authority in written form.
☐ furnished subsequently to this Authority in computer readable form.
☐ The statement that the subsequently furnished written sequence listing does not go beyond the disclosure in the international application as filed has been furnished.
☐ The statement that the information recorded in computer readable form is identical to the written sequence listing has been furnished.

4. The amendments have resulted in the cancellation of:

- ☐ the description, pages:
☐ the claims, Nos.:



**INTERNATIONAL PRELIMINARY
EXAMINATION REPORT**

International application No. PCT/US00/08943

☐ the drawings, sheets:

5. ☐ This report has been established as if (some of) the amendments had not been made, since they have been considered to go beyond the disclosure as filed (Rule 70.2(c)):

(Any replacement sheet containing such amendments must be referred to under item 1 and annexed to this report.)

6. Additional observations, if necessary:

III. Non-establishment of opinion with regard to novelty, inventive step and industrial applicability

1. The questions whether the claimed invention appears to be novel, to involve an inventive step (to be non-obvious), or to be industrially applicable have not been examined in respect of:

☐ the entire international application.

☒ claims Nos. 19,21-25.

because:

☐ the said international application, or the said claims Nos. relate to the following subject matter which does not require an international preliminary examination (*specify*):

☐ the description, claims or drawings (*indicate particular elements below*) or said claims Nos. are so unclear that no meaningful opinion could be formed (*specify*):

☐ the claims, or said claims Nos. are so inadequately supported by the description that no meaningful opinion could be formed.

☒ no international search report has been established for the said claims Nos. 19,21-25.

2. A meaningful international preliminary examination cannot be carried out due to the failure of the nucleotide and/or amino acid sequence listing to comply with the standard provided for in Annex C of the Administrative Instructions:

☐ the written form has not been furnished or does not comply with the standard.

☐ the computer readable form has not been furnished or does not comply with the standard.

IV. Lack of unity of invention

1. In response to the invitation to restrict or pay additional fees the applicant has:

☐ restricted the claims.



INTERNATIONAL PRELIMINARY EXAMINATION REPORT

International application No. PCT/US00/08943

- ☐ paid additional fees.
- ☐ paid additional fees under protest.
- ☒ neither restricted nor paid additional fees.
2. ☐ This Authority found that the requirement of unity of invention is not complied and chose, according to Rule 68.1, not to invite the applicant to restrict or pay additional fees.
3. This Authority considers that the requirement of unity of invention in accordance with Rules 13.1, 13.2 and 13.3 is
- ☐ complied with.
- ☒ not complied with for the following reasons:
see separate sheet
4. Consequently, the following parts of the international application were the subject of international preliminary examination in establishing this report:
- ☐ all parts.
- ☒ the parts relating to claims Nos. 1-18,26-29.

V. Reasoned statement under Article 35(2) with regard to novelty, inventive step or industrial applicability; citations and explanations supporting such statement

1. Statement

Novelty (N)	Yes:	Claims	1-18,20,26-29
	No:	Claims	
Inventive step (IS)	Yes:	Claims	2-17,27-29
	No:	Claims	1,20,26
Industrial applicability (IA)	Yes:	Claims	1-18,20,26-29
	No:	Claims	

2. Citations and explanations **see separate sheet**

VII. Certain defects in the international application

The following defects in the form or contents of the international application have been noted:
see separate sheet



Re Item III

Non-establishment of opinion with regard to novelty, inventive step and industrial applicability

- 1). As no required additional search fees were paid, no additional search was performed for claims 19 and 21-25.

Re Item V

Reasoned statement under Rule 66.2(a)(ii) with regard to novelty, inventive step or industrial applicability; citations and explanations supporting such statement

- 2). Reference is made to the following documents:

D1: WO 99 16102 A

D2: US-A-5 900 618 cited in the application

D3: C.GAO ET AL.: 'Quantitative microwave near-field microscopy of dielectric properties' REVIEW OF SCIENTIFIC INSTRUMENTS, vol. 69, no. 11, November 1998 (1998-11), pages 3846-3851, XP002144502 US

D4: TABIB-AZAR M ET AL: 'NOVEL PHYSICAL SENSORS USING EVANESCENT MICROWAVE PROBES' REVIEW OF SCIENTIFIC INSTRUMENTS,US,AMERICAN INSTITUTE OF PHYSICS. NEW YORK, vol. 70, no. 8, August 1999 (1999-08), pages 3381-3386, XP000870710 ISSN: 0034-6748

- 3). D1 and D2 describe near field microwave microscopes.

Document D1, which is considered to represent the most relevant state of the art, discloses an apparatus and method for contact-imaging (cf. Figs. 1 and 2) of the dielectric permittivity (see Table I), from which the subject-matter of claims 1, 20 and 26 differs only in minor details, which can be found in D2.

Claims 1,20 and 26 thus lack an inventive step.

- 4). The combination of the features of several dependent claims are neither known from, nor rendered obvious by, the available prior art. It has been suggested therefore that a new independent claim be drafted to include these features, bearing in mind that the features known in combination in D1 (or D2) should be placed in the preamble of such a claim in accordance with Rule 6.3(b) PCT.



1
2
3
4
5
6
7
8
9
10
11
12
13
14
15
16
17
18
19
20
21
22
23
24
25
26
27
28
29
30
31
32
33
34
35
36
37
38
39
40
41
42
43
44
45
46
47
48
49
50
51
52
53
54
55
56
57
58
59
60
61
62
63
64
65
66
67
68
69
70
71
72
73
74
75
76
77
78
79
80
81
82
83
84
85
86
87
88
89
90
91
92
93
94
95
96
97
98
99
100

Re Item VII

Certain defects in the international application

- 5). The features of the claims are not provided with reference signs placed in parentheses (Rule 6.2(b) PCT).
- 6). Contrary to the requirements of Rule 5.1(a)(ii) PCT, the relevant background art disclosed in the documents D1-D4 is not mentioned in the description, nor are these documents identified therein.

Quantitative Imaging of Dielectric Permittivity and Tunability

Statement as to Rights to Inventions Made Under Federally-Sponsored Research and Development

5 This invention was made with government support under Contract
Numbers ECS 9632811, DMR 9632521 and DMR 9624021 awarded by the
National Science Foundation. The U.S. Government has certain rights in this
invention.

Background of the Invention

10 *Field of the Invention*

The present invention relates generally to imaging, and more particularly
to measuring dielectric properties using a near-field scanning microwave
microscope.

Related Art

15 Dielectric thin film research has become increasingly important as the
demand grows for smaller, faster, and more reliable electronics. For example,
high permittivity thin films are under study in order to fabricate smaller capacitors
while minimizing leakage. Low permittivity materials are being sought to allow
smaller scale circuits while minimizing undesirable stray capacitance between
20 wires. Nonlinear dielectrics, which have a dielectric permittivity which is a
function of electric field, are being used in tunable devices, particularly at
microwave frequencies. Finally, ferroelectric thin films are a solution for large-
scale, non-volatile memories.

AMENDED SHEET



-2-

5 All of these dielectric thin film technologies demand high-quality, homogeneous films. However, this goal is often difficult to achieve because of the complicated fabrication process involved. Consequently, it is important to have a set of reliable techniques for evaluating thin film properties, such as permittivity and tunability. A number of different techniques are available. One standard low-frequency (≤ 1 MHz) method uses thin film capacitors to measure the normal and in-plane components of the permittivity tensor. Another uses reflection measurements from a Corbino probe. Still another method provides microwave measurements of permittivity by using transmission measurements through a microstrip structure. However, these techniques average over large areas and involve depositing thin film electrodes which itself can alter the properties of the sample. Dielectric resonators have been used as well, but also have the problem of low spatial resolution. More recently, near-field microscopy techniques have allowed quantitative measurements with spatial resolutions much less than the wavelength. These techniques use a resonator which is coupled to a localized region of the sample through a small probe and have the advantage of being non-destructive. However, it is still difficult to arrive at quantitative results and maintain high spatial resolution.

15 Therefore, what is needed is a non-destructive, non-invasive, system and method for imaging quantitative permittivity and tunability at high spatial resolution.

Summary of the Invention

25 The present invention meets the above-mentioned needs by providing a system, apparatus, and method for quantitatively imaging the dielectric properties of bulk and thin film dielectric samples. Permittivity and dielectric tunability are two examples of dielectric properties capable of measurement by the present invention.

AMENDED SHEET



-3-

The system uses a near-field scanning microwave microscope (NSMM). The NSMM is comprised of a coaxial transmission line resonator having one end coupled to a microwave signal source and the other end terminating with an open-ended coaxial probe. The probe, which has a sharp-tipped center conductor extending beyond the outer conductor, is held fixed while the sample is raster scanned beneath the probe tip. A spring-loaded cantilever sample holder gently presses the sample against the probe tip with a force of about 50 μN (microNewtons). A feedback circuit keeps the microwave signal source locked onto a selected resonant frequency of the microscope resonator. Because the electric fields generated by the microwave signal are concentrated at the probe tip, the resonant frequency and quality factor of the resonator are a function of the sample properties near the probe tip. Once the microwave signal has been applied to the sample through the probe tip, it is reflected back through the system. The feedback circuit is then able to receive the reflected microwave signal from the coaxial transmission line resonator and calculate a resonant frequency shift. The resonant frequency shift value is then stored in a computer. The computer also controls the scanning of the sample beneath the probe. To obtain quantitative results, the system uses calibration curves to exhibit the relationship between the calculated resonant frequency shift data values and the dielectric properties of a sample.

The invention described herein has the advantage of being able to provide quantitative results for samples on a length scale of about $1\mu\text{m}$ or less. This allows for the measuring of sample sizes relative to the actual environment in which they will be used.

The invention also has the advantage of providing more accurate quantitative results because the sharp protruding center conductor is represented as a cone during modeling.

AMENDED SHEET



Brief Description of the Figures

The features and advantages of the present invention will become more apparent from the detailed description set forth below and the following figures in which like reference numbers indicate identical or functionally similar elements. Additionally, the left-most digit of a reference number identifies the drawing in which the reference number first appears.

FIG. 1 illustrates the general structure and functionality of an embodiment of the present invention.

FIG. 2 illustrates the use of a spring-loaded cantilever sample support according to an embodiment of the present invention.

FIG. 3 is a diagram of a quantitative modeler used in an embodiment of the present invention.

FIG. 4 illustrates a resonant frequency shift detected by measurements taken when a sample was present versus when a sample was not present.

FIG. 5 shows a perturbation formula used in an embodiment of the present invention.

FIG. 6 is a diagram of the electric equipotential lines for a bulk sample according to a quantitative model of the present invention.

FIG. 7 is a diagram of the electric equipotential fields for a thin film sample according to a quantitative model of the present invention.

FIG. 8 is a diagram illustrating the modeling of the electric field near the microscope probe tip in an embodiment of the present invention.

FIG. 9 is a flow chart illustrating a method for determining dielectric properties according to the present invention.

FIG. 10 is a flow chart depicting an embodiment of a calibration routine of the present invention.

AMENDED SHEET



FIG. 11 is a flow chart depicting an embodiment of a scanning routine of the present invention.

FIG. 12 is a flow chart depicting an embodiment of a probe calibration curve generating routine.

5 FIG. 13 is a diagram representative of quantitative modeling curves generated in an embodiment of the present invention.

FIG. 14 is a diagram representative of a calibration curve generated in an embodiment of the present invention.

10 FIG. 15 illustrates the use of a modulating bias voltage to measure dielectric nonlinearity according to an embodiment of the present invention.

FIG. 16 illustrates a probe tip geometry descriptor according to an embodiment of the present invention.

FIG. 17 is a diagram representative of a calibration curve generated in an embodiment of the present invention.

15 FIG. 18 illustrates frequency shift measurements taken at different heights for several dielectric samples according to an embodiment of the present invention.

20 FIG. 19 is a diagram representative of calibration curves generated for frequency shift measurements taken at heights of 100 μm and 10 μm according to an embodiment of the present invention.

FIG. 20 illustrates the dielectric constant of a LaAlO_3 sample imaged at 100 μm and 9.08 GHz using a 480 μm diameter probe according to an embodiment of the present invention.

25 FIG. 21 is a chart displaying dielectric constant values taken from literature and the dielectric constant values obtained from experimental measurements taken according to a method of the present invention.

FIG. 22a illustrates a dielectric constant image of a test sample taken with a 480 μm probe at 9.08 GHz and 100 μm above the sample according to an embodiment of the present invention.



-6-

FIG. 22b illustrates the topography of a test sample found according to a method of the present invention.

Detailed Description of the Preferred Embodiments

5 The invention described herein is a system, apparatus, and method for displaying the dielectric properties of bulk and thin film samples. The invention uses a near-field scanning microwave microscope (NSMM).

Physical Design for the System of the Present Invention

10 An apparatus according to an embodiment of the present invention is illustrated in FIG. 1. System 100 shows a near-field scanning microwave microscope having an open-ended coaxial probe 130 with a sharp, protruding center conductor 185. A coaxial transmission line resonator 135 is used for producing a resonance between the probe tip 185 and the capacitive coupler 145. The microwave signal source 165 is responsible for generating a microwave
15 signal. The feedback circuit 160 receives a reflected microwave signal from the coaxial transmission line resonator 135. Feedback circuit 160 also keeps the microwave signal source 165 locked onto a predetermined resonance. An additional function of the feedback circuit 160 is to calculate a value for at least one parameter related to a change in the resonance due to the dielectric properties
20 of a sample 125. Two possible parameters measured are resonant frequency shift (Δf) and quality factor (Q). A stage 120 is used to support the sample 125 in contact with the sharp protruding center conductor 185. Alternatively, with respect to FIG. 2 described in more detail below, a further embodiment of the present invention has a spring-loaded cantilever sample holder 210 provided to
25 hold the sample relative to the sharp protruding center conductor 185 and stage 120.



-7-

System 100 further includes motor controllers 115 for manipulating the sample 125 in contact with the sharp protruding center conductor 185 in a first, second, or third direction; for example, the sample can be moved and/or rotated along the x, y and z axes. A coupler 150 is attached between the microwave signal source 165 and the coaxial transmission line resonator 135. Coupler 150 could be a directional coupler, circulator, or other device for directing microwave signals known to one of ordinary skill in the art. The coupler initially directs the microwave signal towards the sample 125 and then directs the reflected microwave signal towards the feedback circuit 160.

A detector 155 is responsible for converting the reflected signal directed towards the feedback circuit 160 into a voltage signal representative of detected power. A computer 105 having both memory and a processor is also shown. The memory of computer 105 stores electric field configuration data files used for quantitative modeling. Computer 105 also stores calibration sample frequency shift values and test sample frequency shift values. The processor of computer 105 mathematically determines the functional relationship between at least one parameter related to a change in the resonant frequency shift and a known dielectric property value of a sample responsible for the change. An example of such a parameter is relative dielectric permittivity (ϵ_r). The processor of computer 105 is then able to receive from feedback circuit 160 resonant frequency shift values for a sample with unknown dielectric properties and determine the value of the unknown dielectric property based upon the model frequency shift-dielectric property relationship. Display device 110 is provided for displaying the value of the dielectric property once it has been determined by the processor 105.

FIG. 2 illustrates an alternative embodiment for the present invention where a spring-loaded sample support 200 is used to support the sample 125 beneath the probe tip 185. Sample support 200 uses a cantilever sample holder 210 having an angled end and a planar surface for supporting sample 125. A first bracing device 230 is fixed to the x-y stage and is joined to sample holder 210 by

-8-

a spring 220. The spring 220 is positioned such that it is in close proximity to the pivot point created when the angled portion of sample holder 210 is brought into contact with a second bracing device 240 also attached to the x-y stage. This spring cantilever design allows the force applied by the probe tip 185 to remain substantially constant during scanning. Excessive wear of the probe tip during contact mode scanning is also reduced. The amount of force applied can be set by selecting an appropriate spring and adjusting the location of the spring and/or sample along the cantilever sample holder 210. In one example, a force of about 50 μN (microNewtons) is applied between the probe tip and sample 125.

System 100 also has a quantitative modeler described in FIG. 3 for determining the model frequency shift-dielectric property relationship. Quantitative modeler 300 receives resonant frequency shift values for calibration samples with known dielectric properties and test samples with unknown dielectric properties from computer 105 memory. Quantitative modeler 300 provides the measured resonant frequency shift data to Model calibration curve generator 310 Probe calibration curve generator 320 and Test sample curve generator 330 in order to generate data (such as, tables, graphs, files or curves) showing the relationship between a measured resonant frequency shift and a particular dielectric property. In particular, Model calibration curve generator 310 generates model calibration curves at different values of a geometric descriptor that show the relationship between a measured resonant frequency shift (Δf) and a dielectric property (e.g. permittivity ϵ_r) for calibration reference samples. The operation of Model calibration curve generator 310 is further described with reference to figures 12 and 13. Probe calibration curve generator 320 and Test sample calibration curve generator 330 generate calibration curves drawn from the model calibration curves and a geometric descriptor value of the probe tip 185. The calibration curves show the relationship between a resonant frequency shift (Δf) measured during scanning and a dielectric property (e.g. permittivity ϵ_r) at a geometric descriptor value of the actual NSMM used in

AMENDED SHEET

imaging. The calibration curve allows a dielectric property to be determined by finding the point on the curve corresponding to the resonant frequency shift measured during scanning. The operation of Probe calibration curve generator 320 and Test calibration curve generator 330 is further described with respect to figures 9, 12, 14 and 17.

It is helpful to begin with discussion of quantitative modeling according to the present invention with reference to figures 4 to 8, and 16. Operation of the present invention is then further described with respect to figures 9-15.

Quantitative Modeling

Calculating the Electric Field Near the Probe Tip

In order to arrive at quantitative results, the inventors developed a physical model for the system, starting with the simplest case of a uniform bulk sample. Because the probe tip length is much smaller than the free space wavelength of the microwaves (~ 4 cm), a static calculation of the microwave electric fields is performed. Cylindrical symmetry further simplifies the problem to two dimensions. Because of the complicated geometry of the probe tip in contact with a potentially multi-layered sample, a finite element model on a grid is used. Using relaxation potential Φ in the region represented by the grid and taking into account any changes in the permittivity ϵ_r , yields:

$$\nabla^2 \Phi + \frac{1}{\epsilon_r} (\nabla \Phi) \cdot (\nabla \epsilon_r) = 0 \quad (1)$$

Using a rectangular grid, the inventors represent the probe tip as a cone with a blunt end of radius r_0 , and perform the calculation in a spreadsheet program.

AMENDED

-10-

From Eq. (1), if Φ_{ij} is the potential at the cell at column i and row j , Φ_{ij} is a weighted average of the values of the four adjacent cells:

$$\Phi_{ij} = \frac{\Phi_{i+1,j} \left(1 + \frac{\Delta r}{r} \right) + \Phi_{i-1,j} + \Phi_{i,j-1} + \Phi_{i,j+1}}{4 + \frac{\Delta r}{r}}, \quad (2)$$

where r is the radius from the cylindrical coordinate axis, referring to FIG. 16, Δr and Δz are the spacing between cells in the r and z directions, respectively, and $\Delta r = \Delta z$. Equation (2) is the simplest case; in practice, the equation is more complicated, such as at the interface between the dielectric sample ($\epsilon_r > 1$) and the air ($\epsilon_r = 1$). Near the probe tip where the electric field is the strongest, and hence, the most critical, the grid spacings Δr and Δz are small and uniform. Inside this box, $\Delta z = \Delta z_{in} = 0.1 \mu\text{m}$, is fixed while the value of $\Delta r = \Delta r_{in}$ is uniform, but adjustable ($0.5 \mu\text{m} \leq \Delta r_{in} \leq 1.0 \mu\text{m}$), to allow for probe tips with different sharpness. In FIG. 16, the geometry descriptor of a probe tip's sharpness is represented with an aspect ratio parameter $\alpha \equiv \Delta z_{in}/\Delta r_{in}$.

The boundaries of the grid should be sufficiently far away in order to minimize the effect of the chosen boundary conditions on the electric field near the probe tip. To accomplish this, outside a region close to the probe tip, the values of Δr and Δz continuously increase with distance away from the probe tip, allowing the outer radius of the grid to be at least 4 mm, and the height of the grid to be 2 mm. The resulting grid consists of 84×117 cells, which is small enough to be a manageable calculation with a modern personal computer. The top and outer boundary conditions are $d\phi/dn = 0$ where n is the coordinate normal to the edge. At the bottom of the grid, which represents the bottom side of the $500 \mu\text{m}$ thick sample, $\phi = 0$ is used for the boundary condition. To match this condition, the sample is placed on top of a metallic layer for scanning; this has the added

benefit of shielding the microscope from the effects of whatever is beneath the sample, which could be difficult to model.

Two possible fitting parameters for the model are the geometry descriptor, i.e., aspect ratio α , and the radius r_0 of the blunt probe end. The inventors found that a satisfactory fit with data could be obtained by fixing $r_0 = (0.6 \mu\text{m})/\alpha$. This leaves α as a single fitting parameter to represent all probes; the inventors have found that typically $1 < \alpha < 2$. When α is small, for example less than 1.5, the probe tip is considered to be blunt. When α is large, for example greater than 1.5, the probe tip is considered to be sharp.

10

Calculating the Frequency Shift of the Microscope

15

Using perturbation theory, the frequency shift of the microscope is calculated as a function of the fields near the probe tip. FIG. 4 illustrates the frequency shift during an unperturbed state, i.e., no sample present and a perturbed state, i.e., sample present beneath the probe. The width of the minima change with respect to the changes in quality factor (Q). With reference to FIG. 5, ϵ_{r1} and ϵ_{r2} are defined as the permittivities of two model samples, the subscripts 1 and 2 indicating the unperturbed and perturbed system. If \vec{E}_1 and \vec{E}_2 are the calculated electric fields inside the two model samples, where $\vec{E} = -\nabla\Phi$, the frequency shift of the microscope upon going from sample 1 to sample 2 is

20

$$\frac{\Delta f}{f} \approx \frac{\epsilon_0}{4W} \int_{V_s} (\epsilon_{r2} - \epsilon_{r1}) \vec{E}_1 \cdot \vec{E}_2 dV \quad (3)$$

where $\epsilon_0 = 8.85 \times 10^{-12}$ F/m is the permittivity of free space, W is the energy stored in the resonator, and the integral is over the volume V_s of the sample. An approximate W is calculated using the equation for the loaded Q of the resonator,

-12-

$Q_L = \omega_0 W/P_l$, where ω_0 is the resonant frequency, and P_l is the power loss in the resonator. In one example, a bare 500 μm thick LaAlO_3 (LAO) substrate is used for the unperturbed system because its properties are well-characterized ($\epsilon_r = 24$) and it is a common substrate for oxide dielectric thin films.

5 FIG. 6 illustrates the electric fields 605 present when a bulk sample 610 is scanned beneath probe tip 185.

Modeling of Dielectric Thin Films

10 FIG. 7 illustrates the modeling of thin films. To provide for imaging of thin films, the finite element model is extended to include a thin film 710 on top of a dielectric substrate 715 having the same thickness as the model samples. As long as the thin film 710 is on a substrate having the same thickness as the model sample, the only perturbation is the thin film (the change in total thickness of the sample is negligible compared to the thick substrate). The electric field 705 in the thin film sample is calculated using the finite element model of the present invention and Eq. (3) to calculate Δf , integrating only over the volume of the thin film. Once a probe's α parameter is found using the process described above for bulk samples, the thin film model is used to obtain a functional relationship between Δf and ϵ_r of the thin film.

15 In producing the quantitative models discussed above, samples are chosen so as to cover a range of permittivity values in which the dielectric permittivity of an unknown sample is expected to fall within. The known values ϵ_r and t (thickness of the thin film 710) and the calculated values α and Φ are all stored in electric field configuration data files respective to each sample. In FIG. 8 for example, quantitative modeling data has been generated using samples with dielectric permittivity values of 10 to 200 and probe tip geometry of $\alpha=1$ and $\alpha=2$.
20 Accordingly, the electric field configuration data files are usable in cases where
25

AMENDED SHEET.

-13-

the dielectric permittivity for an unknown sample can be expected to be between 10 and 200.

The following articles are related to quantitative modeling according to the present invention and are incorporated by reference herein in their entirety:

5 "Imaging of microwave permittivity, tunability, and damage recovery in (Ba, Sr) TiO₃ thin films", D.E. Steinhauer, C.P. Vlahacos, F.C. Wellstood, Steven M. Anlage, C. Canedy, R. Ramesh, A. Stanishevsky, and J. Melngailis, *Applied Physics Letters*, Volume 75, Number 20, p. 3180 (1999); and

10 "Non-Contact Imaging of Dielectric Constant with a Near-Field Scanning Microwave Microscope", C.P. Vlahacos, D. E. Steinhauer, Steven M. Anlage, F.C. Wellstood, Sudeep K. Dutta, and Johan B. Feenstra, *The Americas Microscopy and Analysis*, p. 5, January 2000.

Method of the Present Invention

Dielectric Permittivity Imaging

15 A method for an embodiment of the present invention is illustrated by flowchart 900 of FIG. 9. The method begins with a step 905. In a step 910, system 100 is calibrated according to the probe calibration routine described in FIG. 10 to obtain calibration sample frequency shift values ($\Delta f_{\text{sampleC}}$), a probe tip geometry descriptor, and sample geometry.

Test Sample Scanning

20 In a step 915, a test sample 125 with unknown dielectric properties is scanned according to the routine described in FIG. 11 to obtain test sample resonant frequency shift measurements ($\Delta f_{\text{sampleT}}$). These measurements can also include determining quality factor (Q), and/or tunability information. If the test

AMENDED SHEET

-14-

sample is a thin film then it contains both a dielectric thin film and substrate. Step 915 will now be described with reference to the steps provided in FIG. 11. The method begins with a step 1105. In a step 1110 a resonant frequency of the near-field scanning microwave microscope is selected. In a step 1115 a test sample is placed on the microscope stage. In a step 1120 the probe tip is moved into contact with the test sample. In a step 1125 raster scanning begins. In a step 1130 a position value corresponding to the initial point of contact with the test sample is stored in computer 105 memory as the next scanning point.

In a step 1135 the probe is moved to a predetermined background measurement position where the calibration sample no longer perturbs the resonator. For example, the predetermined background measurement position can be a height 1.5 times greater than the diameter of the microscope transmission line 135, or a height at least approximately 3 millimeters above the calibration sample. In a step 1140 a background resonant frequency shift measurement is taken from the background measurement position. In a step 1145 the probe tip is moved back into contact with the test sample at the next scanning point. In a step 1150 the contact resonant frequency shift at the scanning point is measured. In a step 1155 the difference between the contact resonant frequency shift at the scanning point and the background resonant frequency shift is calculated. In a step 1160 the calculated difference is saved in computer 105 memory as the test sample resonant frequency shift value.

In a step 1165 the microscope probe tip is moved to the next scanning position. In a step 1170 computer 105 determines if the next scanning position is the end of a scan line. If the end of a scan line has not been reached then steps 1150 through 1165 are repeated. Next, at a step 1175 computer 105 determines if the next scanning position is the end of a scan area. If it is not then steps 1135 through 1170 are repeated until the end of a scan area has been reached. At the conclusion of step 915 a set of test sample resonant frequency values have been recorded or stored in computer 105 memory.

APPENDED SHEET

-15-

In a step 920, the calibration sample resonant frequency shift values obtained from step 910 are used to generate a probe calibration curve according to the routine described in FIG. 12. In a step 925, a determination of whether the test sample is a thin film is made. In a step 930, a determination of whether all of the calibration samples have the same thickness as the test sample is made. If the test sample is not a thin film, and all of the calibration samples have the same thickness as the test sample, then in a step 945, one is able to determine an unknown dielectric property for a sample by first retrieving a test sample resonant frequency shift value ($\Delta f_{\text{sampleT}}$) obtained in step 915 and then locating the corresponding Δf value on the probe calibration curve resulting from step 920. The dielectric property of the test sample is equal to the dielectric property corresponding to the Δf value on the probe calibration curve resulting from step 920. If the test sample is a thin film, or if only one calibration sample has the same thickness as the test sample, then in a step 935 a test sample calibration curve is generated. In a step 940 one is able to determine an unknown dielectric property for a test sample by first retrieving a test sample resonant frequency shift value ($\Delta f_{\text{sampleT}}$) obtained in step 915 and then locating the corresponding Δf value on the test sample calibration curve resulting from step 940. The dielectric property of the test sample is equal to the dielectric property corresponding to the Δf value on the test sample calibration curve. The process concludes with a step 950.

In an alternative embodiment, step 920 can be performed prior to step 915.

In a further embodiment, step 910 can be performed after step 915 but before step 920. Furthermore, steps 1135, 1140, and 1145 could alternatively be measured at each point on the sample, any desired number of times during the scan, before the scan, or after the scan.

APPROVED SHEET

-16-

Calibration

To measure the unknown dielectric permittivity (ϵ_r) of a dielectric sample, the NSMM is calibrated to determine the parameter α using at least two samples with known permittivity (ϵ_r) and thickness (t). The thickness of a bulk dielectric test sample or a thin film test sample on top of a dielectric substrate, is referred to as the first determined thickness. For thin film dielectric test samples the thickness of the thin film is referred to as the second determined thickness.

The process of calibrating system 100 is illustrated by flowchart 1000 of FIG. 10. The process starts at a step 1010. At a step 1015, at least two calibration samples that have known dielectric properties are selected. At least two of the calibration samples have the same approximate thickness with one another. In addition, at least one of the calibration samples has the same approximate thickness as the test sample with first determined thickness and unknown dielectric properties. If the test sample contains a thin film, an additional requirement is that the at least one calibration sample with approximate thickness equal to the test sample first determined thickness have the same permittivity as the substrate of the test sample.

Calibration Sample Scanning

In a step 1020, each selected calibration sample is scanned according to the scanning routine described in FIG. 11 to determine respective sets of resonant frequency shift information for samples with known dielectric permittivity values. The method begins with a step 1105. In a step 1110 a resonant frequency of the near-field scanning microwave microscope is selected. In a step 1115 a calibration sample is placed on the microscope stage. In a step 1120 the probe tip is moved into contact with the calibration sample. In a step 1125 raster scanning begins. In a step 1130 a position value corresponding to the initial point of

-17-

contact with the calibration sample is stored in computer 105 memory as the next scanning point. In a step 1135 the probe is moved to a predetermined background measurement position where the calibration sample no longer perturbs the resonator. For example, the predetermined background measurement position can be a height 1.5 times greater than the diameter of the microscope transmission line 135, or a height at least approximately 3 millimeters above the calibration sample. In a step 1140 a background resonant frequency shift measurement is taken from the background measurement position. In a step 1145 the probe tip is moved back into contact with the calibration sample at the next scanning point. In a step 1150 the contact resonant frequency shift at the scanning point is measured. In a step 1155 the difference between the contact resonant frequency shift at the scanning point and the background resonant frequency shift is calculated. In a step 1160 the calculated difference is saved in computer 105 memory as the calibration sample resonant frequency shift value. In a step 1165 the microscope probe tip is moved to the next scanning position. In a step 1170 computer 105 determines if the next scanning position is the end of a scan line. If the end of a scan line has not been reached then steps 1150 through 1165 are repeated. Next, at a step 1175 computer 105 determines if the next scanning position is the end of a scan area. If it is not then steps 1135 through 1170 are repeated until the end of a scan area has been reached. Step 1020 is repeated for each calibration sample.

At a step 1025, a geometry descriptor of the probe tip is determined. The geometry descriptor can be input by a user or calculated by System 100. A geometry descriptor can be any descriptor representative of the geometry of the probe tip. Accordingly, in one embodiment of the present invention, a geometry descriptor is referred to as a first probe tip geometry descriptor value and a second probe tip geometry descriptor value. In another embodiment, an aspect ratio $\alpha = \Delta z / \Delta r$ is used where, Δz is a distance along a z-direction parallel to a length of the

-18-

resonator and the probe tip and Δr is a radius distance extending from the central axis of the probe tip 185 to its outermost surface.

At a step 1030, sample geometry data is input. For example, with bulk samples, sample geometry data includes the thickness of the sample. For thin film samples on a bulk substrate, the thickness of the thin film is provided as well.

Calibration Curve Generation

FIG 12 describes the routine for generating a calibration curve. The routine begins at a step 1205. At a step 1210 electric field configuration data is stored as described in FIG 8. The stored files contain data for model samples having approximately the same thickness as the calibration sample scanned in step 1020. At least one file for each value of α has the same permittivity value as one of the calibration samples scanned in step 1020. This permittivity is defined to give the unperturbed system, with $\Delta f=0$.

At a step 1215 model calibration curves are generated by reading from at least two of the previously stored electric field configuration data files, electric field values and permittivity values for at least two respective probe tip geometry descriptor values. FIG. 13 provides an example of model calibration curves for $\alpha=1$ and $\alpha=2$. To generate the model calibration curve where $\alpha=1$, a first previously stored electric field value (E_1) and a first permittivity value (ϵ_{r1}) is chosen to represent the zero point ($\Delta f=0$). A second electric field configuration data file where $\alpha=1$ is then read to obtain a second previously stored electrical field value (E_2) and a second permittivity value (ϵ_{r2}). A point on the first model calibration curve is then generated by solving the equation

$$\frac{\Delta f}{f} \approx \frac{\epsilon_0}{4W} \int_{V_s} (\epsilon_{r2} - \epsilon_{r1}) \vec{E}_1 \cdot \vec{E}_2 dV$$

AMENDED SHEET

-19-

Multiple points on the first model calibration curve can be generated by repeating step 1215 for different values of ϵ_{r2} and E_2 . The second model calibration curve for $\alpha=2$ is generated as described above except that electric field configuration data files where α equals two are used instead.

5 At a step 1220, a calibration curve is generated using the model calibration curves from step 1215 and the calibration sample frequency shift values from step 1020. A point on the calibration curve is generated by first calculating the difference between two calibration sample frequency shift values. One of the calibration frequency shift values used in the calculation should
10 correspond to zero point permittivity value from step 1215. Once the difference value has been determined it can be plotted with respect to the Δf axis of the model calibration curve. FIG. 14 provides an example where four calibration points have been plotted with respect to the model calibration curve of FIG. 13 to produce a calibration curve for $\alpha=1.5$. The value for α for the probe is
15 determined by observing the position of the curve C_p relative to the curves C_{m2} and C_{m1} .

Test Sample Calibration Curve Generation

If the test sample is a thin film sample, or if only one calibration sample has the same thickness as the first determined thickness of the test sample, then
20 a separate test sample calibration curve must be generated, in step 935.

An example test sample calibration curve C_{ts} is shown in FIG. 17. The curve C_{ts} is used in step 940 to convert the frequency shift values obtained in step 915 to the values of the permittivity of the test sample. The curve C_{ts} can be calculated using one of two methods. For the first method, the calculation is done
25 for the specific value of α determined in step 920 (such as $\alpha = 1.5$, as shown in FIG. 17). For the second method, the calculation is done for two or more values of α , shown in FIG. 17 as the curves C_{ts1} and C_{ts2} . Then, the curve C_{ts} is

AMENDED SHEET



-20-

calculated for the value of α determined in step 920 by interpolating between the curves C_{ts1} and C_{ts2} . The advantage of the second method is that generating the curves C_{ts1} and C_{ts2} can be done in advance just once, requiring less calculation for each scan.

5 For the case where the test sample is a bulk sample, and only one calibration sample has the same thickness as the test sample, the curves in FIG 17 are calculated using the same method as was performed in the previous section with the probe calibration curve. The difference is that a new set of files (represented in FIG. 8) are used, which represent a sample thickness equal to the
10 test sample thickness. The frequency shift measured with the NSMM for the calibration sample having the same thickness as the test sample (done in step 910) is defined as $\Delta f=0$ for the test sample calibration curves in FIG. 17.

For the case of a thin film test sample, the curves C_{ts1} and C_{ts2} in FIG. 17 are calculated according to the routine described in FIG. 12. However, a different
15 set of files represented in FIG. 8 is now used. In this new set, the files represent a thin film having a thickness equal to the second determined thickness of the thin film in the test sample. The volume V_s is the volume of the thin film, rather than the volume of the entire sample. The frequency shift measured with the NSMM for the calibration sample which has the same thickness as the test sample, and
20 the sample permittivity as the test sample substrate, is defined as $\Delta f = 0$ for the curves in FIG. 17.

Nonlinear Dielectric Imaging

FIG. 15 illustrates how electric field-dependent imaging can be accomplished by applying a voltage bias (V_b) 1505 to the probe tip via a bias tee
25 180 in the resonator according to a further feature of the present invention. A metallic layer 1520 beneath the thin film 1510 acts as a grounded counterelectrode.

AMENDED SHEET

-21-

As shown in FIG 15, a sample 125 can be a dielectric thin film 1510. The dielectric thin film 1510 is disposed on a grounded counterelectrode 1520. The grounded counterelectrode 1520 is provided on a substrate 1530. In order to prevent the counterelectrode 1520 from dominating the microwave measurement (modeling of the system has shown this to be a potential problem), the inventors use a high-sheet-resistance counterelectrode, making it virtually invisible to the microwave fields. As a result, the presence of the thin-film counterelectrode 1520 can be safely ignored in the finite element model described above. Because the counterelectrode 1520 is immediately beneath the dielectric thin film, the applied electric field is primarily in the vertical direction, unlike the microwave electric field, which is mainly in the horizontal direction for thin films with large permittivities. Also, by simulating the applied field using a finite element model similar to that presented above, the inventors find that the applied electric field beneath the probe tip is approximately uniform and equal to $E_b = V_b/t_f$, where t_f is the thickness of the dielectric thin film.

By modulating the bias voltage 1505 applied to the probe tip, nonlinear terms in the permittivity can be extracted. Expanding the electric displacement D in powers of the electric field E , and keeping only the nonzero terms yields

$$D_1(E) = \epsilon_{11}E_1 + \frac{1}{2}\epsilon_{113}E_1E_3 + \frac{1}{6}\epsilon_{1133}E_1E_3^2 + \dots \quad (4)$$

where E_1 is the rf electric field in the r direction, and $E_3 = E_b$ is the applied bias electric field in the z direction.

Adding a low-frequency oscillatory component ($\omega_b = 1$ kHz, with an amplitude of $\tilde{V}_b = 1$ V, for example) to the bias voltage, the applied electric field is $E_b = E_b^{dc} + \tilde{E}_b \cos \omega_b t$. The effective rf permittivity is then

-22-

$$\begin{aligned}
\varepsilon_{rf} = & \varepsilon_{11} + \varepsilon_{113} E_b^{dc} + \varepsilon_{1133} \left(\frac{(E_b^{dc})^2}{2} + \frac{\tilde{E}_b}{4} \right) \\
& + (\varepsilon_{113} + \varepsilon_{1133} E_b^{dc}) \tilde{E}_b \cos(\omega_b t) \\
& + \frac{1}{4} \varepsilon_{1133} \tilde{E}_b^2 \cos(2\omega_b t) + \dots
\end{aligned} \tag{5}$$

Note that the components of ε_{rf} at ω_b and $2\omega_b$ are approximately proportional to ε_{113} and ε_{1133} , respectively. Expanding the resonant frequency of the microscope as a Taylor series about $f_0(\varepsilon_{rf} = \varepsilon_{11})$, yields

$$5 \quad f_0[\varepsilon_{rf}(t)] = f_0(\varepsilon_{11}) + \left. \frac{df_0}{d\varepsilon_{rf}} \right|_{\varepsilon_{rf}=\varepsilon_{11}} [\varepsilon_{rf}(t) - \varepsilon_{11}] + \dots \tag{6}$$

Substituting Eq. 5 into Eq. 6, and keeping only the larger terms,

$$\begin{aligned}
f_0(t) \approx & \text{constant} + \varepsilon_{113} \tilde{E}_b \left. \frac{df_0}{d\varepsilon_{rf}} \right|_{\varepsilon_{11}} \cos(\omega t) \\
& + \frac{1}{4} \varepsilon_{1133} \tilde{E}_b^2 \left. \frac{df_0}{d\varepsilon_{rf}} \right|_{\varepsilon_{11}} \cos(2\omega t).
\end{aligned} \tag{7}$$

Thus, the components of the frequency shift signal at ω_b and $2\omega_b$ can be extracted to determine the nonlinear permittivity terms ε_{113} and ε_{1133} . These nonlinear terms can be measured simultaneously with the linear permittivity (ε_{11}) while scanning.

10

AMENDED SHEET

As an alternative, the electric field E_b could be applied in the horizontal direction using thin film electrodes deposited on top of the dielectric thin film. The advantage here is that diagonal nonlinear permittivity tensor terms could be measured, such as ϵ_{111} and ϵ_{1111} ; the disadvantage in this case is that imaging is limited to the small gap between the electrodes.

Simultaneously Measuring Sample Topography

Using a spring-loaded sample holder such as that shown in FIG. 2, one can also measure sample topography. This is accomplished by measuring the deflection of the sample holder during a scan. Because the probe tip is held fixed, the sample holder will deflect depending on the topography of the sample. For example, if the sample has a bump on top of it, the sample holder will deflect downward. One can record this deflection during a scan, and obtain a topographical image corresponding to the same region as the microwave image(s).

The measurement of the deflection of the sample holder could be accomplished using one of many techniques, including an optical sensor, a capacitive sensor, an interferometer, etc.

Overview

The microwave microscope, as covered in patent 5,900,618, consists of a resonator contained in a microwave transmission line. One end of the resonator is an open-ended coaxial probe, which is held close to the sample, and the other end is coupled to a microwave source with a coupling capacitor. A sample is scanned beneath the probe. Because of the concentration of the microwave fields at the probe center conductor, the resonant frequency and quality factor Q of the resonator are perturbed depending on the properties of the sample near the probe

RECEIVED SHEET



-24-

center conductor. One quantity recorded while scanning is the resonant frequency shift (Δf) of the resonator.

Two modes of operation are non-contact mode and contact mode. In non-contact mode, the preferred embodiment is with the probe center conductor flush with the face of the probe, so that the end of the center conductor is in the same plane as the end of the outer conductor. A sample is scanned beneath the probe with a small gap of 10-100 μm between the probe and the sample. In contact mode imaging, the center conductor extends beyond the outer conductor, and has a sharp point. The sample holder gently presses the sample against the probe tip with a small force.

The invention involves calibration using dielectric samples with known permittivity. In the case of non-contact mode, the calibration data is interpolated, allowing one to scan dielectric samples with the same thickness as the calibration samples, and to convert the microscope frequency shift into the local permittivity of the sample. In the case of contact-mode imaging, a physical model is used to generate the relationship between the frequency shift of the microscope and the local permittivity of the sample. Because of the use of the model with contact-mode imaging, quantitative imaging in this case is not limited to samples which have the same thickness as the calibration samples. The contact-mode imaging can be used for both bulk and thin-film samples.

In contact mode, a low-frequency electric field can also be applied to the sample, so that permittivity can be measured as a function of the applied electric field. Thus, dielectric nonlinearity can be measured as well as the linear permittivity.

When scanning in contact mode, an optical sensor can be used to measure the deflection of the sample holder, and hence, the sample, as the sample is scanned in contact with the probe tip. The deflection is exactly equal to the topographic changes in the sample. Thus, by recording this reflection at the same

AMENDED SHEET

-25-

time that Δf is measured, the sample topography can be imaged simultaneously with the permittivity.

In one embodiment of non-contact mode imaging, the local dielectric constant of a material is determined by measuring the frequency shift of the microscope as a function of height above the sample. Areas as small as 100 μm in diameter can be measured.

An unknown sample is scanned and a dielectric constant is measured as a function of position as long as the height of the probe above the sample is accurately known.

The technique can be performed quickly and at many locations on a bulk dielectric material.

The techniques can be done over a very broad range of frequencies simply by choosing other resonant modes of the microscope. In principle one can measure between about 100 MHz and 50 GHz.

The technique can be applied over a broad range of temperatures, from 1.2K to well above room temperature, possibly as high as 1000°C.

Non-Contact Imaging of Dielectric Constant with a Near-Field Scanning Microwave Microscope

In another embodiment of the present invention, a non-contact technique for imaging dielectric constant using a resonant near-field scanning microwave microscope is provided. By measuring the shift in the system's resonant frequency during a scan over an insulating sample, one can obtain quantitative images of dielectric variations. In one example, the inventors scanned seven samples with dielectric constants ϵ_r ranging from 1 to 230, using a 480 μm diameter probe at a height of 100 μm and a frequency of 9.08 GHz. The technique achieves an accuracy of about 25% for $\epsilon_r=230$ and less than 2% for $\epsilon_r=2.1$, limited mainly by variations in the probe-sample separation.

AMENDED SHEET

-26-

This approach offers a fast, simple, broadband method to image dielectrics using readily available microwave components.

In one embodiment, resonant near-field scanning microwave microscope consists of a 1m long coaxial transmission line which is capacitatively coupled to a microwave source at one end and terminated by an open-ended coaxial probe at the other end. This arrangement creates a resonant circuit in which the resonant frequency f_0 and quality factor Q are modified when a sample approaches the open end of the probe (see inset in Fig. 18). By using a frequency-following feedback circuit the invention keeps the microscope source locked on resonance. The shift of the system's resonant frequency Δf as the sample under the probe is scanned. The variations in Δf are directly related to spatial variations in dielectric constant in the sample. In addition, however, topographic changes will also give rise to changes in Δf .

Calibration Example

To calibrate the system, the inventors constructed a test sample by placing six pieces of different dielectric material into the bottom of a square plastic mould and pouring epoxy into the mould. In addition, silicone adhesive was used to hold each piece down. After the epoxy cured, the test sample was removed from the mould, polished, and positioned on the XY table. The materials embedded in the epoxy were silicon, glass microscope slide, SrTiO_3 , Teflon, sapphire, and LaAlO_3 . All six pieces were approximately 500 μm thick and about 6 mm x 8 mm in size. The overall thickness of the test sample was 6 mm.

The frequency shift Δf versus height h above the six pieces having dielectric constants ranging from 2.1 to about 230 is measured. The inventors also tested the epoxy which has an unknown dielectric constant. Each piece, as well as the probe, was flat and smooth on the scale of 5 μm as judged by an optical microscope. For these measurements, a probe with a 480 μm center

AMENDED SHEET

-27-

conductor diameter and a source frequency of 9.08 GHz was used in one example of implementation. For each scan, the probe was first brought in contact with a dielectric sample and the frequency shift Δf was recorded as the height was systematically increased. The results are plotted in Fig. 18. Samples with the largest dielectric constant produced the largest frequency shift, as expected. The largest shift observed was -26.2 MHz, when the probe was in contact with a SrTiO_3 sample with $\epsilon_r=230$. The smallest shift found was -1.2 MHz when the probe was in contact with a Teflon sample with $\epsilon_r=2.1$. As can be seen from Fig. 18, the frequency shift is essentially zero above 1 mm and saturates when the probe-sample distance is smaller than a few microns.

The inventors used the above information to construct an empirical calibration curve that directly relates the frequency shift to the dielectric constant ϵ_r . In order to construct the calibration curve the inventors took the difference between the frequency shift at two different heights h_1 and h_2 , i.e., $f_d=\Delta f(h_2)-\Delta f(h_1)$, where h_2 is far away ($h_2>1000 \mu\text{m}$). By taking the difference, the effect of drift in the microwave source frequency is eliminated. As shown in Fig. 19, two calibration curves of f_d versus ϵ_r can be constructed, one curve for $h_1=10 \mu\text{m}$ and $h_2=1.1 \text{ mm}$ and the other for $h_1=100 \mu\text{m}$ and $h_2=1.1 \mu\text{m}$. The parameters in each calibration curve are set with an empirical function (solid lines in Fig. 19), allowing us to easily transform any measured frequency shift to a dielectric constant. From these curves one can see that one can enhance the sensitivity to the dielectric constant considerably by using a small probe height. On the other hand, at closer probe-sample separations the influence of topographic features will be enhanced.

AMENDED SHEET

-28-

Imaging Results

To test the dielectric imaging capabilities of our system, the inventors next scanned a single sample of LaAlO_3 which had an 8 x 5 mm triangular shape and a thickness of 510 μm . The inventors placed the sample directly on the metal scanning table and recorded the frequency shift as a function of position. The data was taken at 9.08 GHz using the 480 μm probe at heights of 100 μm and 1.1 mm. The two data sets are subtracted and a 100 μm calibration curve is used to transform the resulting frequency shift image into a dielectric constant image. Figure 20 shows the resulting contour image of dielectric constant versus position. The dielectric constant varies from about 20 to 25 over the sample and equals 1 when the probe is away from the sample. For comparison, the reported value of relative permittivity for LaAlO_3 at room temperature is $\epsilon_r=23.9$ at 18 GHz. In this image, the main variation in ϵ_r over the sample is due to a slight tilt in the sample surface of about 20 μm . The edges of the sample show a smaller value of ϵ_r due to averaging over the inner conductor of the probe. The width of the affected region is in good agreement with the expected spatial resolution of about 500 μm .

The inventors next recorded a frequency shift image of the six-piece test sample using a probe-sample separation of 100 μm and the 480 μm diameter probe at 9.08 GHz. As before, using the $\epsilon_r(f_0)$ calibration, the frequency shift image is transformed into a dielectric constant image (see Fig. 22a). The darker regions in Fig. 22a indicate a higher dielectric constant (larger frequency shift) and the lighter regions indicate a smaller dielectric constant (smaller frequency shift). Figure 22b shows the corresponding surface plot representation. Note that the z-axis in Fig. 22b uses a logarithmic scale to allow us to show the large range of dielectric constants present in the sample. As expected, the largest dielectric constant materials (SrTiO_3 and LaAlO_3) are the highest surfaces and the smallest dielectric constant materials (Teflon and vacuum) are the lowest. Further, notice

PAGE 8 OF 8 SHEET

that the Teflon sample forms a depression in Fig. 22b, indicating that the dielectric constant of Teflon is lower than the surrounding epoxy. Note that voids in the epoxy can easily be seen as irregularly shaped low-dielectric regions (white regions in Fig. 22a) in the epoxy. Fig. 21 summarizes the dielectric constants for the six test materials and provides comparative data taken from literary sources.

From Fig. 22b, it is apparent that there is some noise in our images of dielectric constant. In our system, the predominant sources of random errors are noise in our recording electronics and fluctuations in the source frequency. To establish the precision to which ϵ_r can be determined, we determined the standard deviation in ϵ_r over a small region near the center of the LaAlO_3 sample in Fig. 20; we found $\Delta \epsilon_r = 0.06$ for a sampling time of 30 ms. Similarly, over the Teflon in Fig. 22a, the standard deviation in ϵ_r was 7×10^{-4} for a sampling time of 30 ms. From Fig. 22 we can also estimate the absolute accuracy of our technique. For $\epsilon_r = 230$ (SrTiO_3) the accuracy is about 25% while for $\epsilon_r = 2.1$ (Teflon) the accuracy is better than 2%. The main source of these errors is topographic variations. In our test sample, even after polishing, there are small height variations of about $30 \mu\text{m}$ (e.g. between the sapphire and SrTiO_3 in Fig. 22) between the different dielectrics. Such height variations cause an additional frequency shift, resulting in an error in the measured dielectric constant. In this regard, an accurate measurement of the dielectric constant of a single flat dielectric sample is considerably easier. However, the image of the composite sample clearly demonstrates the strength and sensitivity of this non-contact technique to measure variations in ϵ_r .

Conclusion

While various embodiments of the present invention have been described above, it should be understood that they have been presented by way of example, and not limitation. It will be apparent to persons skilled in the relevant art(s) that

-30-

various changes in form and detail can be made therein without departing from the spirit and scope of the invention. Thus the present invention should not be limited by any of the above-described exemplary embodiments, but should be defined only in accordance with the following claims and their equivalents.

8

-31-

~~What Is Claimed Is:~~

CLAIMS

1. A method for contact imaging of dielectric permittivity using a near-field scanning microwave microscope having a resonator with a probe tip comprising the steps of:

- 5 (a) calibrating the near-field scanning microwave microscope to determine a geometry descriptor of the probe tip;
- (b) generating calibration curves;
- 10 (c) scanning a test sample in contact with the probe tip at scanning locations and generating at least one test sample frequency shift value at each scanning location; and
- (d) determining the dielectric permittivity of the test sample at the sample locations based on the respective generated test sample frequency shift values and the generated calibration curves.

- 15 2. The method of claim 1, wherein said calibrating step (a) includes the steps of:

- (i) selecting a resonant frequency of the near-field scanning microwave microscope;
- 20 (ii) scanning each of said at least two calibration samples, where for each scan the probe tip is first brought into contact with each of said at least two calibration samples;
- (iii) moving the microscope probe to a predetermined background measurement position;
- 25 (iv) measuring a background resonant frequency at said predetermined background measurement position;

12-11-2001

-32-

- (v) moving the probe tip into contact with said one of said at least two calibration samples at a scanning position;
- (vi) measuring a contact resonant frequency at said scanning position;
- (vii) calculating the difference between said contact resonant frequency and said background resonant frequency;
- (viii) storing in memory said calculated difference as a calibration sample resonant frequency shift value;
- (ix) moving the sample to the next scanning position;
- (x) determining if said next scanning position is the end of a scan line;
- (xi) repeating steps (vi) through (x) until said end of a scan line has been reached;
- (xii) moving the sample to the next scan line;
- (xiii) determining if said next scan line is the end of a scan area;
- (xiv) repeating steps (iii) through (xiii) for each of said at least two calibration samples until said end of a scan area has been reached.

3. The method of claim 2, wherein the resonator includes a microscope transmission line, and wherein said step (iii) comprises moving the microscope probe to a height 1.5 times greater than the diameter of the microscope transmission line.

AMENDED SHEET



-33-

4. The method of claim 2, wherein said step (iii) comprises moving the microscope probe to a height where the calibration sample no longer perturbs the resonator.
5. The method of claim 2, wherein said step (iii) comprises moving the microscope probe to a height at least approximately 3 millimeters above the calibration sample.
6. The method of claim 1, wherein the geometry descriptor comprises an aspect ratio of the probe tip, and the calibration step (a) further includes calculating the aspect ratio of the microscope probe tip as $\Delta z/\Delta r$, where Δz is a distance along a z-direction parallel to a length of the resonator and the probe tip and Δr is a radius distance extending from the central axis of the probe tip to its outermost surface.
7. The method of claim 1, wherein the scanning step (c) includes the steps of:
- (i) selecting a resonant frequency of the near-field scanning microwave microscope;
 - (ii) placing said test sample on the microscope stage;
 - (iii) moving the probe tip into contact with said test sample;
 - (iv) storing a position value corresponding to the point of contact with said test sample;
 - (v) moving the probe to a predetermined background measurement position;
 - (vi) measuring a background resonant frequency at said background measurement position;

AMENDED SHEET

-34-

- 5 (vii) moving the probe tip into contact with said test sample at the scanning position;
- (viii) measuring the contact resonant frequency at said scanning position;
- 10 (ix) calculating the difference between said contact resonant frequency and said background resonant frequency;
- (x) storing in memory said calculated difference as a test sample resonant frequency shift value;
- (xi) moving the sample to the next scanning position;
- (xii) determining if said next scanning position is the end of a scan line;
- (xiii) repeating steps (viii) through (xii) until said end of a scan line has been reached;
- 15 (xiv) moving the sample to the next scan line;
- (xv) determining if said next scan line is the end of a scan area;
- (xvi) repeating steps (v) through (xv) until said end of a scan area has been reached.

20 8. The method of claim 7, wherein the resonator includes a microscope transmission line, and wherein said step (v) comprises moving the microscope probe to a height that is at least approximately 1.5 times greater than the diameter of the microscope transmission line.

25 9. The method of claim 7, wherein said step (v) comprises moving the probe to a height where the test sample no longer perturbs the resonator.

AMENDED SHEET

-35-

10. The method of claim 7, wherein said step (v) comprises moving the probe to a height at least approximately 3 millimeters above the test sample.
11. The method of claim 1, wherein the scanning step (c) includes placing a bulk test sample on the microscope stage.
12. The method of claim 11, wherein the generating a calibration curve step (b) includes the steps of:
- (i) storing electric field configuration data files, wherein the data corresponds to a model sample having approximately the same first thickness and further having approximately the same permittivity as one of said at least two calibration samples with known dielectric properties; and wherein the data stored is representative of electric field values at respective ϵ_r and α over a predetermined range of ϵ_r and α , where ϵ_r is a dielectric permittivity value and α is the probe tip geometry descriptor;
 - (ii) generating a first model calibration curve using said stored electric field configuration data;
 - (iii) generating a second model calibration curve using said stored electric field configuration data;
 - (iv) generating a probe calibration curve using said first and second generated model calibration curves and said generated calibration sample frequency shift values; and

AMENDED SHEET,

-36-

- (v) determining the geometry descriptor of the probe tip at the time of scanning of the test sample based upon the positioning of said generated probe calibration curve in relation to said first and second generated model calibration curves.

5

13. The method of claim 12 wherein the generating a first model calibration curve using said previously stored electric field configuration data (ii) includes the steps of:

10

- (1) reading from a first electric field configuration data file where α = a first probe tip geometry descriptor value, a first previously stored electric field value (E_1) and a first permittivity value (ϵ_{r1});

15

- (2) reading from a second electric field configuration data file where α = a first probe tip geometry descriptor value, a second previously stored electrical field value (E_2);

20

- (3) calculating a point on the first model calibration curve by solving the equation

$$\frac{\Delta f}{f} \approx \frac{\epsilon_0}{4W} \int_{V_s} (\epsilon_{r2} - \epsilon_{r1}) \vec{E}_1 \cdot \vec{E}_2 dV ; \text{ and}$$

25

- (4) repeating steps (1) through (3) until a predetermined number of points on the first model calibration curve have been generated.

AMENDED SHEET



-37-

14. The method of claim 12 wherein the generating a second model calibration curve using said previously stored electric field configuration data files step (iii) includes the steps of:

(1) reading from a first previously stored electric field configuration data file where α =a second probe tip geometry descriptor value, a first previously stored electric field value (E_1) and a first permittivity value (ϵ_{r1});

(2) reading from a second previously stored electric field configuration data file where α = a second probe tip geometry descriptor value, a second previously stored electric field value (E_2) and a second permittivity value (ϵ_{r2});

(3) calculating a point on the second model calibration curve by solving the equation

$$\frac{\Delta f}{f} \approx \frac{\epsilon_0}{4W} \int_{V_s} (\epsilon_{r2} - \epsilon_{r1}) \vec{E}_1 \cdot \vec{E}_2 dV ; \text{ and}$$

(4) repeating steps (1) through (3) until a predetermined number of points on the second model calibration curve have been generated.

15. The method of claim 1, wherein the scanning step (c) includes arranging a thin film test sample on top of a dielectric substrate having approximately the same first determined thickness and the same permittivity as at least one of said calibration samples and then placing said arrangement on the microscope stage.

RECEIVED



-38-

16. The method of claim 15, wherein the generating a calibration curve includes the steps of:

(i) storing electric field configuration data files

wherein the data corresponds to a model sample having a thin film of approximately the same second determined thickness and a known dielectric permittivity value arranged on top of said dielectric substrate having approximately the same first determined thickness and the same permittivity as at least one of said calibration samples with known dielectric properties; wherein the stored data files are representative of electric field values at respective ϵ_r and α over a predetermined range of ϵ_r and α , wherein ϵ_r is a dielectric permittivity value for the model sample thin film and α is representative of a probe tip geometry descriptor;

(ii) generating a first test sample calibration curve

using said stored electric field configuration data files;

(iii) generating a second test sample calibration curve

using said stored electric field configuration data files;

(iv) generating an additional test sample calibration

curve using said first and second test sample calibration curves and said generated test sample frequency shift values;

17. The method of claim 16 wherein the generating a first test sample calibration curve using said previously stored electric field configuration data files step (ii) includes the steps of:

(1) reading from a first electric field configuration

data file where α = a first probe tip geometry descriptor value, a first previously stored electric field value (E_1) and a first permittivity value (ϵ_{r1}) where ϵ_{r1} is the permittivity of said thin film having approximately the same second determined thickness and known dielectric permittivity;

(2) reading from a second electric field configuration

APPROVED



-39-

data file where α = a first probe tip geometry descriptor value, a second previously stored electric field value (E_2) and a second permittivity value (ϵ_{r2}) where ϵ_{r2} is the permittivity of said thin film having approximately the same second determined thickness and known dielectric permittivity;

- 5 (3) calculating a point on the first test sample calibration curve by solving the equation

$$\frac{\Delta f}{f} \approx \frac{\epsilon_0}{4W} \int_{V_s} (\epsilon_{r2} - \epsilon_{r1}) \vec{E}_1 \cdot \vec{E}_2 dV ; \text{ and}$$

- (4) repeating steps (1) through (3) until a predetermined number of points on the first test sample calibration curve have been generated.
- 10

18. The method of claim 16 wherein the generating a second test sample calibration curve using said previously stored electric field configuration data files step (iii) includes the steps of:

- (1) reading from a first previously stored electric field configuration data file where α = a second probe tip geometry descriptor value, a first previously stored electric field value (E_1) and a first permittivity value (ϵ_{r1}) where ϵ_{r1} is the permittivity of said thin film having approximately the same second determined thickness and known dielectric permittivity;
- 15

- (2) reading from a second previously stored electric field configuration data file where α = a second probe tip geometry descriptor value, a second previously stored electric field value (E_2) and a second permittivity value (ϵ_{r2}) where ϵ_{r2} is the permittivity of said thin film having approximately the same second determined thickness and known dielectric permittivity;
- 20

- (3) calculating a point on the second test sample calibration curve by solving the equation
- 25

AMENDED SHEET

-40-

$$\frac{\Delta f}{f} \approx \frac{\epsilon_0}{4W} \int_{V_s} (\epsilon_{r2} - \epsilon_{r1}) \vec{E}_1 \cdot \vec{E}_2 dV ; \text{and}$$

(4) repeating steps (1) through (3) until a predetermined number of points on the second test sample calibration curve have been generated.

- 5 19. An apparatus for displaying dielectric properties comprising:
- (a) a near-field scanning microwave microscope having an open-ended coaxial probe with a sharp, protruding center conductor;
- (b) a coaxial transmission line resonator that has a resonant frequency;
- 10 (c) a microwave source coupled to said coaxial transmission line resonator through a capacitive coupler for generating said voltage;
- (d) a spring-loaded cantilever for supporting said sample in contact with said sharp protruding center conductor;
- (e) a bias tee coupled to said coaxial transmission line resonator for applying a local electric field to said sample in contact with said sharp protruding center conductor;
- 15 (f) a first motor controller for manipulating said sample in contact with said sharp protruding center conductor in a first direction;
- (g) a second motor controller for manipulating said sample in contact with said sharp protruding center conductor in a second direction;
- 20 (h) a third motor controller for manipulating said sample in contact with said sharp protruding center conductor in a third direction;
- (i) a coupler joined to said microwave source and said coaxial transmission line resonator;
- 25 (j) a detector for converting the microwave signal from said coupler into an output signal;
- (k) a feedback circuit receives the output signal from said

AMENDED SHEET

-41-

detector and measures a shift change in resonance frequency, wherein said feedback circuit keeps said microwave source locked onto a predetermined resonant frequency;

(l) a processor for determining between at least one
5 parameter related to a change in said resonant frequency and a known dielectric property value of a sample responsible for said change; wherein the processor is further able to receive from said feedback circuit said value for at least one parameter related to a change in said resonant frequency due to an unknown dielectric property of said sample and determine the value of said unknown
10 dielectric property; and

(m) a display device for imaging the value of said unknown dielectric property once said value is determined by said processor.

20. A system for quantitatively modeling and imaging of dielectric properties, comprising:

- 15 (a) a memory device that stores
- (i) files of electric field values, ϵ_r , and α over a predetermined range of ϵ_r and α , where ϵ_r is a dielectric permittivity value and α is representative of said probe tip geometry descriptor;
 - 20 (ii) calibration sample resonant frequency shift values;
 - (iii) test sample resonant frequency shift values;
- (b) a model calibration curve generator that generates two model calibration curves using the stored files in said memory;
- 25 (c) a probe calibration curve generator that generates a probe calibration curve using said generated model calibration curves and said calibration sample frequency shift values.

AMENDED SHEET

-42-

- (d) a test sample calibration curve generator that generates a test sample calibration curve using additional model calibration curves and additional calibration sample frequency shift values;

5

21. A spring-loaded sample holder comprising:

- (a) a sample support having an angled end and a planar surface for supporting a sample;
- (b) a first bracing device in contact with the angled end of said sample support so as to create a pivot point;
- (c) a spring mounted to the sample support; and
- (d) a second bracing device in contact with said spring for holding the spring in place.

10

22. The method of claim 21, wherein a probe is held fixed and in contact with the sample.

15

23. The method of claim 22, wherein the sample holder and sample are scanned horizontally.

24. The method of claim 23, wherein a sensor measures the vertical displacement of the sample holder, such that this displacement is a function of the topography of the sample.

20

25. An apparatus for imaging a sample using a near-field scanning microwave microscope, comprising:

a bias tee in a coaxial transmission line resonator for applying a low-frequency bias voltage to a microscope probe tip and wherein the low-frequency bias voltage is independent of a

REMOVED SHEET

-43-

microwave signal, whereby a local electric field can be applied to a sample to allow for nonlinearity and tunability measuring.

26. A method for non-contact imaging of dielectric permittivity using a near-field scanning microwave microscope having a resonator with a probe tip comprising the steps of:

- 5
- (a) calibrating the near-field scanning microwave microscope using at least three dielectric samples with known dielectric properties;
- (b) generating calibration curves;
- 10 (c) scanning a test sample with the probe at a predetermined scanning height and generating at least one test sample frequency shift value at said predetermined scanning height; and
- (d) determining the dielectric permittivity of the test sample based on the generated test sample resonant frequency shift value and the generated calibration curves.
- 15

27. The method of claim 26, wherein said calibrating step (a) includes the steps of:

- 20 (i) selecting a resonant frequency of the near-field scanning microwave microscope;
- (ii) placing one of said at least three calibration samples beneath the probe;
- (iii) positioning the probe at a first predetermined height;
- 25 (iv) measuring a resonant frequency at said first predetermined height;

AMENDED SHEET

-44-

- (v) moving the probe to a second predetermined height;
- (vi) measuring the resonant frequency at said second predetermined height;
- 5 (vii) calculating the difference between said resonant frequency at said first predetermined height and said resonant frequency at said second predetermined height;
- 10 (viii) storing in memory said calculated difference as a calibration sample resonant frequency shift value;
- (ix) repeating steps (ii) through (viii) for each of said at least two calibration samples.

28. The method of claim 26, wherein said generating calibration curves step (b) includes the step of plotting said calibration frequency shift values as a function of dielectric constant (ϵ_r) and frequency shift.

29. The method of claim 26, wherein said scanning a test sample step (c) includes the steps of:

- (i) selecting a resonant frequency of the near-field scanning microwave microscope;
- 20 (ii) placing said test sample beneath the probe;
- (iii) positioning the probe at a first predetermined height;
- (iv) measuring a resonant frequency at said first predetermined height;
- 25 (v) moving the probe to a second predetermined height;

APPROVED

-45-

- (vi) measuring the resonant frequency at said second predetermined height;
- (vii) calculating the difference between said resonant frequency at said first predetermined height and said resonant frequency at said second predetermined height;
- (viii) storing in memory said calculated difference as a test sample resonant frequency shift value.

5

COPY SHEET



PATENT COOPERATION TREATY

PCT

INTERNATIONAL SEARCH REPORT

(PCT Article 18 and Rules 43 and 44)

Applicant's or agent's file reference 1797.020PC02	FOR FURTHER ACTION see Notification of Transmittal of International Search Report (Form PCT/ISA/220) as well as, where applicable, item 5 below.	
International application No. PCT/US 00/ 08943	International filing date (day/month/year) 05/04/2000	(Earliest) Priority Date (day/month/year) 10/09/1999
Applicant ANLAGE, Steven, Mark et al.		

This International Search Report has been prepared by this International Searching Authority and is transmitted to the applicant according to Article 18. A copy is being transmitted to the International Bureau.

This International Search Report consists of a total of 4 sheets.

☐ It is also accompanied by a copy of each prior art document cited in this report.

1. Basis of the report

- a. With regard to the language, the international search was carried out on the basis of the international application in the language in which it was filed, unless otherwise indicated under this item.

☐ the international search was carried out on the basis of a translation of the international application furnished to this Authority (Rule 23.1(b)).

- b. With regard to any nucleotide and/or amino acid sequence disclosed in the international application, the international search was carried out on the basis of the sequence listing :

☐ contained in the international application in written form.

☐ filed together with the international application in computer readable form.

☐ furnished subsequently to this Authority in written form.

☐ furnished subsequently to this Authority in computer readable form.

☐ the statement that the subsequently furnished written sequence listing does not go beyond the disclosure in the international application as filed has been furnished.

☐ the statement that the information recorded in computer readable form is identical to the written sequence listing has been furnished

2. ☐ Certain claims were found unsearchable (See Box I).

3. ☒ Unity of invention is lacking (see Box II).

4. With regard to the title,

☒ the text is approved as submitted by the applicant.

☐ the text has been established by this Authority to read as follows:

5. With regard to the abstract,

☒ the text is approved as submitted by the applicant.

☐ the text has been established, according to Rule 38.2(b), by this Authority as it appears in Box III. The applicant may, within one month from the date of mailing of this international search report, submit comments to this Authority.

6. The figure of the drawings to be published with the abstract is Figure No.

☒ as suggested by the applicant.

☐ because the applicant failed to suggest a figure.

☐ because this figure better characterizes the invention.

1

☐ None of the figures.



INTERNATIONAL SEARCH REPORT

International application No.
PCT/US 00/08943

Box I Observations where certain claims were found unsatisfactory (Continuation of item 1 of first sheet)

This International Search Report has not been established in respect of certain claims under Article 17(2)(a) for the following reasons:

1. ☐ Claims Nos.:
because they relate to subject matter not required to be searched by this Authority, namely:

2. ☐ Claims Nos.:
because they relate to parts of the International Application that do not comply with the prescribed requirements to such an extent that no meaningful International Search can be carried out, specifically:

3. ☐ Claims Nos.:
because they are dependent claims and are not drafted in accordance with the second and third sentences of Rule 6.4(a).

Box II Observations where unity of invention is lacking (Continuation of item 2 of first sheet)

This International Searching Authority found multiple inventions in this international application, as follows:

1. ☐ As all required additional search fees were timely paid by the applicant, this International Search Report covers all searchable claims.

2. ☐ As all searchable claims could be searched without effort justifying an additional fee, this Authority did not invite payment of any additional fee.

3. ☐ As only some of the required additional search fees were timely paid by the applicant, this International Search Report covers only those claims for which fees were paid, specifically claims Nos.:

4. ☒ No required additional search fees were timely paid by the applicant. Consequently, this International Search Report is restricted to the invention first mentioned in the claims; it is covered by claims Nos.:

1-18, 20, 26-29

Remark on Protest

- ☐ The additional search fees were accompanied by the applicant's protest.
- ☐ No protest accompanied the payment of additional search fees.

FURTHER INFORMATION CONTINUED FROM PCT/ISA/ 210

1. Claims: 1-18,20,26-29

Quantitative imaging dielectric permittivity

2. Claims: 19(partially), 21-24

Spring loaded sample holder

3. Claims: 19(partially), 25

Bias tee



A. CLASSIFICATION OF SUBJECT MATTER
IPC 7 G01R27/26

According to International Patent Classification (IPC) or to both national classification and IPC

B. FIELDS SEARCHED

Minimum documentation searched (classification system followed by classification symbols)

IPC 7 G01R G01N

Documentation searched other than minimum documentation to the extent that such documents are included in the fields searched

Electronic data base consulted during the international search (name of data base and, where practical, search terms used)

C. DOCUMENTS CONSIDERED TO BE RELEVANT

Category *	Citation of document, with indication, where appropriate, of the relevant passages	Relevant to claim No.
Y	<p>WO 99 16102 A (UNIV CALIFORNIA) 1 April 1999 (1999-04-01) abstract; claims 10,24; figures 2,16 page 2, line 15 -page 4, line 7 page 8, line 20 -page 9, line 9 page 13, line 8 - line 29 page 15, line 7 -page 16, line 20 page 19, line 2 - line 8 page 20, line 3 - line 5 page 21, line 16 -page 22, line 9 page 43, line 7 - line 10</p> <p>---</p> <p>-/--</p>	1,20,26

☒ Further documents are listed in the continuation of box C.

☒ Patent family members are listed in annex.

* Special categories of cited documents :

- *A* document defining the general state of the art which is not considered to be of particular relevance
- *E* earlier document but published on or after the international filing date
- *L* document which may throw doubts on priority claim(s) or which is cited to establish the publication date of another citation or other special reason (as specified)
- *O* document referring to an oral disclosure, use, exhibition or other means
- *P* document published prior to the international filing date but later than the priority date claimed

T later document published after the international filing date or priority date and not in conflict with the application but cited to understand the principle or theory underlying the invention

X document of particular relevance; the claimed invention cannot be considered novel or cannot be considered to involve an inventive step when the document is taken alone

Y document of particular relevance; the claimed invention cannot be considered to involve an inventive step when the document is combined with one or more other such documents, such combination being obvious to a person skilled in the art.

Z document member of the same patent family

Date of the actual completion of the international search

8 August 2000

Date of mailing of the international search report

30.08.2000

Name and mailing address of the ISA

European Patent Office, P.B. 5818 Patentlaan 2
NL - 2280 HV Rijswijk
Tel. (+31-70) 340-2040, Tx. 31 651 epo nl,
Fax: (+31-70) 340-3016

Authorized officer

FRITZ, S

C.(Continuation) DOCUMENTS CONSIDERED TO BE RELEVANT

Category *	Citation of document, with indication, where appropriate, of the relevant passages	Relevant to claim No.
A	C.GAO ET AL.: "Quantitative microwave near-field microscopy of dielectric properties" REVIEW OF SCIENTIFIC INSTRUMENTS, vol. 69, no. 11, November 1998 (1998-11), pages 3846-3851, XP002144502 US abstract; figure 1 ---	1,20,26
Y	US 5 900 618 A (S.M.ANLAGE ET AL.) 4 May 1999 (1999-05-04) cited in the application abstract; claim 17; figures 1A,6-9 column 1, line 47 -column 2, line 15 column 7, line 66 -column 8, line 24 column 8, line 45 - line 47 ---	1,20,26
A	TABIB-AZAR M ET AL: "NOVEL PHYSICAL SENSORS USING EVANESCENT MICROWAVE PROBES" REVIEW OF SCIENTIFIC INSTRUMENTS,US,AMERICAN INSTITUTE OF PHYSICS. NEW YORK, vol. 70, no. 8, August 1999 (1999-08), pages 3381-3386, XP000870710 ISSN: 0034-6748 abstract; figures 1-3 -----	1,20,26



INTERNATIONAL SEARCH REPORT

Information on patent family members

International Application No

P S 00/08943

Patent document cited in search report		Publication date	Patent family member(s)	Publication date
WO 9916102	A	01-04-1999	AU 1061599 A EP 1018138 A	12-04-1999 12-07-2000
US 5900618	A	04-05-1999	NONE	

INTERNATIONAL SEARCH REPORT

International Application No.

PCT/US 00/08943

A. CLASSIFICATION OF SUBJECT MATTER
IPC 7 G01R27/26

According to International Patent Classification (IPC) or to both national classification and IPC

B. FIELDS SEARCHED

Minimum documentation searched (classification system followed by classification symbols)
IPC 7 G01R G01N

Documentation searched other than minimum documentation to the extent that such documents are included in the fields searched

Electronic data base consulted during the international search (name of data base and, where practical, search terms used)

C. DOCUMENTS CONSIDERED TO BE RELEVANT

Category *	Citation of document, with indication, where appropriate, of the relevant passages	Relevant to claim No.
Y	WO 99 16102 A (UNIV CALIFORNIA) 1 April 1999 (1999-04-01) abstract; claims 10,24; figures 2,16 page 2, line 15 -page 4, line 7 page 8, line 20 -page 9, line 9 page 13, line 8 - line 29 page 15, line 7 -page 16, line 20 page 19, line 2 - line 8 page 20, line 3 - line 5 page 21, line 16 -page 22, line 9 page 43, line 7 - line 10 --- -/-	1,20,26

☒ Further documents are listed in the continuation of box C.☒ Patent family members are listed in annex.

* Special categories of cited documents:

- "A" document defining the general state of the art which is not considered to be of particular relevance
"E" earlier document but published on or after the international filing date
"L" document which may throw doubts on priority claim(s) or which is cited to establish the publication date of another citation or other special reason (as specified)
"O" document referring to an oral disclosure, use, exhibition or other means
"P" document published prior to the international filing date but later than the priority date claimed

- "T" later document published after the international filing date or priority date and not in conflict with the application but cited to understand the principle or theory underlying the invention
"X" document of particular relevance; the claimed invention cannot be considered novel or cannot be considered to involve an inventive step when the document is taken alone
"Y" document of particular relevance; the claimed invention cannot be considered to involve an inventive step when the document is combined with one or more other such documents, such combination being obvious to a person skilled in the art
"&" document member of the same patent family

Date of the actual completion of the international search

8 August 2000

Date of mailing of the international search report

30 Oct 2000

Name and mailing address of the ISA

European Patent Office, P.B. 5818 Patentlaan 2
NL - 2280 HV Rijswijk
Tel. (+31-70) 340-2040, Tx. 31 651 epo nl,
Fax: (+31-70) 340-3016

Authorized officer

FRITZ, S



INTERNATIONAL SEARCH REPORT

International Application No
PCT/US 00/08943

C.(Continuation) DOCUMENTS CONSIDERED TO BE RELEVANT

Category *	Citation of document, with indication, where appropriate, of the relevant passages	Relevant to claim No.
A	C.GAO ET AL.: "Quantitative microwave near-field microscopy of dielectric properties" REVIEW OF SCIENTIFIC INSTRUMENTS, vol. 69, no. 11, November 1998 (1998-11), pages 3846-3851, XP002144502 US abstract; figure 1 ---	1,20,26
Y	US 5 900 618 A (S.M.ANLAGE ET AL.) 4 May 1999 (1999-05-04) cited in the application abstract; claim 17; figures 1A,6-9 column 1, line 47 -column 2, line 15 column 7, line 66 -column 8, line 24 column 8, line 45 - line 47 ---	1,20,26
A	TABIB-AZAR M ET AL: "NOVEL PHYSICAL SENSORS USING EVANESCENT MICROWAVE PROBES" REVIEW OF SCIENTIFIC INSTRUMENTS,US,AMERICAN INSTITUTE OF PHYSICS. NEW YORK, vol. 70, no. 8, August 1999 (1999-08), pages 3381-3386, XP000870710 ISSN: 0034-6748 abstract; figures 1-3 -----	1,20,26



INTERNATIONAL SEARCH REPORT

Int. Application No.
PCT/US 00/08943

Box I Observations where certain claims were found unsearchable (Continuation of item 1 of first sheet)

This International Search Report has not been established in respect of certain claims under Article 17(2)(a) for the following reasons:

1. ☐ Claims Nos.:
because they relate to subject matter not required to be searched by this Authority, namely:

2. ☐ Claims Nos.:
because they relate to parts of the International Application that do not comply with the prescribed requirements to such an extent that no meaningful International Search can be carried out, specifically:

3. ☐ Claims Nos.:
because they are dependent claims and are not drafted in accordance with the second and third sentences of Rule 6.4(a).

Box II Observations where unity of invention is lacking (Continuation of item 2 of first sheet)

This International Searching Authority found multiple inventions in this international application, as follows:

1. ☐ As all required additional search fees were timely paid by the applicant, this International Search Report covers all searchable claims.

2. ☐ As all searchable claims could be searched without effort justifying an additional fee, this Authority did not invite payment of any additional fee.

3. ☐ As only some of the required additional search fees were timely paid by the applicant, this International Search Report covers only those claims for which fees were paid, specifically claims Nos.:

4. ☒ No required additional search fees were timely paid by the applicant. Consequently, this International Search Report is restricted to the invention first mentioned in the claims; it is covered by claims Nos.:
1-18, 20, 26-29

Remark on Protest

- ☐ The additional search fees were accompanied by the applicant's protest.
- ☐ No protest accompanied the payment of additional search fees.



INTERNATIONAL SEARCH REPORT

International Application No. PCT/US 00/08943

FURTHER INFORMATION CONTINUED FROM PCT/ISA/ 210

1. Claims: 1-18,20,26-29

Quantitative imaging dielectric permittivity

2. Claims: 19(partially), 21-24

Spring loaded sample holder

3. Claims: 19(partially), 25

Bias tee



.

.

PCT

WORLD INTELLECTUAL PROPERTY ORGANIZATION
International Bureau



INTERNATIONAL APPLICATION PUBLISHED UNDER THE PATENT COOPERATION TREATY (PCT)

(51) International Patent Classification ⁶ : H01J 37/20, G01B 7/34	A1	(11) International Publication Number: WO 99/16102
		(43) International Publication Date: 1 April 1999 (01.04.99)
(21) International Application Number: PCT/US98/19764		(81) Designated States: AL, AM, AT, AU, AZ, BA, BB, BG, BR, BY, CA, CH, CN, CU, CZ, DE, DK, EE, ES, FI, GB, GE, GH, GM, HU, ID, IL, IS, JP, KE, KG, KP, KR, KZ, LC, LK, LR, LS, LT, LU, LV, MD, MG, MK, MN, MW, MX, NO, NZ, PL, PT, RO, RU, SD, SE, SG, SI, SK, SL, TJ, TM, TR, TT, UA, UG, UZ, VN, YU, ZW, ARIPO patent (GH, GM, KE, LS, MW, SD, SZ, UG, ZW), Eurasian patent (AM, AZ, BY, KG, KZ, MD, RU, TJ, TM), European patent (AT, BE, CH, CY, DE, DK, ES, FI, FR, GB, GR, IE, IT, LU, MC, NL, PT, SE), OAPI patent (BF, BJ, CF, CG, CI, CM, GA, GN, GW, ML, MR, NE, SN, TD, TG).
(22) International Filing Date: 22 September 1998 (22.09.98)		
(30) Priority Data: 60/059,471 22 September 1997 (22.09.97) US		
(71) Applicant: THE REGENTS OF THE UNIVERSITY OF CALIFORNIA [US/US]; 21st floor, 300 Lakeside Drive, Oakland, CA 94612-3550 (US).		
(72) Inventors: XIANG, Xiao-Dong; 215 Kevington Place, Alameda, CA 94502 (US). GAO, Chen; Apartment #318, 434 Central Avenue, Alameda, CA 94501 (US).		
(74) Agents: ROSS, Pepi et al.; Suite 3300, Four Embarcadero Center, San Francisco, CA 94111 (US).		

Published

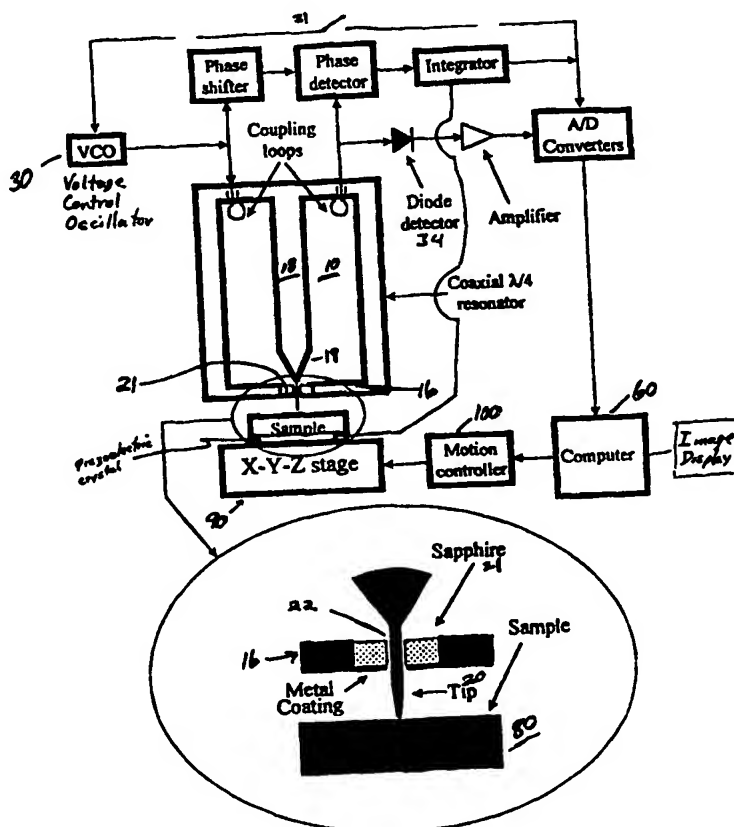
With international search report.

Before the expiration of the time limit for amending the claims and to be republished in the event of the receipt of amendments.

(54) Title: SCANNING EVANESCENT ELECTRO-MAGNETIC MICROSCOPE

(57) Abstract

A scanning microscope uses near-field evanescent electromagnetic waves emitted from a sharpened metal tip (20) to probe sample (80) properties. The sharpened tip (20), which is electrically and mechanically connected to a central electrode (18), extends through and beyond an aperture (22) in an endwall (16) of a microwave resonating device, such as a microwave cavity resonator (10). The microscope is capable of high resolution imaging and quantitative measurement of the electrical properties of a sample, such as the dielectric constant, tangent loss, conductivity, and complex electrical impedance measurements.



FOR THE PURPOSES OF INFORMATION ONLY

Codes used to identify States party to the PCT on the front pages of pamphlets publishing international applications under the PCT.

AL	Albania	ES	Spain	LS	Lesotho	SI	Slovenia
AM	Armenia	FI	Finland	LT	Lithuania	SK	Slovakia
AT	Austria	FR	France	LU	Luxembourg	SN	Senegal
AU	Australia	GA	Gabon	LV	Latvia	SZ	Swaziland
AZ	Azerbaijan	GB	United Kingdom	MC	Monaco	TD	Chad
BA	Bosnia and Herzegovina	GE	Georgia	MD	Republic of Moldova	TG	Togo
BB	Barbados	GH	Ghana	MG	Madagascar	TJ	Tajikistan
BE	Belgium	GN	Guinea	MK	The former Yugoslav Republic of Macedonia	TM	Turkmenistan
BF	Burkina Faso	GR	Greece	ML	Mali	TR	Turkey
BG	Bulgaria	HU	Hungary	MN	Mongolia	TT	Trinidad and Tobago
BJ	Benin	IE	Ireland	MR	Mauritania	UA	Ukraine
BR	Brazil	IL	Israel	MW	Malawi	UG	Uganda
BY	Belarus	IS	Iceland	MX	Mexico	US	United States of America
CA	Canada	IT	Italy	NE	Niger	UZ	Uzbekistan
CF	Central African Republic	JP	Japan	NL	Netherlands	VN	Viet Nam
CG	Congo	KE	Kenya	NO	Norway	YU	Yugoslavia
CH	Switzerland	KG	Kyrgyzstan	NZ	New Zealand	ZW	Zimbabwe
CI	Côte d'Ivoire	KP	Democratic People's Republic of Korea	PL	Poland		
CM	Cameroon	KR	Republic of Korea	PT	Portugal		
CN	China	KZ	Kazakhstan	RO	Romania		
CU	Cuba	LC	Saint Lucia	RU	Russian Federation		
CZ	Czech Republic	LI	Liechtenstein	SD	Sudan		
DE	Germany	LK	Sri Lanka	SE	Sweden		
DK	Denmark	LR	Liberia	SG	Singapore		
EE	Estonia						

SCANNING EVANESCENT ELECTRO-MAGNETIC MICROSCOPE

5

10 This invention was made with U. S. Government support under Contract No. DE-AC03-76SF00098 between the U.S. Department of Energy and the University of California for the operation of Lawrence Berkeley Laboratory. The U. S. Government may have certain rights in this invention.

15 This is a continuation-in-part of application serial number 08/717,321, filed September 20, 1996 and incorporated herein by reference. This invention claims benefit of provisional application serial number 60/059,471 filed September 22, 1997, and incorporated herein by reference.

Background of the Invention

Field of the Invention

20 This invention relates generally to scanning probe microscopy and more specifically to scanning evanescent near field microwave and electromagnetic spectroscopy.

Description of the Related Art

25 Scanning probe type microscopes have typically been used to create visual images of a sample material. The image obtained may reflect any of a number of distinct electrical or magnetic properties of the sample material, depending on the parameter measured by the probe tip. For example the tip may image electron tunneling, atomic force, absorption and refraction of propagating or evanescent electromagnetic waves, or other parameters. The tip may be in contact with the sample or it may be a short distance above the sample.

30 A thorough discussion of scanning probe microscopes is presented by R. Wiesendanger,

"Scanning Probe Microscopy and Spectroscopy: Methods and Applications" Cambridge University Press, 1994. Efforts in improving Scanning Probe Microscopes (SPMs) have focused almost entirely on increasing their resolution and sensitivity. While it is generally recognized that obtaining quantitative data to associate with the image detail would be highly desirable, two major technological barriers have prevented such instruments from being developed.

First, microscopy signals, as obtained from SPMs often are a combined function of topography and physical properties of the material. Separating them requires measuring at least two independent signals. For example, in scanning tunneling microscopy, the tunneling current is a function of both the tip to sample distance and the density of states. A recently developed scanning near-field optical microscope can measure optical signals such as luminescent spectra or optical index of refraction in addition to shear force, which can be used to determine the distance between tip and sample.

Second, to obtain quantitative information regarding the physical sample being imaged, complicated electromagnetic field equations in the region of the tip and sample must be solved. A review of this work is discussed by C. Girard and A. Dereux in Rep. Prog. Phys., vol. 657, 1996. Although numerical methods based on finite element analysis have been used to solve the field distribution around a near-field optical microscope tip, the complicated computational process involved, such as solving the Maxwell equations under real boundary conditions on a scale of a wavelength or less, is not practical in routine applications. The problem has been complicated for the work done in the past, because the microscopes were required to operate below a cut-off frequency and so suffered severely from waveguide decay, having a typical attenuation of 10^{-3} to 10^{-6} (R.F. Soohoo, J. Appl. Phys. 33:1276, 1962; E.A. Ash and G. Nichols, Nature, 237:510, 1972). In aperture or tapered waveguide probes, a linear improvement in resolution causes an exponential reduction in sensitivity. M. Fee, S. Chu, and T.W. Hansch, improved sensitivity and resolution to the micron level (Fee, M. et al., Optics Commun., 63:219, 1988) by using a transmission line probe with a reduced cross-section. However, further improvement in resolution was still accompanied by significant transmission line decay.

The unshielded far-field wave propagation components around the tip of the transmission line probe significantly limited the resolution of the microscope, and particularly interfered with its use for quantitative analysis.

5 It would be highly desirable to have a scanning probe microscope capable of making images of features having submicron resolution and additionally capable of making quantitative measurements of the physical properties of the imaged features.

Summary of the Invention

10 The invention comprises a near field scanning evanescent-wave microscope wherein a probe tip primarily emits an evanescent wave and wherein interfering propagating wave emissions are minimized. Propagating waves have low resolution while evanescent waves have high resolution. This feature is crucial for quantitative measurements, where only the near-field evanescent wave is modeled. A high resolution image is generated by scanning a sample with a novel evanescent wave probe on the inventive microscope. Furthermore, the inventive microscope provides complex electrical
15 impedance values that are calculated from measured data and which are associated with the resolved image features. The complex impedance, including dielectric constant, loss tangent and conductivity can be measured for materials having properties that range from insulators to superconductors.

20 The inventive microscope is capable of quantitative measurements of dielectric properties and surface resistance with submicron resolution. By monitoring the resonance frequency (f_r) and quality factor (Q) of a resonant coaxial cavity coupled to the tip, the electrical properties of the sample are measured. One embodiment of the SEMM comprises a $\lambda/4$ coaxial resonator operating at frequency (f_r) of roughly 1 GHz coupled to a sharp tip protruding from a narrow hole. When the probe tip is brought near a
25 sample, f_r and Q shift. The inventive microscope is capable of converting the measured f_r and Q shifts to electrical parameters of the sample. Since the extremely small tip radius determines the extent of the field distribution, this microscope is capable of submicron resolution. For dielectric samples, the interaction between the probe tip and the sample is dependent on the dielectric constant and tangent loss of the nearby sample. For a
30 metallic sample, the interaction depends on the surface resistance of the sample.

The probe itself, comprising either a resonator or a conventional coaxial body, is a key inventive feature of the microscope. An important novel feature of the probe tip is a conducting endwall having an aperture, through which the center conducting element of the coaxial cable or resonator extends without shorting to the endwall. Another key feature of the inventive microscope is the computing element programed to convert measured changes in resonant frequency (or reflected electromagnetic wave) and measured changes in the quality factor to quantitative electrical parameters of the sample. An additional important feature of the inventive microscope is a means to maintain a constant separation distance between the tip and the sample while measurement scans of the sample are performed.

Summary Description of the Drawings

Figure 1 is a diagrammatic view of the various components which comprise the imaging evanescent near field microscope system.

Figure 2 is a diagrammatic view of the various components which comprise the quantitative evanescent near field microscope system.

Figure 3 shows the image charge distribution for a thick sample in contact with the end of the probe tip. The q_n series represents the charge redistribution on the tip; the q_n' series represents the effect of polarization of the dielectric sample; and the q_n'' is the effective value of q_n inside the sample.

Figure 4 shows the image charge distribution for the configuration with an air gap between a thick sample and the end of the probe tip. Symbols q_n , q_n' , and q_n'' have the same meaning as in Figure 3.

Figure 5 shows a graph of measured and fitted resonant frequency as a function of the distance between the end of the probe tip and the sample for a MgO single crystal.

Figure 6 shows distribution of image charges for a tip-sample configuration in which the sample comprises a thin film (ϵ_2) on a thick substrate (ϵ_1) and in which there is an air gap (g) between the probe tip and the film surfaces. Symbols q_n , q_n' , and q_n'' have the same meaning as in Figure 3. The q_n' series represents the effect of polarization of the dielectric film induced by the field of the tip. The q_n'' series

represents the reaction on the film from the polarized substrate. The q_n'' series represents the reaction on the tip from the polarized substrate, and the q_n''' series represents the polarization of the dielectric film caused by q_n''' , etc. This analysis is analogous to a three-mirror system in optics.

5 Figure 7 shows the intrinsic spatial resolution, in units of tip radius, R_0 , of the SEMM as a function of dielectric constant.

Figure 8 shows the multiple image charge analysis of tip-sample interaction between the end of the probe tip and a conducting sample.

10 Figure 9 shows the magnetic field distribution on the surface of a conducting material surrounding the proximity of the probe tip.

Figure 10 shows the radial distribution for the magnetic field on the surface of a conducting material surrounding the proximity of the probe tip, for different probe tip radii, a_0 .

15 Figure 11 shows measured data points (triangles) and a best fit calculated curve from SEMM signals as a function of gap size between the probe tip and a copper sample using the resonant frequency equation 12.

Figure 12 shows measured data points (triangles) and a best fit calculated curve from SEMM signals as a function of gap size between the probe tip and a copper sample using the quality factor equation 19.

20 Figure 13 shows the spatial frequency spectra of the magnetic field on the surface of a conducting material for five different values of a_0 .

Figure 14 shows the power dissipated, S , in a conducting sample as a function of a_0 , the ratio of the gap distance to the radius of the probe tip.

25 Figure 15 shows on the left, a topographic image of a LiNbO_3 sample having periodically poled domains. The image on the right is of a simultaneously obtained first harmonic image in which the contribution from sample-probe geometry has been excluded. These images were obtained using the inventive feed back control component to control sample to tip distance.

30 Figure 16 shows an embodiment of the inventive probe tip comprising a coaxial cable instead of a resonator.

Figure 17 shows a change in frequency as a function of gap distance for a known metal, the curve being useful as a calibration curve for the gap distance controller.

Figure 18 shows results obtained using the SEMM to image conducting silver sections having differing heights but constant conductivity.

5 Figure 19 shows results obtained using the SEMM to image conducting metal sections having differing heights and differing conductivity.

Detailed Description of the Invention

The present invention is described in part in copending application serial number 08/717,321, and described in at least one embodiment by T. Wei and X.-D. Xiang in Appl.
10 Phys. Lett., 68, 3506(1996). An image resolution of about 100 nm on dielectric material has been achieved with a sensitivity of about 10^{-3} .

The present invention improves the visual image resolution of the scanning evanescent electromagnetic microscope and extends its utility to essentially simultaneous measurement of quantitative microscopy. The microscope is referred to as a SEMM,
15 originally for Scanning Evanescent Microwave Microscope, and alternatives, because the microscope is not limited to the microwave region, for "Scanning Evanescent electroMagnetic Microscope". Using the SEMM, quantitative microscopy can be used to obtain the complex electrical impedance of dielectric, ferroelectric, and conducting materials with submicron resolution. Use of the SEMM is not limited to the microwave
20 region. Rather the electromagnetic frequency of the inventive microscope is limited on the high end by the electron mobility in the sample being measured (that is the plasma frequency of the material) and on the low end by the practicality of the physical dimension of the resonant cavity portion of the probe tip. For a sample made from copper, frequencies ranging from the infrared region of the electromagnetic spectrum to the
25 microwave region can be used on the scanning evanescent wave microscope. If the resonance is replaced by a coaxial cable having an end wall connected to the coaxial shielding element, the low end of the measurement frequency is essentially d.c.

To understand the invention it is helpful to review some fundamental physics of evanescent-wave microscopy. The evanescent-waves in this context refer to
30 electromagnetic waves with wave-vectors of imaginary number not originating from

dissipation. In fact, the evanescent electromagnetic waves are the photon equivalent of quantum mechanic electron waves in the classically forbidden region (within a barrier). In the far-field description of electromagnetic waves, an orthogonal eigenfunction set of Hilbert space is chosen as the plane waves whose wave vectors are any real number satisfying Helmholtz equation (as a consequence, these plane waves are propagating waves). Any propagating wave (for example, a propagating spherical wave from a point source) can be expanded as the superposition of these plane waves. The magnitudes of the wave vectors are solely determined by the frequency and speed according to Maxwell equation, i.e. $k=2\pi(\epsilon\mu/c)^{1/2}=2\pi/\lambda=(k_x^2+k_y^2+k_z^2)^{1/2}$. For propagating waves, k_x , k_y , and k_z are real numbers and thus must be smaller than k (in free space $k=k_0$). These waves only have resolving power on the order of λ . However, these plane waves can not be used to reconstruct, for example, a spherical wave whose wave front has a radius less than the wavelength λ . Therefore, a true complete set of Hilbert space should include plane waves whose wave-vectors are any complex number satisfying the Maxwell equation to construct such a spherical wave. Since imaginary wave vectors are allowed, the components (k_x , k_y , and k_z) can then be any value and still satisfy the Maxwell equation. Here the "plane waves" whose lateral components $k_r=(k_x^2+k_y^2)^{1/2}$ are larger than k will have higher lateral resolving power (on the order of $1/k_r$). However, since they must have imaginary components k_z to satisfy the Maxwell equation, these waves are "evanescent" and can not propagate much more than a wavelength λ . Different methods of evanescent-wave microscopy use different means to obtain strong evanescent waves and strong interaction between the evanescent wave and the substance under inspection. For example, a metal sphere or tip fed by a wave source with a radius of r ($\ll \lambda$) will generate evanescent waves (to form a spherical wave on the metal surface satisfying the boundary conditions) whose wave vectors range up to $k_r \sim 1/r$ and resolving power up to $\sim r$. Interaction between the tip and sample (with high effective dielectric constant) may further increase the high k_r components and resolution as a result of decreasing the effective tip radius from a polarizing effect. Since these waves decay over a distance r in free space, the sample has to be brought to within r of the tip to obtain strong interaction. Note,

these waves are not necessarily evanescent in conducting materials since $k_c = 2\pi/\lambda_c$ in conducting materials is many orders of magnitude larger than that in free space.

The inventive scanning evanescent microscope uses an evanescent wave to image the surface with high resolution and to obtain a quantitative measurement of the complex electrical impedance associated with detail resolved in the image. The inventive apparatus uses the near-field interaction between the evanescent waves around the tip and the samples under scan.

Figure 1 shows the inventive near field microscope system utilizing the novel evanescent probe structure comprising a microwave resonator such as illustrated microwave cavity 10 having generator 30 electrically connected to cavity 10 to feed an input signal, through a coaxial line 32, into a coupled loop input 12 on cavity 10. A coupled loop output 14 of cavity 10 is connected to a detector 40 through a second coaxial line 42. Detector 40, in turn, feeds the output signal to a data acquisition unit 50. The data from data acquisition unit 50 is then fed into a computer 60 which converts the data into an image viewable at image display 70 connected to computer 60. Other means besides coupled loops or tuned loops can be used to couple energy to and from the resonant cavity, as described in detail in the text "Microwave Engineering" by D. M. Pozar, (Addison-Wesley Publishing Co, New York, 1990).

The Structure of the Tip

One of the best prior art probe tips comprised an open-ended coaxial cable which included a center conducting wire surrounded by an insulator and enclosed in an external shield. This type of tip generates both a near-field evanescent wave, which doesn't propagate more than a few wavelengths (λ) before it attenuates and thus results in high resolution measurements, and a far-field propagating wave. The propagating wave is undesirable because it interferes with the near-field evanescent wave. In order to minimize the propagating wave, researchers attempted to use coaxial cables having smaller and smaller diameters, but eventually large energy loss and difficult physical construction to avoid electrical breakdown between the shield and center wire became a problem. Because of the practical limitation in diameter of the conventional coaxial cable design, the present inventors developed a configuration in which the center wire was sharpened

and extended a distance beyond the shielding, or a sharpened tip was mechanically and electrically connected to the center wire. An additional inventive shielding element was added to the bottom edge of the coaxial cable in order to minimize any electromagnetic fields created between the sharpened end of the probe and the end of the external shielding, which when left open can allow far-field propagating wave to reach the sample and dominate the near-field evanescent wave. In addition, the present inventors added a resonator which was located immediately above or near the probe tip so that evanescent waves could be generated and sensed with greater efficiency and sensitivity, although the resonator is not a necessary component for every application.

The inventive SEMM tip limits the creation of propagating waves so that high resolution evanescent wave measurements can be made effectively. One feature of the inventive tip that limits creation of far-field propagating waves is a conductive shielding element that extends over the portion of the coaxial cable that otherwise would have been open. Referring to Figures 1 and 2, at the end from which the probe tip 20 extends, a new electrically conducting shielding element 16 is located so that its outer edge connects to the exterior coaxial shield 17 and its inner edge circles, or surrounds, the probe tip without electrically shorting to it. The conducting shielding element 32 is preferably thin, on the order of $1\text{ }\mu\text{m}$, to avoid causing excess loss. It is preferably physically supported by a low loss insulator like sapphire. In essence, the outer shield 32 is brought around the end portion 16 of the insulator but has an opening, or aperture 22 through which the probe can extend without electrically shorting to the shield. The aperture is conveniently circular but does not have to be circular. The aperture is smaller than either the coaxial cable or a resonator that is used to generate the evanescent wave. Conveniently the end portion of the insulator forms a plane that is approximately normal to the line of the probe portion, however a tapered surface could span part of the distance between the outer shield and probe as long as the sensitivity of the probe remains acceptable and degradation of the Q factor is avoided. The Q factor is a quality factor; it equals the ratio of the total energy in the resonator and the energy that is dissipated from the resonator ($Q = E_{\text{total}}/E_{\text{dissipated}}$). The Q factor is a function of the geometry of the cavity and tapering the

walls of the cavity may lower it (as well as lowering the sensitivity) unacceptably for any given desired measurement. Preferably $Q = 2\pi E_{\text{total}}/E_{\text{dissipated}}$.

As shown in both Figures 1 and 2, a sharpened metal tip 20 which, in accordance with the invention acts as a point-like evanescent field emitter as well as a detector,
5 extends through a cylindrical opening or aperture 22 in endwall 16 of cavity 10, as will be described in more detail below. Mounted immediately adjacent sharpened tip 20 is a sample 80. Sample 80 is mounted to a movable target mount or stepper mechanism 90 which can be moved in either the X, or Y or Z axis by an X-Y-Z scanning controller 100 which, in turn, is controlled by signals from computer 60.

10 Microwave generator 30, detector 40, data acquisition unit 50, computer 60, display 70, movable target mount 90, and X-Y-Z scanning control 100 all comprises commercially available equipment. For example, microwave generator 30 is available from the Programmed Test Source Company as model PTS1000, detector 40 is available from Pasternack Enterprises as model PE800-50, data acquisition unit 50 is available from
15 National Instruments as model PC-TIO02150, computer 60 may comprises any standard programmable computer, display 70 may comprise any commercially available monitor, movable target mount or stepper mechanism 90 is available from the Ealing Company as model 61-0303, and X-Y scanning control 100 is available from the Ealing Company as model 37-1039. Design principles for a quarter wave cavity, such as cavity 10, may be
20 found in "Radio Engineer Handbook" by F.E. Terman.

Cavity 10 comprises a standard quarter or half wave cylindrical microwave cavity resonator having a central metal conductor 18 with a tapered end 10 to which is attached sharpened metal tip or probe 20. An optional spacer, made of an insulation material such as Teflon, may be used to assist in maintaining the central positional of central conductor
25 18 coaxially within cavity 10. As shown, probe tip 20 extends through and beyond aperture 22 formed in endwall 16.

Metal Probe Tip Thickness

Metal probe tip 20 has a sharpened end thereon which may be as fine as about 100 Angstroms in diameter. The sharpened end of tip 20 will usually vary in diameter from
30 as small as about 100 Angstrom (10 nm) to as large as about 100 μm , and preferably

ranges from about 200 Angstroms (20nm) to about 20 μ m. Sharpened metal probe tip 20 may be formed, for example, by electrochemically etching one section of a wire which might have an initial diameter of from about 1 μ m to about 0.2 millimeters (mm) prior to the electrochemical etch. Sharpened metal probe tip 20 may be connected to tapered end 19 of central conductor 18 by welding or any other suitable means which will provide a secure mechanical and electrical connection between tip 20 and tapered probe end 19.

The Diameter of the Aperture

Experimentally, the minimum diameter of aperture 22 has been determined to be the minimum diameter which maintains the high Q and sensitivity of the resonator. The aperture opening must be small enough that a propagating wave is not emitted that will interfere with the evanescent wave measurement. To maintain the high Q, the minimum diameter of aperture 22 should be greater than the thickness of endwall 16. That is, endwall thickness t divided by aperture diameter d must be much less than unity ($t/d \ll 1$) to maintain high Q (or low loss) of the resonator. Ideally, the endwall should be made by plating a good conducting film (silver or copper) of about 1-2 μ m thick on a low loss insulating plate (~1 mm thick), such as sapphire or $LaAlO_3$ to reduce the thickness t while maintaining rigidity (mechanical vibration is not desired). The aperture diameter is also related to the diameter of the metal probe tip which passes through and beyond aperture 22. The minimum aperture diameter, therefore, will usually be at least about 200 Angstroms (20 nm). If the diameter of aperture 22 is too large, however, the resolution will be reduced. It has been found, however, that the diameter of aperture 22 may be as large as 3 mm while still maintaining satisfactory resolution. Typically, the diameter of aperture 22 will range from about 500 Angstroms (50 nm) to about 1 mm.

Extension of Metal Tip through and Beyond Aperture

As shown in both Figures 1 and 2, sharpened metal probe tip 20 extends through and beyond cylindrical aperture 22 in endwall 16 of resonator 10. The reason why probe tip 20 must extend beyond aperture 22 a distance comparable to the diameter of aperture 22, in accordance with the invention, is to reduce the effect of the size of the aperture on the resolution. That is, the reason probe tip 20 extends through and beyond aperture 22, instead of terminating at aperture 22, as in prior art structure, is to provide increased

spacial resolution, dependent dimensionally on the radius of probe tip 20 rather than the diameter of aperture 22. The extension of probe tip 20 beyond aperture 22 also is helpful and convenient for the scanning of the sample. The length of the portion of sharpened metal probe tip 20 which extends through and beyond aperture 22 is related to the diameter of aperture 22. This length of probe tip 20 extending through and beyond aperture 22 will range from about $\frac{1}{3}$ of the diameter of aperture 22 to about 3 times the diameter of aperture 22. The preferred ratio of extension length to aperture diameter has been found to be about 1. The extension length should be further selected to be the length that does not give rise to a large background signal (caused by radiation from the aperture which interacts with the sample) while still giving rise to a strong signal by the tip-sample interaction.

The Resonator

Still referring to the embodiment of Figures 1 and 2, cavity 10, including shielding 32 and endwall 16, is formed of metal but preferably comprises a diamagnetic material such as copper or silver, rather than a ferromagnetic material, so that a modulating magnetic field can be used in connection with cavity 10. The diameter (or diameters if the size varies) of cavity 10 will determine the Q factor of the cavity, while the length of cavity 10 will equal the wavelength (at the resonant frequency) divided by 4, i.e. cavity length = $\lambda/4$ (a quarter wavelength cavity). Usually the cavity diameter should be large enough and the diameter ratio of cavity 10 to central electrode 18 should be about 3.6 to provide an optimum Q. The Q of a microwave cavity or resonator may be defined as the quality factor of the cavity, and should be kept as high as possible. The sensitivity of the near field microscope can be improved by increasing the input microwave power and unloaded Q, denoted Q_u , of the resonator with an optimal coupling which is achieved by adjusting the coupling strength so that the loaded Q, denoted Q_b , is $2/3$ of Q_u .

The resonator cavity volume is filled with a dielectric material, preferably one having low loss. The resonant wavelength is directly proportional to the square root of relative dielectric constant that fills the cavity, that is, $\lambda = \epsilon^{1/2}/\lambda_0$. The relative dielectric constant is proportional to the dielectric constant of a vacuum. Thus using a dielectric having a large ϵ , decreases the resonant frequency of the cavity or decreases the size of

cavity needed for a give resonant range. Sample dielectric materials that can be advantageously used to fill the resonator cavity include air, Strontium Titanate (SrTiO_3), and sapphire (Al_2O_3).

5 The resonator height is in integral multiples of $\lambda/4$, that is $n \lambda/4$ where n is an integer. If the resonator is an open resonator n is an even integer, if the resonator is closed n is an odd integer.

Use of a coaxial cable instead of a resonator

10 The resonator can be replaced with a standard coaxial cable. Figure 16 shows an embodiment of the inventive probe tip using a conventional coaxial cable in place of a resonator. An electromagnetic energy source 40 delivers electromagnetic energy to the cable. The coaxial cable has an outer electric shielding element 52 that surrounds an insulator element 44 and a central conducting element 48. The central conducting element extends beyond the end of the coaxial cable and is either sharpened into a tip or a fine sharp tip is attached to it 20. At the end of the coaxial portion of the cable, a thin metal endwall 46 is attached to the insulator that is interposed between the shielding 52 and the center conductor 48. The endwall thickness is guided by the same consideration as for the conductive endwall 16 at the end of the resonator. The endwall 46, located at the end of the coaxial cable, has an orifice of sufficient size to allow the center cable 48 to pass through it without electrically shorting the center probe to the endwall.

20 The inventive probe comprising a coaxial cable, additionally has a directional coupler 42 located between the endwall 46 and the source 40. The directional coupler 42 couples the source electromagnetic wave to the cable. The electromagnetic wave propagates down the cable to the end and is reflected back by the end wall. Interaction between the probe tip 60 and the sample being scanned modifies the properties of the reflected wave. The reflected wave is coupled to a detector by directional coupler 42 and the amplitude and phase of the reflected wave are measured by the detector. Quantitative values of the physical properties of the sample, such as complex conductivity, dielectric constant, tangent loss, conductivity, and other electrical parameters are determined using equations programed into the SEMM.

25

Quantitative Measurement of the Complex Electrical Impedance of a Dielectric or Ferromagnetic

Using the inventive SEMM with a shielded probe tip with resonator that minimizes or eliminates far-field wave components, dielectric materials have been imaged having a spatial resolution of 100 nm and sensitivity of 1×10^{-3} . Furthermore, using a computation of an analytic expression of the field distribution around the probe tip, a quantitative measurement was taken of the complex electrical impedance dielectric material. Thus a map of electrical impedance values was constructed that matched resolution and sensitivity of the image, and wherein the measured complex electrical impedance values were correlated to features visualized on the image.

Referring again to Figure 2, in one embodiment, the coaxial resonator has a height of $\lambda/4$. A sapphire disk 21 with a center hole only slightly larger than that of the tip wire was located in the end plate. The tip diameter was between about 50 μm and about 100 μm . A metal layer of about 1 μm was coated on the outside surface of the sapphire disk to shield the tip from far-field propagating components. The metal coating thickness is determined by the skin-depth to avoid the formation of a micro-transmission line, which would have heavy loss near the aperture. In one embodiment, the sapphire disk serves to minimize vibration and is bonded to the probe tip using insulating glue. In addition, insulating glue having low energy loss may be used to fix the tip wire with respect to the endwall shielding so that the tip does not vibrate against the shielding.

In a different embodiment, the entire resonant cavity is filled with a dielectric material such as SrTiO_3 . In that case the height of the resonant cavity is greatly reduced as the resonant wavelength is inversely proportional to the square root of the relative dielectric constant of the material that fills the cavity. Considering that $\lambda = (c/f) \epsilon^{-1/2}$, for $f = 1 \text{ GHz}$ and $\epsilon = 300$, for SrTiO_3 , λ is about 1.73 cm and $\lambda/4$, the height of the resonator, is only about 0.43 cm. The resonant diameter may shrink significantly also.

As explained in copending application serial number 08/717,321, an image is obtained by placing the tip of the resonator in direct physical contact with the sample to be imaged, and scanning the tip across the surface of the sample. The resonator is driven at a frequency that is slightly higher or lower than the resonant frequency of the resonator.

The change in the resonant frequency is then measure by recording the output power at the input frequency (measured as the detector output voltage). As the tip scans the sample, the resonant frequency of the resonator is reduced as a function of the relative conductivity of different regions of the sample. Thus, for example very fine niobium wires coated on, say, silicon dioxide, can be successfully imaged to a spatial resolution of about 5 μm (about $\lambda/100,000$).

In the present invention, in addition to detecting relative differences in conductivity of the surface of the sample, a quantitative measurement is obtained of the complex electrical impedance. This is possible because the resonant frequency, f_r , and the quality factor, Q , shifts as functions of the dielectric constant and loss tangent of any material, such as the sample material, located near the probe tip. In the past this functional relationship was not well enough known, however, to obtain quantitative information about the dielectric constant, loss tangent, or complex electrical impedance, from a measured shifts in f_r or Q .

The present invention comprises a scanning evanescent wave resonant-probe microscope having a computing element capable of correctly relating a series of measured shifts in f_r and Q to the complex electrical impedance, (e.g. dielectric constant, loss tangent, or conductivity) at a series of locations on the sample surface. The computing element is programmed to calculate values of ϵ and tangent losses ($\tan \delta$) at a series of different frequencies.

The calculations are made from a mathematical model that is thoroughly described in a paper entitled, "Quantitative Microwave Near-Field Microscopy of Dielectric Properties", submitted by the inventors to Review of Scientific Instruments, accepted for publication, and incorporated herein by reference.

Using the inventive microscope, the probe tip is placed either in direct soft contact with the sample, or a small gap is preserved between the probe tip and the sample. There are several steps to making measurements of a dielectric sample, described in detail below. In summary, one method of measuring a dielectric constant and loss tangent of a sample comprises,

a) determining a reference resonant frequency f_0 of the probe by

- i) locating the probe far enough away from the sample material that it is not influenced by the sample;
- ii) sweeping a frequency range;
- iii) plotting frequency versus power;
- 5 iv) fitting a curve to find the maximum frequency, called f_0 ;
- b) determining Q_0 by dividing f_0 by the frequency difference at two half power amplitude points;
- c) calculating the coefficient M from the equation $S = MQ_0^2$ where S is the power at f_0 ;
- 10 d) calibrating the geometric factors A , B , and R_0 , in equations 5 and 6 using a sample of known dielectric constant;
- e) placing a probe tip of a scanning evanescent electromagnetic wave microscope near or in soft contact with the sample;
- f) measuring the shift in resonant frequency caused by the proximity of the sample near the probe tip;
- 15 g) measuring the quality factor shifts caused by the proximity of the sample near the probe tip; and
- h) calculating the dielectric constant and loss tangent using a pair of equations chosen from the group comprising soft contact equations 2 and 3, probe-sample gap equations 5 and 6, or the Thin Film equations.
- 20

Alternatively, the frequency versus power curve in the procedure above can be determined using a Lorentz line type fit to obtain f_0 and Q_0 .

Soft Contact Measurements of Dielectrics

- 25 When using evanescent waves and a tip radius that is much smaller than the probe wavelength, the electromagnetic wave can be treated as quasi-static, that is, the wave nature of the field can be ignored. In addition, the sample material in the vicinity of the small probe tip is reasonably considered as homogeneous and isotropic in its dielectric properties.

Thus $\epsilon = \epsilon' + j\epsilon''$ and ϵ is $\gg \epsilon_0$, and $\epsilon' \gg \epsilon''$, where ϵ is the complex dielectric constant, ϵ' is the real component of the dielectric constant, ϵ'' is imaginary component of the dielectric constant, and ϵ_0 is the dielectric constant of free space.

Furthermore, $\mu = \mu' + j\mu''$ and $\mu \sim \mu_0$; where μ is the complex magnetic permeability of the sample; μ' is the real component of the magnetic permeability, and μ'' is the imaginary component of the magnetic permeability, and μ_0 is the magnetic permeability of free space.

Figure 3 shows a diagram of the measurement geometry. The probe tip 20 is in soft contact with the surface of a dielectric material 80 having a thickness much larger than the tip radius. For example, the sample thickness may be more than 2 times as thick as the tip radius. More preferably it is 5 times as thick. To the first order, the probe tip is represented as a charged conducting sphere under the same potential as the end point or tip of the center conductor in the endwall of the resonator, since the tip only extends out a length several orders of magnitude smaller than the wavelength beyond the cavity. The dielectric sample under the tip is polarized by the electric field of the tip and thus acts electrically on the tip causing a redistribution of charges on the tip to maintain the equipotential surface of the conducting sphere. The action on the tip is represented by an image charge q_1' located in the sample; the redistribution of charge in the probe tip is represented by another image charge q_2 inside the spherically modeled tip end. This action and redistribution repeats itself, that is it is iterative until equilibrium is attained. Three series of image point charges are formed that meet the boundary conditions at both tip and dielectric sample surfaces as shown in Figure 3. The peak value of the field distribution inside the sample can be expressed as a superposition of contributions from the series of point charges q_n'' , the effective value of q_n in the sample. The expression for the field distribution is,

$$\vec{E}_1 = \frac{q}{2\pi(\epsilon + \epsilon_0)} \sum_{n=1}^{\infty} \frac{1}{n} b^{n-1} \frac{r\vec{e}_r + (z + R_0/n)\vec{e}_z}{[r^2 + (z + R_0/n)^2]^{3/2}} \quad (1)$$

where $b = (\epsilon - \epsilon_0)/(\epsilon + \epsilon_0)$, $q = 4\pi \epsilon_0 R_0 V_0$; R_0 is the radius of the tip, and \vec{e}_r and \vec{e}_z are the unit vectors along the directions of the cylindrical coordinates r and z , respectively. This field distribution satisfies Coulomb's law and the boundary conditions on the surfaces of

both the dielectric sample and the conducting sphere terminus of the probe tip. In this model the majority of the electromagnetic energy is concentrated in the cavity and the field distribution inside the cavity is not disturbed by any tip-sample interaction. Therefore, perturbation theory for electromagnetic resonators, where the frequency is perturbed slightly to find the resonant frequency or the amplitude of the energy deposited in the cavity is perturbed, can be used to calculate the f_r and Q shifts that would result from a particular dielectric material, as noted in equations (2) and (3).

$$\frac{\Delta f_r}{f_r} = - \frac{\int_v (\Delta \epsilon \vec{E}_1 \cdot \vec{E}_0 + \Delta \mu \vec{H}_1 \cdot \vec{H}_0) dv}{\int_v (\epsilon_0 E_0^2 + \mu_0 H_0^2) dv} = A \left[\frac{\ln(1-b)}{b} + 1 \right] \quad (2)$$

$$\Delta \left(\frac{1}{Q} \right)_d = \frac{\int_v (\Delta \epsilon'' \vec{E}_1 \cdot \vec{E}_0 + \Delta \mu'' \vec{H}_1 \cdot \vec{H}_0) dv}{\int_v (\epsilon_0 E_0^2 + \mu_0 H_0^2) dv} = - \frac{\Delta f_r}{f_r} \tan \delta \quad (3)$$

where E_0 , H_0 , and E_1 , H_1 , refer to the electric and magnetic field before and after the perturbation, respectively, λ is the wavelength, $A = 4\pi \epsilon_0 R_0 (V_0^2 / E_{\text{total}})$ is a constant determined by the geometry of the tip-resonator assembly ($A \sim 16 R_0 \ln(R_2/R_1)/\lambda$ for an ideal $\lambda/4$ coaxial resonator), and $\tan \delta = \epsilon''/\epsilon'$. V_0 is the voltage on the probe tip.

Considering first the shift in resonant frequency, Equation (2) shows that the shift in resonant frequency is proportional to the radius R_0 of the probe tip. This is because the electric field near a conducting sphere, which is how the probe tip is modeled, at a given voltage is inversely proportional to the sphere radius and the total contribution to the signal is the integration of the square of the electrical field magnitude divided by the volume of the sample.

Considering now the shift in quality factor Q, the extra current required to support a charge redistribution on the spherical probe tip end when it is brought near a dielectric induces resistivity loss. This results in a shift in Q that is expressed as,

$$\Delta \left(\frac{1}{Q} \right)_c = -B \frac{\Delta f_r}{f_r} \quad \text{and the total Q shift is} \quad (4)$$

$$\Delta\left(\frac{1}{Q}\right)_i = -(B + \tan \delta) \frac{\Delta f_r}{f_r}$$

The $\tan \delta$ is referred to as the loss tangent.

Using equations 2, 3, and 4, quantitative measurements of the local complex dielectric constant for samples having a thickness much greater than the probe tip radius can be made. The sample thickness may be at least about two times as thick as the probe tip radius. Preferably the sample thickness is at least five times as thick as the probe tip radius. Even more preferably the sample thickness is at least 10 times greater than the probe tip radius. The constants A and B are found by calibration against a standard sample such as sapphire that has a known dielectric constant and loss tangent. Table I lists relative dielectric constants ϵ_r and loss tangents for a number of materials measured using the inventive SEMM. The relative dielectric constants are relative to measurements taken in a vacuum or air. The measurements were calibrated against a sapphire single crystal ($\epsilon_r = 11.6$ and $\tan \delta = 2 \times 10^{-5} \sim 0$ at 10 GHz). These values for sapphire and the reported values on the table were obtained from T. Konaka, et al., J. Supercond. 4:283(1991). The measured values agree extremely well with the literature values, which differ functionally in that they are measured as averages over large volumes).

Table I. Measured Dielectric Constants and Tangent Losses for Single Crystals

Material	Measured ϵ_r	Reported ϵ_r	Measured $tg\delta$	Reported $tg\delta$
YSZ	30.0	29	1.7×10^{-3}	1.75×10^{-3}
LaGaO ₃	23.2	25	1.5×10^{-3}	1.80×10^{-3}
CaNdAlO ₄	18.2	19.5	1.5×10^{-3}	$0.4 - 2.5 \times 10^{-3}$
TiO ₂	86.8	85	3.9×10^{-3}	4×10^{-3}
BaTiO ₃	295	300	0.47	0.47
YAlO ₃	16.8	16	-	8.2
SrLaAlO ₄	18.9	20		
LaAlO ₃	25.7	24		2.1×10^{-5}
MgO	9.5	9.8		1.6×10^{-5}

LiNbO ₃ (X-cut)	32.0	30		
----------------------------	------	----	--	--

Air-Gap Measurements of Dielectrics

It is sometimes preferable not to have the probe tip in direct contact with the sample. In this case, iterative relationships are derived for the image charges as shown in Figure 4.

$$a'_n = 1 + a' - \frac{1}{1 + a' + a'_{n-1}}$$

$$q_n = t_n q$$

$$t_n = \frac{b}{1 + a' + a'_{n-1}} t_{n-1}$$

where $a' = g/R_0$ and g is the gap distance between the sample and the probe tip.

The initial conditions of the iterations are $a'_1 = 1 + a' = 1 + g/R_0$ and $t_1 = 1$. Using a perturbation method similar to the one described above,

(5)

$$\frac{\Delta f_r}{f_r} = -A \sum_{n=1}^{\infty} \frac{b t_n}{a'_1 + a'_n}$$

$$\Delta \left(\frac{1}{Q} \right)_i = -(B + \tan \delta) \frac{\Delta f_r}{f_r}$$

(6)

Figure 5 shows the measured resonant frequency f_r as a function of the gap distance for a Magnesium Oxide (MgO) single crystal (data points are shown as triangles). The best fitted curve using modeling equation 5 is also shown. For MgO, $\epsilon_r = 9.5$, $R_0 = 12.7 \mu\text{m}$, and $A = 1.71 \times 10^{-3}$. The excellent agreement between the measurement and the mathematical model used in the present inventive microscope indicates that the quasi-static and spherical tip approximations support accurate measurements.

It is important to estimate the effect of the air gap relative to measurements made using the soft contact measurement. For the soft contact measurement a' , which equals g/R_0 , approaches zero. For the air gap measurements,

$$a'_n \sim \frac{1}{n} + \frac{2n^2 + 1}{3n} a'$$

and

$$t_n = \frac{b^{n-1}}{n} \left(1 - \frac{n^2}{3} a\right)$$

then,

$$\frac{\Delta f_r}{f_r} \rightarrow -A \sum_{n=1}^{\infty} \frac{b^n}{n+1} \left[1 - \frac{(n+1)^2}{3} a'\right] \approx \left(\frac{\Delta f_r}{f_r}\right)_0 + A a' \frac{b(2-b)}{3(1-b)^2} \quad (7)$$

where $(\Delta f_r/f_r)_0$ refers to the frequency shift when the tip comes in soft contact with the samples which can be evaluated from Equation 2. Equation 7, shows that even if the tip to sample distance is maintained within 1 nm (for example $a' \sim 10^{-2}$ for an 100 nm probe tip radius), the effect of such an air gap can not be neglected because the second term of Equation 6 has a relatively small denominator $(1-b \sim 2\epsilon_0/\epsilon)$. For an $\epsilon_r=10$ the difference is about 10% and increases rapidly to 50% for $\epsilon_r=35$.

Thin Film Measurements

One application of the inventive SEMM is measuring the dielectric constant of thin films. In this respect it is important to understand that many films traditionally considered thin films would interact with the inventive probe as a bulk sample because of the extreme sharpness with which the probe tip can be made. The penetration depth of the field is calculated using Equation 1 to be about the same as the radius of the probe tip, R_0 .

In the case that the film thickness is on the order of R_0 or smaller, the image charge model discussed above is not useful because of divergence of the image charges, as illustrated in Figure 6. Typically, numerical methods such as finite element analysis are necessary for such thin films. However, modeling the contribution of the substrate to the

reaction on the tip, provides a good approximation using the image charge approach. Clearly the contribution from the substrate decreases as the film thickness and dielectric constant increases. This contribution was modeled by replacing the effect of reaction from the complicated image charges with an 'effective charge' using the following equations:

$$b_{eff} = b_{20} + (b_{10} - b_{20}) \exp\left[-0.18 \frac{a}{(1 - b_{20})}\right]$$

- 5 where $b_{20} = (\epsilon_2 - \epsilon_0)/(\epsilon_2 + \epsilon_0)$, $b_{10} = (\epsilon_1 - \epsilon_0)/(\epsilon_1 + \epsilon_0)$, and ϵ_2 and ϵ_1 are the dielectric constants of the film and substrate, respectively; $a = d/R_0$ and d is the thickness of the film. In choosing this formalism both infinitely thin and infinitely thick film limitations are accounted for. The constant, 0.18, was determined through a series of calibrations and its value can be further refined. The present invention is not limited to this particular value
- 10 in the equation. Using a similar process as described above yields:

$$\begin{aligned} \frac{\Delta f_r}{f_r} &= -A \sum_{n=1}^{\infty} \sum_{m=0}^{\infty} b_{eff}^{n-1} b_{20}^m b_{21}^m \left[\frac{b_{20}}{n+1+2mna} - \frac{b_{21}}{n+1+2(m+1)na} \right] \\ \Delta\left(\frac{1}{Q}\right)_i &= A \left\{ \tan \delta_2 \sum_{n=1}^{\infty} \sum_{m=0}^{\infty} b_{eff}^{n-1} b_{20}^m b_{21}^m \left[\frac{1}{n+1+2mna} - \frac{1}{n+1+2(m+1)na} \right] + \right. \\ &\quad \left. \frac{2\epsilon_2\epsilon_1 \tan \delta_1}{(\epsilon_2 + \epsilon_1)(\epsilon_2 + \epsilon_0)} \sum_{n=1}^{\infty} \sum_{m=0}^{\infty} \frac{b_{eff}^{n-1} b_{20}^m b_{21}^m}{n+1+2(m+1)na} \right\} - B \left(\frac{\Delta f_r}{f} \right) \end{aligned}$$

where $b_{21} = (\epsilon_2 - \epsilon_1)/(\epsilon_2 + \epsilon_1)$, $\tan \delta_2$ and $\tan \delta_1$ are the tangent losses of the film and substrate.

The above two equations can be referred to as the Thin Film Equations.

Table II shows the results of measuring dielectric constants for thin films using the inventive SEMM and a conventional inter-digital contact electrode at 1 GHZ.

Table II. Measured dielectric constants and tangent losses of various thin films By SEMM and interdigital electrode technique, both measured at 1 GHZ.

Films	SEMM measurement		Interdigital electrodes	
	ϵ_p	$\tan \delta$	ϵ_p	$\tan \delta$
SrTiO ₃	292	0.01	297	0.01
Ba _{0.8} Sr _{0.2} TiO ₃	888	0.19	868	0.10
Ba _{0.6} Sr _{0.4} TiO ₃	707	0.14	727	0.07

Intrinsic Spatial Resolution

Intrinsic spatial resolution is an important figure of merit for microscopes. The intrinsic resolution of the inventive microscope was estimated using equation 2 to calculate numerically the contribution to $(\Delta f/f_r)$ from small vertical columns as a function of lateral location (r) relative to the center of the tip for materials of different dielectric constants. The contribution was shown to decrease quickly as r increase, especially when ϵ was large. The radius where the contribution from the volume inside the radius r reached 50% of the total contribution was defined as the intrinsic spatial resolution. In that case, the estimated resolution was about two orders of magnitude smaller than the tip radius at the moderate ϵ_r (~50) and decreased slightly as ϵ_r increased. This is illustrated in Figure 7. This behavior can be understood by considering that the effective probing charge on the probe tip is attracted downwards to the sample by the polarized dielectric sample. the higher the dielectric constant is, the shorter the effective distance is between the charge and sample. As a result, the field distribution inside the sample is concentrated

in a very small region just below the tip apex with the polarization perpendicular to the sample surface, and f_i and Q shifts are dominated by the contribution from this small region. Experiments on dielectric materials having moderate dielectric constants have shown that 100 nm resolution can be achieved with a tip radius of several microns. The figure of merit of a near-field microscope is the ratio of the wavelength inside the sample and the spatial resolution. For the present embodiment a figure of merit of about 4×10^5 was calculated as follows and verified by measurement..

$$\lambda_0 = c/f = 30 \text{ cm.}$$

$$\lambda = \lambda_0 \epsilon^{-1/2} = \lambda_0 / 50^{1/2} = 30\text{cm}/7.1 = 4.2 \text{ cm}$$

The spatial resolution was 100 nm so the Figure of Merit is,

$$\lambda/100\text{nm} = 4.2 \text{ cm} / 10^{-5} \text{ cm} = 4.2 \times 10^5.$$

Because the electromagnetic wavelength in metals is several (at least four) orders of magnitude smaller than that in free space, samples of electrically conducting materials are not suitable for this resolution analysis.

Sensitivity Analysis

The resonant system can be analyzed using an equivalent lumped series resonant circuit as shown in Fig.2 with effective capacitance C , inductance L and resistance R (for an ideal quarter-wave resonator):

$$C = \frac{2\pi\epsilon_0}{\ln(R_2/R_1)} l$$

$$L = \frac{\mu_0}{2\pi} l \ln(R_2/R_1)$$

$$R = \frac{2R_s}{\pi^3} \left(\frac{1}{R_2} + \frac{1}{R_1} \right) l$$

where $l \approx \lambda/4$ is the effective cavity length, R_s is the surface resistance of cavity material, R_2 and R_1 are the radii of center and outer conductors, respectively; ϵ_0 and μ_0 are the permittivity and permeability of free space, respectively. The uncoupled (Q_u) and coupled (Q_c) quality factors of the resonant system are given by:

$$Q_u = \frac{1}{\omega_r C R}$$

$$Q_c = \frac{1}{\omega_r C} \frac{1}{R + R_0/p^2}$$

- 5 where R_0 is the internal resistance of the source, $\omega_r = 2\pi f_r = 1/\sqrt{LC}$ and f_r is the resonant frequency, and $p \propto (h/l) \cdot \cos \theta$ is the coupling factor (h is the equivalent coupling length and θ is the angle between the coupling loops and the radius direction). The power delivered by the source, P_0 , the power delivered into the cavity, P , and energy stored in the cavity, E , are expressed as:

$$P_0 = \frac{1}{2} \left(\frac{V}{p} \right)^2 \frac{1}{R + R_0/p^2}$$

$$P = \frac{1}{2} \left(\frac{V}{p} \right)^2 \frac{R}{(R + R_0/p^2)^2}$$

$$E = \frac{P_0 Q_c}{\omega_r} = \frac{P Q_u}{\omega_r} = \frac{1}{2} \left(\frac{V}{p} \right)^2 C Q_c^2 = \frac{1}{4} C V_0^2 = \frac{\pi \epsilon_0 \lambda}{8 \ln(R_2/R_1)} V_0^2$$

- 10 where V_0 is the open end peak voltage. As the signal S detected by the diode detector is proportional to the square of the voltage in coupling loop, we have:

$$S = M Q_c^2 \quad (7A)$$

at the resonant frequency, where M is a constant that is determined by measuring Q from the frequency response of a known material.

At the same time, the output signal of the phase detector can be expressed as:

$$V \propto \frac{1}{\sqrt{2}} V_0 z + V_n$$

- 5 where $z = 2Q_c(\omega_0 - \omega_p)/\omega_r$, ω_0 is the circular frequency of the source, V_n is the noise voltage. Then, the output power caused by $\delta\omega = (\omega_0 - \omega_p)$ is:

$$P \propto P_s + P_n = 4PQ_c^2 \left(\frac{\delta\omega}{\omega_r}\right)^2 + P_n$$

To estimate the Johnson noise limited sensitivity, let us consider a matched lossy network at physical temperature T as shown in Fig.3. The energy flow to left and right of the reference plane are equal in thermal equilibrium:

$$k_B TB / N + P_n = k_B TB$$

- 10 where $N = Q_u/(Q_u - Q_c)$ is the insertion loss, k_B is Boltzmann's constant, and B is the bandwidth of the data acquisition. Finally, the noise power is:

$$P_n = k_B TB \frac{Q_c}{Q_u}$$

The Johnson noise limited sensitivity is then determined by $P_s = P_n$:

$$\frac{\delta\epsilon}{\epsilon} = \frac{1}{A} \sqrt{\frac{k_B TB}{4PQ_c Q_u}}$$

As PQ_c takes its maximum value a $Q_c = \frac{2}{3}Q$ (the best working condition which can be achieved by adjusting the angle of coupling loop θ), the minimum detectable $(\delta\epsilon/\epsilon)$ is estimated to be:

$$\left(\frac{\delta\epsilon}{\epsilon}\right)_{\min} = \frac{1}{8\pi R_0 V_0 f_r} \sqrt{\frac{3k_B T B c}{2\epsilon_0 Q_u \ln(R_2/R_1)}}$$

where c is the speed of light in free space. Suppose the vacuum breakdown voltage between the shielding coating and tip wire is $V_0 = 10$ V (for a gap of 10 mm between the tip wire and shielding coating), the estimated sensitivity is about 1×10^{-5} for $R_0 = 1$ μ m, $f_r = 1$ GHz, $T = 300$ K, $B = 100$ kHz, $Q_u = 1700$, and $R_2/R_1 = 5$. To obtain such sensitivity, a microwave source with frequency stability of $df/f = 1 \times 10^{-8}$ is required. Sensitivity is limited to 1×10^{-3} by the stability of the analog voltage controlled oscillator (VCO) (10^{-6}) used in the system. The equation above shows that the sensitivity increases linearly with tip radius, R_0 . As the resolution decreases linearly with tip radius shown in the above text, the conflict between resolution and sensitivity has reached the best possible compromise from physical point of view.

Quantitative Measurement of the Conductivity of an Electrically Conducting Sample

The classical skin-depth concept of conducting materials (still often used in evanescent wave microscopy) can be shown as no longer valid in describing the interaction between evanescent electromagnetic waves and conducting materials. The classical skin-depth concept is derived from the interaction between a conducting surface and propagating plane waves whose k vector components (k_x , k_z) must be smaller than k_0 .

As $k_c \gg k_0$, there is little difference between refracted waves inside the conducting materials for different k_z and the overall physical parameters can be calculated with a single valued $k_r = k_0$. On the other hand, the value of the k vector components (k_r , k_z) for the evanescent plane waves involved in interaction between the evanescent wave and the sample are multi-valued and can be much higher than k_0 . The overall physical parameter has to be calculated for each different k vector component value and integrated. We present here a calculation of detailed field configuration and evanescent electromagnetic wave interaction with conducting materials. It should enable a wide range of scientific applications in quantitative evanescent electromagnetic waves microscopy. In principal the results are applicable to evanescent wave microscopy of frequencies up to the far infrared, as long as the wavelength is much larger than the dimension of the interaction region. In addition, since the electric field configuration considered here is identical to the electrostatic field configuration in various scanning probe microscopes, it should also enable a wide range of quantitative microscopy using scanning probe microscopes. i)

15

The inventive SEMM is based on a high quality factor (Q) microwave coaxial resonator with a sharpened metal tip mounted on the center conductor. The tip extends beyond an aperture formed on a thin metal shielding end-wall of the resonator. The tip and the shielding structure are designed so that the propagating far-field components are shielded within the cavity whereas the non-propagating evanescent waves are generated at the tip. This feature is crucial for both high resolution and quantitative analysis. Because it is not mathematically feasible to model the interactions of both evanescent and

20

propagating waves, (where the latter are leaked from the resonator), quantitative microscopy would not be possible without the inventive microscope configuration. In contrast to conventional antenna probes (a far-field concept), the inventive probe does not emit significant energy (and therefore provides a very high Q to boost the sensitivity).

5 Only when the tip is close to the sample will the evanescent waves on the tip interact with the material. The interaction gives rise to a frequency and Q change of the cavity and consequently the microscopy of the electrical impedance.

In brief, measurements of the conductivity of electrically conducting samples comprises the following steps

- 10 a) determining a reference resonant frequency f_0 of the probe by
- i) locating the probe far enough away from the sample material that it is not influenced by the sample;
 - ii) sweeping a frequency range;
 - iii) plotting frequency versus power;
 - 15 iv) fitting a curve to find the maximum frequency, called f_0 ;
- b) determining Q_0 by dividing f_0 by a the frequency difference at two half power amplitude points;
- c) calculating the coefficient M from the equation $S = MQ_0^2$ where S is the power at f_0 ;
- 20 d) placing a probe tip of a scanning evanescent electromagnetic wave microscope near the sample;

- e) calibrating the geometric factors A, B, and R_0 , in equations 12 and 19 by measuring and fitting the frequency and quality factors as a function of a gap distance, g, between the probe tip and a reference sample of known conductivity;
- f) measuring the shift in resonant frequency caused by the proximity of the sample near the probe tip;
- g) calculating g from equation 12;
- h) measuring the shift in quality factor caused by the proximity of the sample near the probe tip; and
- i) calculating the conductivity using equation 19.

When a conducting material is placed in the vicinity of the tip (modeled as a sphere), it will interact with the tip causing charge and field redistribution. The first order field redistribution can be obtained by treating the material as an ideal conductor with infinite conductivity. Under the quasi-static approximation (the wavelength is much larger than the effective region of field distribution), the surface of the conducting material is a charge mirror and the tip-sample interaction can be represented as a multiple image charge process as shown in Fig. 8. The electric field in the tip-sample region can be calculated as the superposition of contributions from all the charges:

$$\vec{E} = \frac{1}{4\pi\epsilon_0} \sum_{n=1}^{\infty} q_n \left\{ \frac{r\vec{e}_r + (z + a_n R_0)\vec{e}_z}{[r^2 + (z + a_n R_0)^2]^{3/2}} - \frac{r\vec{e}_r + (z - a_n R_0)\vec{e}_z}{[r^2 + (z - a_n R_0)^2]^{3/2}} \right\} \quad (8)$$

and the electromagnetic fields on the surface of the conducting material are:

$$\vec{E}_z(r) = \frac{R_0}{2\pi\epsilon_0} \sum_{n=1}^{\infty} \frac{a_n q_n}{[r^2 + (a_n R_0)^2]^{3/2}} \begin{pmatrix} - \\ e_z \end{pmatrix} \quad (9)$$

$$\vec{H}_\phi(r) = \frac{3R_0}{2\pi\epsilon_0\mu_0} \sum_{n=1}^{\infty} \frac{a_n q_n}{[r^2 + (a_n R_0)^2]^{5/2}} \begin{pmatrix} - \\ e_\phi \end{pmatrix} \quad (10)$$

where ϵ_0 and μ_0 are the permittivity and permeability of free space, R_0 is the tip

radius, \vec{e}_r and \vec{e}_z are the unit vectors along the directions of the cylindrical coordinates

5 r and z , $a_n R_0$ and q_n are the position and charge of the n th image inside the tip, respectively.

a_n and q_n have the following iterative relations:

$$\begin{cases} a_n = 1 + a_0 - \frac{1}{1 + a_0 + a_{n-1}} \\ q_n = \frac{q_{n-1}}{1 + a_0 + a_{n-1}} \end{cases} \quad (11)$$

with initial conditions: $a_1 = 1 + a_0$ and $q_1 = 4\pi\epsilon_0 R_0 V_0$, where $a_0 = h / R_0$, h is the tip-

sample distance and V_0 is the tip voltage. As equation 8 satisfies the Coulomb's law and

10 the boundary conditions on both the surfaces of the tip and the conducting material, it is the correct and sole solution of this problem. Although we are dealing with electromagnetic waves here (\vec{E} and \vec{H}) fields are related through the Maxwell equation), the electric field configuration solved here is identical to the electrostatic field configuration in various SPMs.

The typical \tilde{H} field intensity profile obtained from equation 10 (Fig. 9) forms the shape of a volcano. The radial distributions for different tip-sample distances are depicted in Fig.10. The figure indicates that the size of caister (a measure of spatial resolution of the microscope) decreases and the intensity of the field increases with decreasing tip-sample distance, respectively.

We analyze the system through an equivalent series RLC circuit of the resonator. The tip is represented as a small capacitor, C' , whose capacitance depends on the tip-sample interaction, parallel to the main capacitor of the resonant circuit. The relative resonant frequency shift is then proportional to the variation of C' . This variation can also be represented by the variation of the total charge on the tip, i.e. the sum of all sample-induced (image) charges:

$$\frac{\Delta f}{f} = -A \left\{ \sum_{n=1}^{\infty} q_n - q_1 \right\} = -A \sum_{n=2}^{\infty} q_n$$

(12)

This result is universal for all conducting materials (independent of conductivity) if the good metal condition is satisfied, i.e. $\sigma \gg \omega \epsilon$, where σ , ϵ are the conductivity, dielectric constant of the conducting material respectively, and ω is the circular frequency of the microwave (e.g., $\sigma / \omega \epsilon$ of Cu at 1 GHZ is on the order of 10^9). Fig.11 shows the measured f as a function of tip-sample distance for Cu and the best fit to equation

12. The fitting determines $A = 2.82 \times 10^{-3}$ and $R_0 \approx 8 \mu m$ (consistent with observation).

To calculate the energy dissipated inside the conducting materials, the second order approximation and subsequently the refraction of evanescent electromagnetic wave on the surface of conducting materials and the decay behavior inside the materials must be considered. In the following paragraphs, we will first discuss the refraction of evanescent electromagnetic waves on the surface of conducting materials. Then, the wave decay and dissipation inside the conducting materials are computed to derive the conductivity quantitatively from the SEMM signals.

The wave equations for electromagnetic waves in air and in conducting materials have the form of:

$$\begin{cases} \nabla^2 u + k_0^2 u = 0 & z < 0 \quad (\text{in air}) \\ \nabla^2 u + k_c^2 u = 0 & z \geq 0 \quad (\text{in conducting material}) \end{cases}$$

(13)

where u is any component of the electromagnetic wave, k_0 and k_c are (complex)

eigen-wave vectors for air and conducting material, respectively. $k_c^2 = \omega^2 \epsilon \mu (1 + i \sigma / \omega \epsilon)$

and $k_0^2 = \omega^2 \epsilon_0 \mu_0$, where μ is the permeability of the conducting material. $|k_c^2| \gg k_0^2$

even for lightly doped semiconductors (e.g. Si with dopant level of 10^{15} and resistivity of $3 \Omega\text{cm}$) in the microwave frequency range of $<10 \text{ GHz}$ ($|k_c^2 / k_0^2| \geq 60$).

From the boundary condition, when a wave is incident on the surface of conducting material from air (either propagating or evanescent), the lateral component of the wave vector crosses the interface continuously, i.e. $\vec{k}_0 \times \vec{n} = \vec{k}_c \times \vec{n}$, where \vec{n} is the unit vector perpendicular to the interface, \vec{k}_c represents the refracted wave vector of \vec{k}_0 . When the incident wave is a propagating wave, the perpendicular component of its wave vector in air, k_{0z} ($= k_0 \cos \theta$, where θ is the incident angle), is real, and the lateral component, k_{0r} ($= \sqrt{k_0^2 - k_{0z}^2} = k_0 \sin \theta$) is limited to be less than k_0 . Therefore, the refracted wave vector inside the conducting material of a propagating wave is always nearly perpendicular to the surfaces, i.e. $k_{cz} = \sqrt{k_c^2 - k_{0r}^2} \cong k_c$ because k_{0r} is negligible compared to $|k_c|$.

Consequently, the decay length is independent of the incident angle. From this point of view, it is usually stated that the conducting material has a unique surface impedance (or surface resistance) at a certain frequency independent of the incident angle (i.e. the lateral component of the wave vector) of the incident electromagnetic wave in the microwave region. It is based on this fact that the conventional skin-depth concept is derived.

However, the situation is completely different for evanescent waves. In this situation, the corresponding k_{0r} can be any value, comparable or even larger than $|k_c|$, and is no longer negligible. As a result, the decay length (determined by the imaginary part of k_{cr}) depends on k_{0r} and must be calculated for each k_{0r} value. The classical skin-depth concept fails here. Any theory on evanescent wave microscopy of conducting materials that does not specifically consider this fact is flawed.

To further elaborate the above analysis, we expand the surface field $\tilde{H}_s(r)$ into different lateral components using the concept of the spatial frequency as in Fourier optics:

$$\tilde{H}_s(k_{0r}) = \frac{1}{2} \int \tilde{H}_s(\tilde{r}) \exp(i\tilde{k}_{0r} \cdot \tilde{r}) d\tilde{s}$$

(14)

The calculated spatial frequency spectra for different ratios of tip-sample distances to tip radius (a_0) are shown in Fig.12. It is clear that a cut-off spatial frequency exists for certain R_0 and a_0 . It is also clear from the figure that the smaller the tip-sample distance (i.e. smaller the a_0/R_0) is, the more intense the high spatial frequency components are. Also found in Fig.12 is that the increase of the intensity with respect to the decrease of a_0 is very rapid in the high k_{0r} range and quite slow in the low k_{0r} range of the spectra. In other

words, the field intensity increase associated with the decrease of the tip-sample distance is mainly concentrated in the high spatial frequency region.

The corresponding perpendicular wave vector component inside the conducting material k_{cz} can be obtained:

$$5 \quad k_{cz} = \sqrt{k_c^2 - k_{0r}^2} = \sqrt{\frac{2i}{\delta^2} - k_{0r}^2} = k_{cz}^r + ik_{cz}^i$$

(15)

where k_{cz}^r and k_{cz}^i denote the real and imaginary parts of k_{cz} , $\sigma = 2\sigma/(\omega\mu\epsilon)$ is the classical skin-depth for metals and semiconductors, or penetration depth for superconductors. The corresponding electromagnetic field inside the conducting material

10 has the form of:

$$\vec{H}_c(k_{0r}) = \vec{H}_s(k_{0r}) \exp[i(k_{cz}^r z + k_{0r} r) - k_{cz}^i z]$$

(16)

$$\vec{E}_c(k_{0r}) = \nabla \times \vec{H}_c(k_{0r}) / (\sigma - i\omega\epsilon)$$

(17)

15 and the total power flowing into and dissipated in the conducting material can be derived as:

$$S = \int \bar{n} \cdot \bar{S} dk_{or}^2 = \frac{1}{2} \int \text{Re} \{ \bar{n} \cdot (\bar{E}_c \times \bar{H}_c^*) \} dk_{or}^2$$

(18)

where $\bar{S} = \frac{1}{2} \text{Re} \{ \bar{E} \times \bar{H}^* \}$ is the Poynting vector. The Q shift caused by the power dissipated in the conducting material is:

$$\Delta \frac{1}{Q} = BS$$

(19)

where B is a constant which can be obtained by calibration in a fashion similar to the A in equation 12.

If $k_{or} \ll 1/\delta$, the above approach yields the same result as the classical skin-depth

approach. However, the situation changes dramatically if $k_{or} \sim 1/\delta$ or $k_{or} \gg 1/\delta$. This is clearly demonstrated in Fig. 13 and Fig. 14.

Also shown in Fig. 13 is the measured Q -distance curve and its best fit with equation 19 for Cu. The fit gives $B = 1.52 \times 10^{-7}$ and a conductivity of $6.2 \times 10^7 \text{ S/m}$

(characterized with the conventional skin-depth of $\delta \approx 2 \mu\text{m}$) which is in good agreement

with the conductivity of Cu ($5.8 \times 10^7 \text{ S/m}$). Plot together is the fit using the classical skin-depth concept. The difference is quite large in the region of small tip-sample distance.

Measurement of other Electrical Parameters using the inventive SEMM

Other electrical parameters such as capacitance and Coulomb force can be measured quantitatively using the inventive SEMM. The electric field configuration solved here is identical to the static electric field configuration in various SPMs, such as scanning capacitance microscopy. The complete expression for the capacitance between the tip and sample can be written as

$$C' = \frac{\sum_{n=1}^{\infty} q_n}{V_0}$$

for both conducting and dielectric samples. For conducting materials, we found that when the distance is less than one tenth of the tip radius, the capacitance can be expressed very well with the following equation:

$$C' = -1.26 \times 10^{-10} R_0 \log(a_0) + 1.11 \times 10^{-10} R_0 (\text{Farad})$$

The Coulomb force between tip and sample is

$$F = \frac{d(\frac{1}{2} C' V_0^2)}{dh} = -2.74 \times 10^{-11} \frac{R_0}{h} V_0^2 (\text{Newton})$$

These relations can be used to obtain quantitative microscopy for various SPMs.

Distance regulation of a SEMM

Rapid progress in the electronic/optical industries requires the ability to image electrical properties with high resolution. We have developed a scanning evanescent electromagnetic microscope (SEMM) capable of quantitative measurements of dielectric properties and surface resistance with submicron resolution. By monitoring the resonance frequency (f_r) and quality factor (Q) of a coaxial cavity, we measure the dielectric properties of the sample. The shift in f_r corresponds to the dielectric constant of the material (ϵ) while the shift in Q corresponds to the tangent loss ($\tan \delta$). By modeling the tip as a monopole and calculating a series of image charges, we estimate the local ϵ and $\tan \delta$. Since the tip radius determines the extent of the field distribution, this microscope is capable of submicron resolution. To enable the quantitative characterization of materials, it is useful to operate at a known distance. We have operated in a soft contact mode, but this mode degrades resolution and even soft contact can damage the tip and sample. Here we describe several different means to regulate the tip-sample separation and allow quantitative non-constant measurements of metallic and insulating surfaces with high resolution.

Quantitative modeling of the SEMM response has been performed in the case of metals and insulators. The resultant curve has been fitted theoretically (Figure 11). For the case of good metals, the resultant shift in f_r does not depend appreciably on the surface resistance. However, the shift in Q is a function of the surface resistance. Since the frequency shift does not vary with conductivity, it can be used to control the tip-sample separation by maintaining the separation so as to induce a constant frequency shift.

Through such methods, the surface topography can be imaged. Through quality factor measurements and theoretical calculations, the conductivity of the metal can be imaged simultaneously.

Metals: For the case of metals, as the shift in f_r is essentially constant, we can maintain a constant tip-sample separation by adjusting the tip-sample separation to maintain a constant f_r in the cavity. The ability to perform non-contact imaging of the surface resistance opens up a variety of possible applications. One such, of some interest to the microwave community, is the profiling of outgrowths in high T_c films.

A quantitative, analytic model for the tip-response for dielectric and metallic material was developed. Since the SEMM operates in the extreme near-field region, with resolution $\sim \lambda/10^6$, we can employ the quasi-static approximation. The local electrical properties were estimated by modeling the tip as a metallic sphere and calculating a series of image charges. Quantitative modeling of the SEMM response was performed in the cases of metals and insulator. Quantitative comparisons of the tip response with the modeled response have been conducted as a function of distance and sample properties and have demonstrated accuracy within 5% on sample of widely varying dielectric and metallic properties.

For metals, the resulting expression is

$$\Delta f/f = -A \sum q_n / V_0,$$

where the summation is from $n=2$ to infinity, and where A is a geometric factor.

The q_n is given by an iterative relation:

$$q_n = q_{n-1} / (1 + a_0 + a_{n-1}) ; \text{ and}$$

$$a_n = 1 + a_0 - [1 / (1 + a_0 + a_{n-1})]$$

with initial conditions: $a_1 = 1 + a_0$ and $q_1 = 4\pi\epsilon_0 R_0 V_0$, where $a_0 = g/R_0$, and g is the tip-sample separation, R_0 the tip radius, and V_0 the tip voltage. For $a_0 \ll 1$, this expression converges slowly owing to the slow divergence of image charges from the tip. However,

$$\Delta f/f = -1.14A \log_{10}(a_0)$$

agrees well for $a_0 < 0.1$. Since these expressions are independent of conductivity for good metals, the frequency shift is used as a distance measure and the surface resistance is measured separately.

By varying the tip-sample separation over a metallic substrate, the frequency response can be measured. After calibration of the cavity to determine the geometrical constant A , the theoretical curve can be fit and R_0 and the absolute separation at a given f_r may be extracted. (Figure 17)

The design of our microscope is based on a previously constructed SEMM. From the calibration curves, a frequency f_{RF} is chosen to correspond to some tip-sample separation. To regulate the tip-sample distance, we employ a phase-locked loop, where connection 31 on Fig. 2 is open. A constant RF frequency f_{RF} is input into the cavity and the cavity output is mixed with a signal coming from a reference path. The length of the reference path is adjusted so that the output of the mixer is zero when f_r matches f_{RF} . The output of the phase detector is fed to an integrator, which regulates the tip-sample distance by changing the extension of a piezoelectric actuator (Burleigh PZS-050) to maintain the integrator output near zero. For samples exhibiting a uniform frequency shift, this

corresponds to a constant tip-sample separation. The measurement is limited to approximately 30 Hz by vibration and the rather low resonance frequency of the actuator. To measure Q , the amplitude of the cavity resonance is measured simultaneously. Using the calibration curves (f_r versus d), a resonance frequency that corresponds to some chose
5 tip-sample separation is chosen for the cavity. The resonance frequency chosen is fed into the cavity and the output of the phase defector is used to regulate the applied voltage to the piezoelectric actuator. Sample topography is measured by monitoring the variation in voltage applied to the actuator.

To demonstrate the ability to separate topographic and electrical information, we
10 imaged a set of metallic squares of varying height on a metallic film (Fig.18). This sample consists of 100 nm, 200 nm, and 400 nm Ag squares on a 2.1 μm Ag substrate on a sapphire substrate. They were 250 μm by 250 μm and separated by a distance of 60 μm . The topographic image shows clear variations in height for the different squares. The loss image is essentially featureless.

15 To demonstrate the ability to image surface resistance, we imaged squares of varying resistivity (Fig. 19). This simple consists of Mn, Cr, and Zr squares deposited on 75 nm Pt on a silicon substrate. The variations in the topographic image correspond to real variations in height as measured by a profilometer. The variations in the loss image are clearly visible and correspond to variations in resistivity.

20 Poled Single Crystals: For materials in which the frequency shift is constant (i.e. poled single crystals), the tip-sample distance (d) can be controlled by adjusting the distance to maintain a constant frequency shift. We have implemented a feedback loop

using a phase-sensitive detector to force a piezoelectric actuator (Burleigh PZS-050) to maintain a constant f_r . For samples exhibiting a uniform frequency shift, this corresponds to a constant tip-sample separation. Sample topography is measured by monitoring the variation in voltage applied to the actuator. By simultaneous measurement of an additional
5 signal, variations in sample properties can be imaged in conjunction with topography. Variations in the transmitted power correspond to variations in tangent loss or surface resistance. By application of an alternating voltage with frequency between that of the tip-sample feedback loop and the cavity bandwidth and measurement of the variation in the output of the phase detector, the first order nonlinear dielectric constant (ϵ_{ijk}) can also be
10 measured. (Figure 15) This image was taken of a periodically poled single-crystal LiNbO₃ wafer. The topographic image is essentially featureless, with the exception of a constant tilt. The nonlinear image features a reversal in phase by the reversal of polarization in the alternating domains.

Other: Apertureless reflectance-mode near-field optical microscopy (apertureless
15 NSOM) can also be used for distance regulation of a SEMM. The variation of material properties at optical frequencies is less than the variation at lower frequencies, making apertureless NSOM suitable for distance regulation. 'Conventional' near-field optics relies on the use of a tapered waveguide geometries of transmission or absorption. This waveguide can either confine or sample light from a region near an aperture with size
20 smaller than the wavelength of light. This form of near-field optics requires the fabrication of a complex probe. In apertureless NSOM, a sharp, optically conducting tip is moved close to the sample and a highly focused spot illuminate the tip-sample region. This

contrasts with earlier apertureless NSOMs in which the tip was illuminated from below. These apertureless NSOMs are limited to use on optically transparent samples. The scattered light varies with the tip-sample separation and may be used for distance control, either by measurement of the amplitude or of the polarization of the scattered light. To
5 reduce the effects of background illumination, we propose the use of a Schwartzchild lens, where a dark central region reduces the scattered background. Additionally, a vertical dither may be used to reduce the effects of a far-field background. This dither should enable the detection of only that component of the optical signal that varies over small length scales. This method allow for control the tip-sample separation in an SEMM with
10 high resolution over a broad range of substrates in combination with simultaneous measurements of the sample's electrical properties.

The tip-sample distance may also be regulated by differential measurement of the frequency shift. Vibrating the sample position, for example by placing a peizoelectric element under the sample, causes a change in resonance frequency and its harmonics.
15 These changes are measured using, for example, a lock-in amplifier.

The changes in resonance frequency will have sharper distance dependence than the microscope signal and can be used for distance control. For frequency shifts whose distance dependence resembles a power law, the variation of f_r at the frequency of the cavity dither will vary inversely with an additional factor of the tip-sample separation. If
20 this vertical dither is small by comparison to the tip-sample separation, the total variation in acquired signal will be small, permitting simultaneous measurement of topography and the sample properties.

The frequency shift and harmonic intensity are independent functions of the dielectric constant and the tip-sample distance, g , and give rise to two independent equations:

$$f_r = f_1(\epsilon, g) \quad (20)$$

$$5 \quad \frac{d(f_r)}{d g} \Big|_{r=\omega} = f_2(\epsilon, g) \quad (21)$$

where the f_r are described in Equation 5 above. To use equation 5 in equation 20, $\Delta f_r = f_r - f_0$. In addition, the denominator, in equation 5, f_r is substituted with f_0 , which will have very little affect on the outcome because of the relative size of the numbers. Equation 5
 10 is then solved for f_r and used as equation 20. Equation 21 is the first derivative taken with respect to g . The equations 20 and 21 are solved simultaneously to yield the dielectric constant, ϵ , and the gap distance, g .

The description of illustrative embodiments and best modes of the present invention is not intended to limit the scope of the invention. Various modifications, alternative
 15 constructions and equivalents may be employed without departing from the true spirit and scope of the appended claims.

We claim:

1. A scanning electromagnetic wave microscope probe comprising,
 - a) a coaxial cable having a center conducting element;
 - b) an insulating material surrounding the center conducting element;
 - 5 c) an exterior electrically conducting shielding element that surrounds the insulating material;
 - d) an electrically conducting endwall having an aperture, the endwall connected to the shielding element;
 - 10 e) a sharpened tip that is electrically connected to the center conducting element located in a manner to extend through and beyond the aperture in the endwall.
2. The apparatus of claim 1 wherein the probe comprises a stripline coaxial cable.
3. A scanning electromagnetic wave microscope probe comprising,
 - a) a resonator having a center conducting element;
 - 15 b) a cavity surrounding the center conducting element;
 - c) an exterior electrically conducting shielding element that surrounds the cavity;
 - d) an electrically conducting endwall having an aperture, the endwall connected to the shielding element; and
 - 20 e) a sharpened tip that is electrically connected to the center conducting element located in a manner to extend through and beyond the aperture in the endwall.
4. The apparatus of claim 3 further comprising a second electrically conducting frontwall positioned a distance above the endwall wherein the distance is between
25 $1/4 \lambda$ and an integer number, n , of $1/4 \lambda$ units.

5. The apparatus of claim 4 wherein the frontwall is electrically shorted to the center conductor and the distance between the frontwall and the endwall is $n (1/4 \lambda)$ where n is an odd integer.
6. The apparatus of claim 4 wherein the frontwall is not electrically shorted to the center conductor and the distance between the frontwall and the endwall is $n (1/4 \lambda)$ where n is an even integer.
7. The apparatus of claim 4 wherein the shielding element is held in place relative to the center conductor with insulating glue.
8. The apparatus of claim 3 wherein the cavity contains an insulating material.
9. A scanning electromagnetic wave microscope comprising,
 - a) a scanning electromagnetic wave microscope probe having an aperture in an electrically conducting endwall and having a center conducting element comprising a sharpened tip that extends through the aperture beyond the endwall;
 - b) a frequency detector for calculating an initial and a final resonant frequency of the resonator, called a frequency shift; and
 - c) a power detector for calculating an initial and final ratio of electromagnetic energy dissipated and stored in the resonator, called a Q shift.
10. The microscope of claim 9 further comprising computer means for calculating a dielectric constant of a dielectric material near the electrode probe tip as a function of the shift of resonant frequency or change in reflected wave caused by the proximity of the dielectric material to the probe tip.
11. The microscope of claim 10 wherein the computer means are programed to calculate the dielectric constant from the equation 2.
12. The microscope of claim 9 further comprising computer means for calculating a loss tangent of a dielectric material near the electrode probe tip as a function of the shift of Q shift caused by the proximity of the dielectric material to the probe tip.

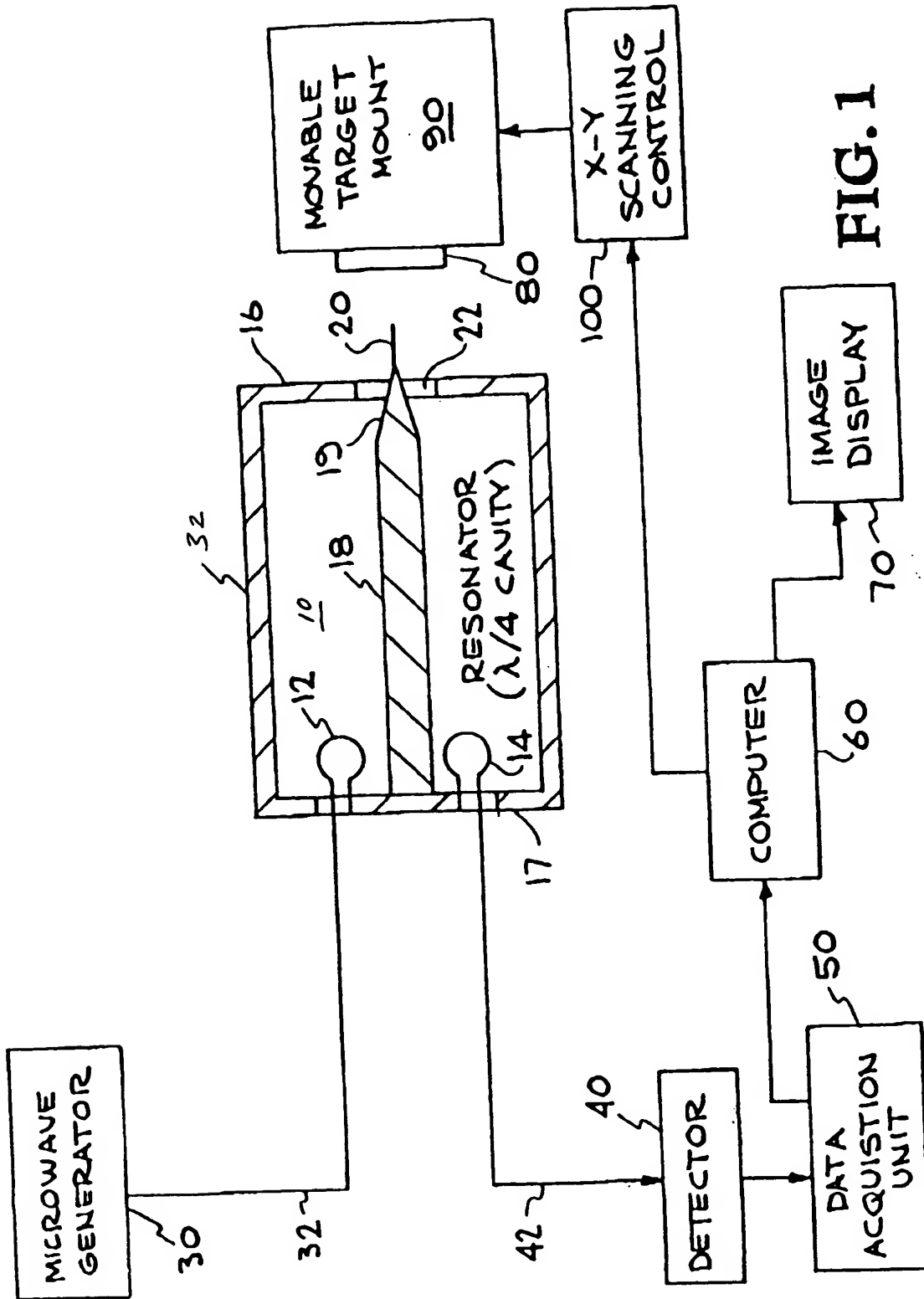
13. The microscope of claim 12 wherein the computer means are programed to calculate the loss tangent from the equation 3.
14. The microscope of claim 9 wherein the power detector is a diode detector.
15. The microscope of claim 9 wherein the frequency detector comprises a phase shifter, phase detector, and integrator.
16. The microscope of claim 9 wherein the probe has a resonator and wherein the cavity is filled with a dielectric material.
17. The microscope of claim 16 wherein the dielectric material is sapphire.
18. The microscope of claim 17 wherein the dielectric material is SrTiO_3 .
19. The microscope of claim 9 wherein the probe tip extends a distance beyond the aperture between about 1/3 and about 3 times the largest distance across the aperture.
20. The microscope of claim 9 wherein the aperture in the resonator endwall is circular and the diameter is between about 20 nanometers and about 3 millimeters.
21. The microscope of claim 9 wherein the frequency generator comprises a voltage controlled oscillator.
22. The microscope of claim 21 wherein the frequency generator operates in the microwave region.
23. The microscope of claim 9 wherein frequency controllers is digital.
24. A method of measuring a dielectric constant and loss tangent of a sample comprising:
- j) determining a reference resonant frequency f_0 of the probe by
 - v) locating the probe far enough away from the sample material that it is not influenced by the sample;

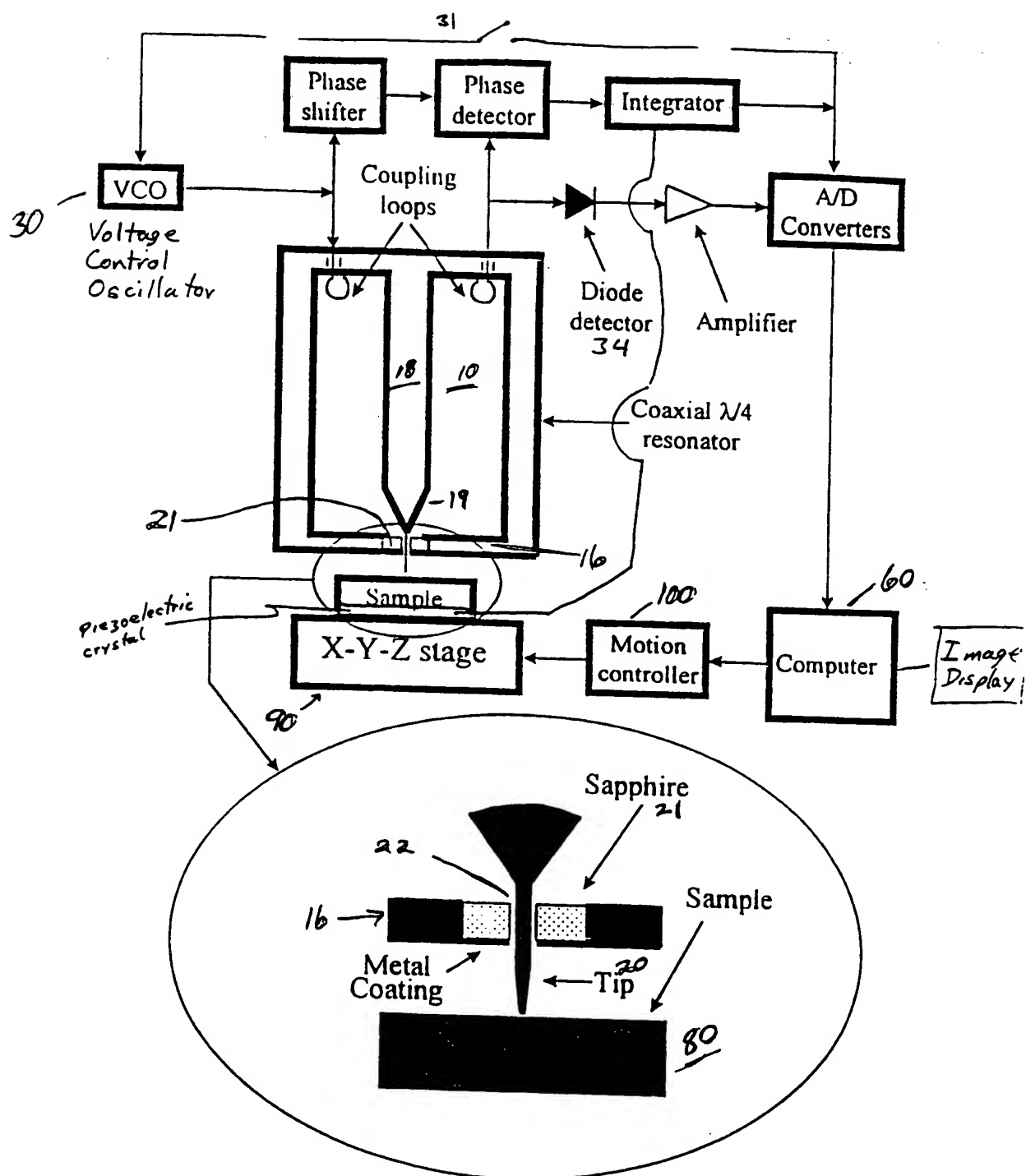
- vi) sweeping a frequency range;
- vii) plotting frequency versus power;
- viii) fitting a curve to find the maximum frequency, called f_0 ;
- 5 k) determining Q_0 by dividing f_0 by a the frequency difference at two half power amplitude points;
- l) calculating the coefficient M from the equation $S = MQ_0^2$ where S is the power at f_0 ;
- m) calibrating the geometric factors A, B, and R_0 , in equations 5 and 6 using a sample of known dielectric constant;
- 10 n) placing a probe tip of a scanning evanescent electromagnetic wave microscope near or in soft contact with the sample;
- o) measuring the shift in resonant frequency caused by the proximity of the sample near the probe tip;
- p) measuring the quality factor shifts caused by the proximity of the sample near the probe tip; and
- 15 q) calculating the dielectric constant and loss tangent using a pair of equations chosen from the group comprising soft contact equations 2 and 3, probe-sample gap equations 5 and 6, or the Thin Film equations.
- 25. Determining the frequency versus power curve in claim 24 by using a Lorentz line type fit to obtain f_0 , and Q_0 .
- 20 26. A method of measuring conductivity of a conducting sample comprising:
 - a) determining a reference resonant frequency f_0 of the probe by
 - i) locating the probe far enough away from the sample material that it is not influenced by the sample;
 - 25 ii) sweeping a frequency range;
 - iii) plotting frequency versus power;
 - iv) fitting a curve to find the maximum frequency, called f_0 ;
 - b) determining Q_0 by dividing f_0 by a the frequency difference at two half power amplitude points;

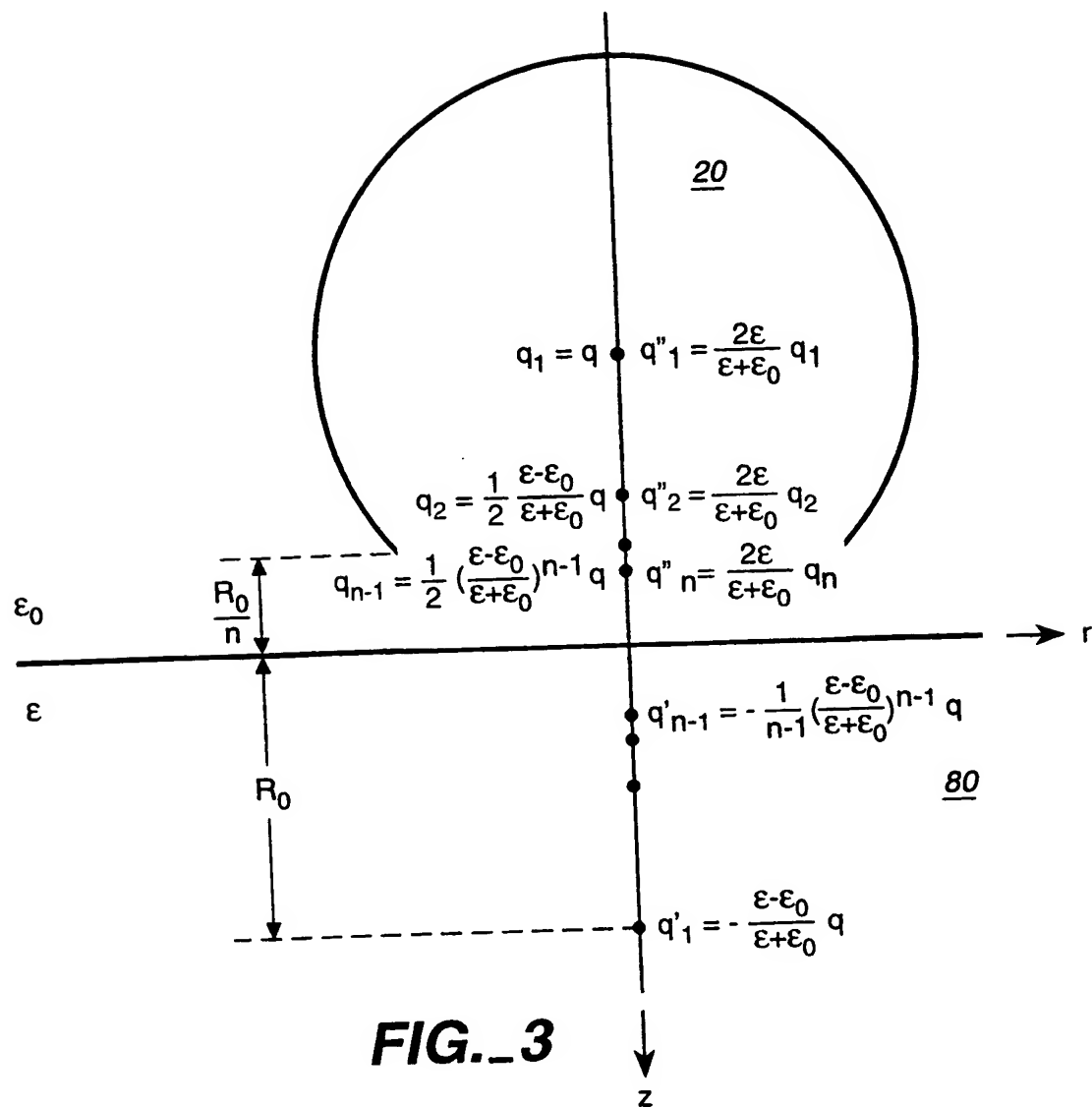
- c) calculating the coefficient M from the equation $S = MQ_0^2$ where S is the power at f_0 ;
- d) placing a probe tip of a scanning evanescent electromagnetic wave microscope near the sample;
- 5 e) calibrating the geometric factors A , B , and R_0 , in equations 12 and 19 by measuring and fitting the frequency and quality factors as a function of a gap distance, g , between the probe tip and a reference sample of known conductivity;
- 10 f) measuring the shift in resonant frequency caused by the proximity of the sample near the probe tip;
- g) calculating g from equation 12;
- h) measuring the shift in quality factor caused by the proximity of the sample near the probe tip; and
- i) calculating the conductivity using equation 19.
- 15 27. A method of regulating a distance between a probe tip of a scanning evanescent electromagnetic wave microscope and a conducting sample being scanned comprising,
 - a) selecting a preferred distance, g_p , between the tip and sample;
 - b) determining a reference resonant frequency f_0 of the probe by
 - 20 i) locating the probe far enough away from the sample material that it is not influenced by the sample;
 - ii) sweeping a frequency range;
 - iii) plotting frequency versus power;
 - iv) fitting a curve to find the maximum frequency, called f_0 ;
 - 25 c) determining Q_0 by dividing f_0 by a the frequency difference at two half power amplitude points;
 - d) calibrating the geometric factors A , B , and R_0 , in equations 12 and 19 by measuring and fitting the frequency and quality factors as functions of a gap distance, g , between the probe tip and a reference sample of known conductivity;
 - 30

- e) measuring the resonant frequency and obtaining the absolute difference between it and the reference frequency;
 - f) calculating the change in gap distance required to return the gap distance to g_p ;
 - 5 g) electromechanically adjusting the distance between the probe tip and the sample being scanned to equal g_p ; and
 - h) repeating steps e) through g) at a set interval period until the scanning process is complete.
28. A method of regulating a distance between a probe tip of a scanning evanescent electromagnetic wave microscope and a dielectric sample being scanned comprising,
- 10
- a) selecting a preferred distance, g_p , between the tip and sample;
 - b) determining a reference resonant frequency f_0 of the probe by
 - 15 i) locating the probe far enough away from the sample material that it is not influenced by the sample;
 - ii) sweeping a frequency range;
 - iii) plotting frequency versus power;
 - iv) fitting a curve to find the maximum frequency, called f_0 ;
 - c) determining Q_0 by dividing f_0 by a the frequency difference at two half power amplitude points;
 - 20 d) calculating the coefficient M from the equation $S = MQ_0^2$ where S is the power at f_0 ;
 - e) calibrating the geometric factors A, B, and R_0 , in equations 5 and 6 using a sample of known dielectric constant;
 - 25 f) vibrating the sample so as to vary the gap distance, g, between the tip and the sample, wherein the vibration amplitude is small such as that caused by a piezo-electric element and wherein the frequency of vibration is within the frequency difference of element c) above;
 - g) measuring an averaged shift in resonant frequency and a first harmonic intensity;
 - 30

- 5
- h) solving equations 20 and 21 for g ;
 - i) calculating the change in gap distance required to return the gap distance to g_p ;
 - j) electromechanically adjusting the distance between the probe tip and the sample being scanned to equal g_p ; and
 - k) repeating steps e) through g) at a set interval period until the scanning process is complete.



Figure 2



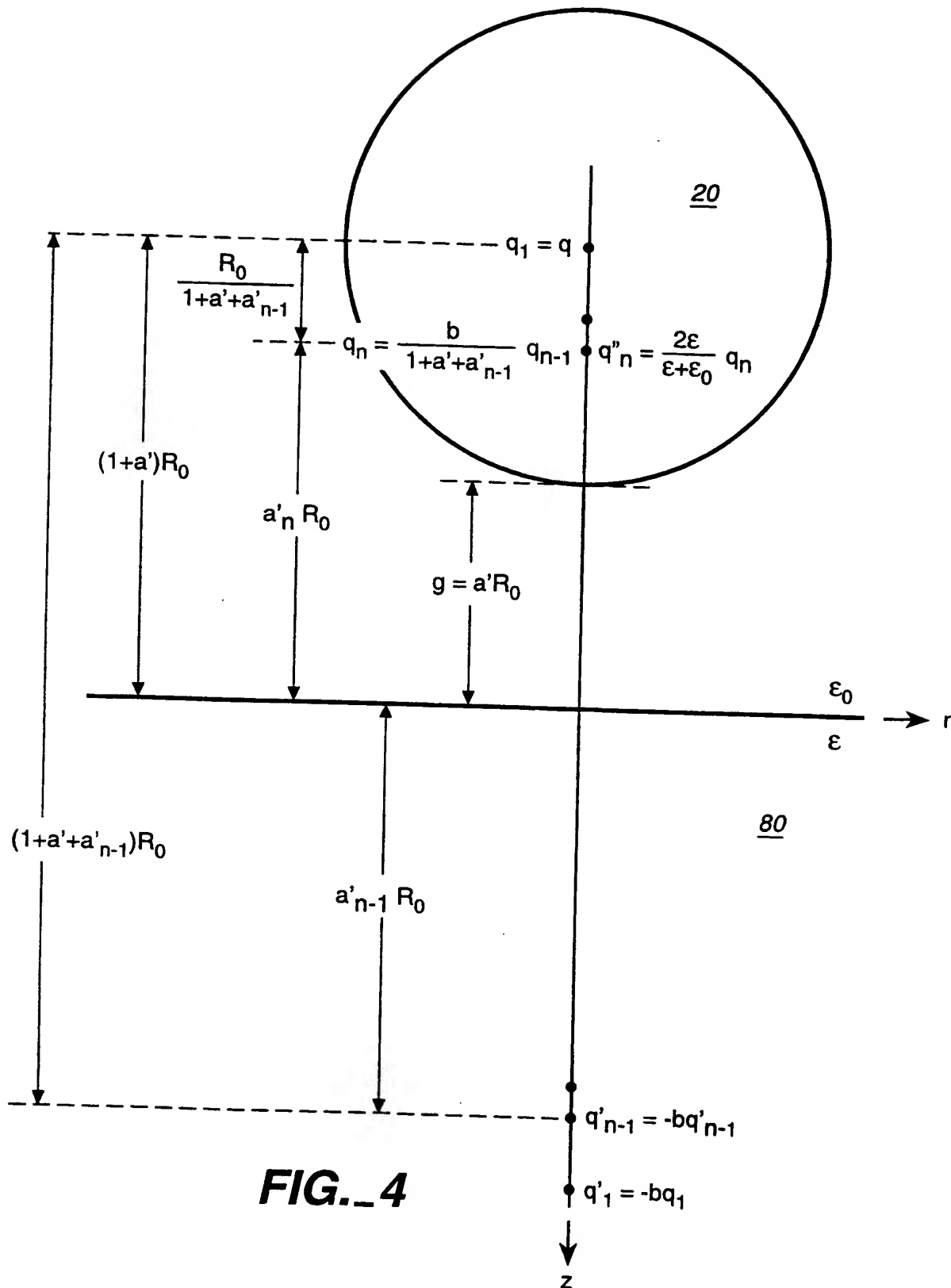


FIG._4

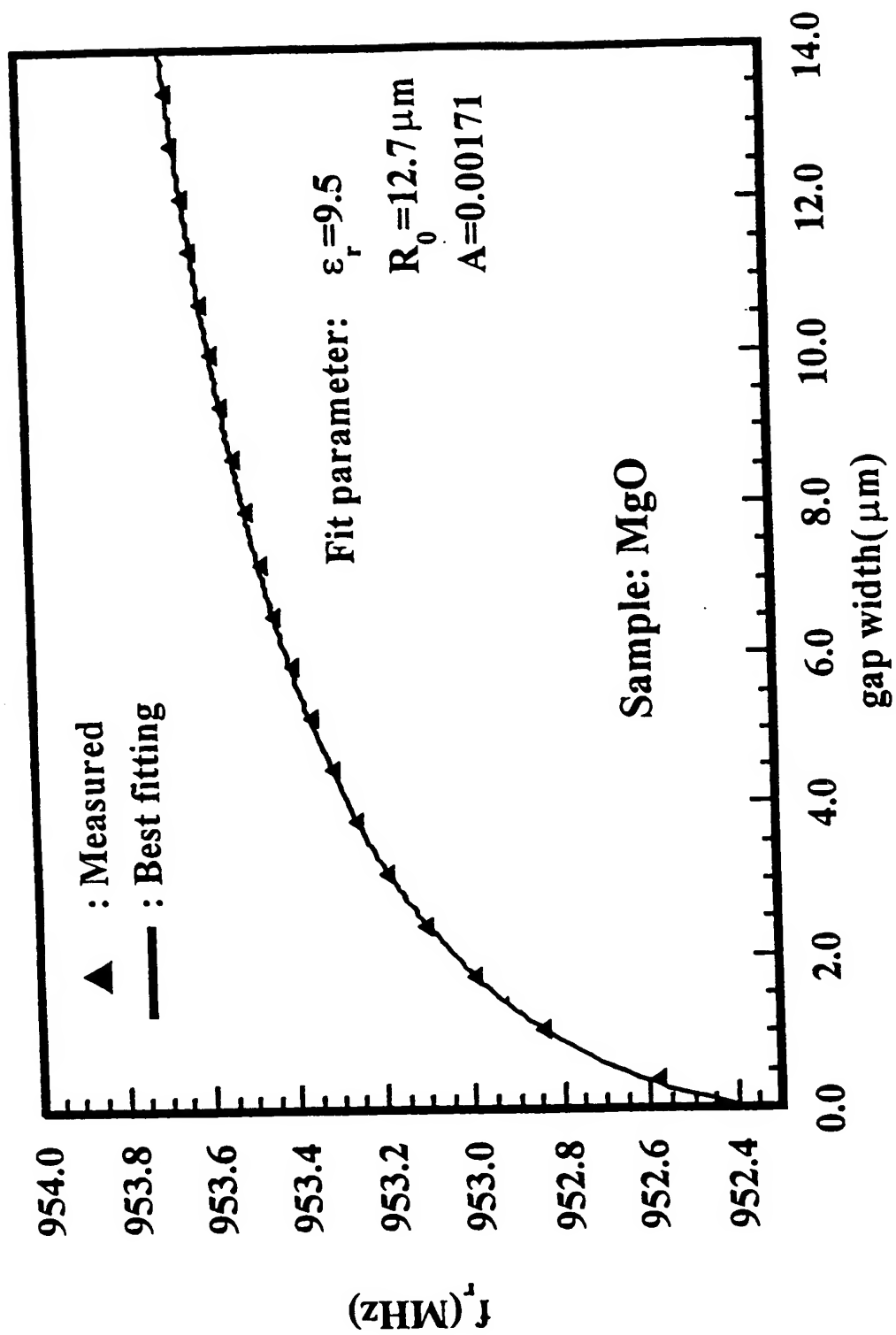
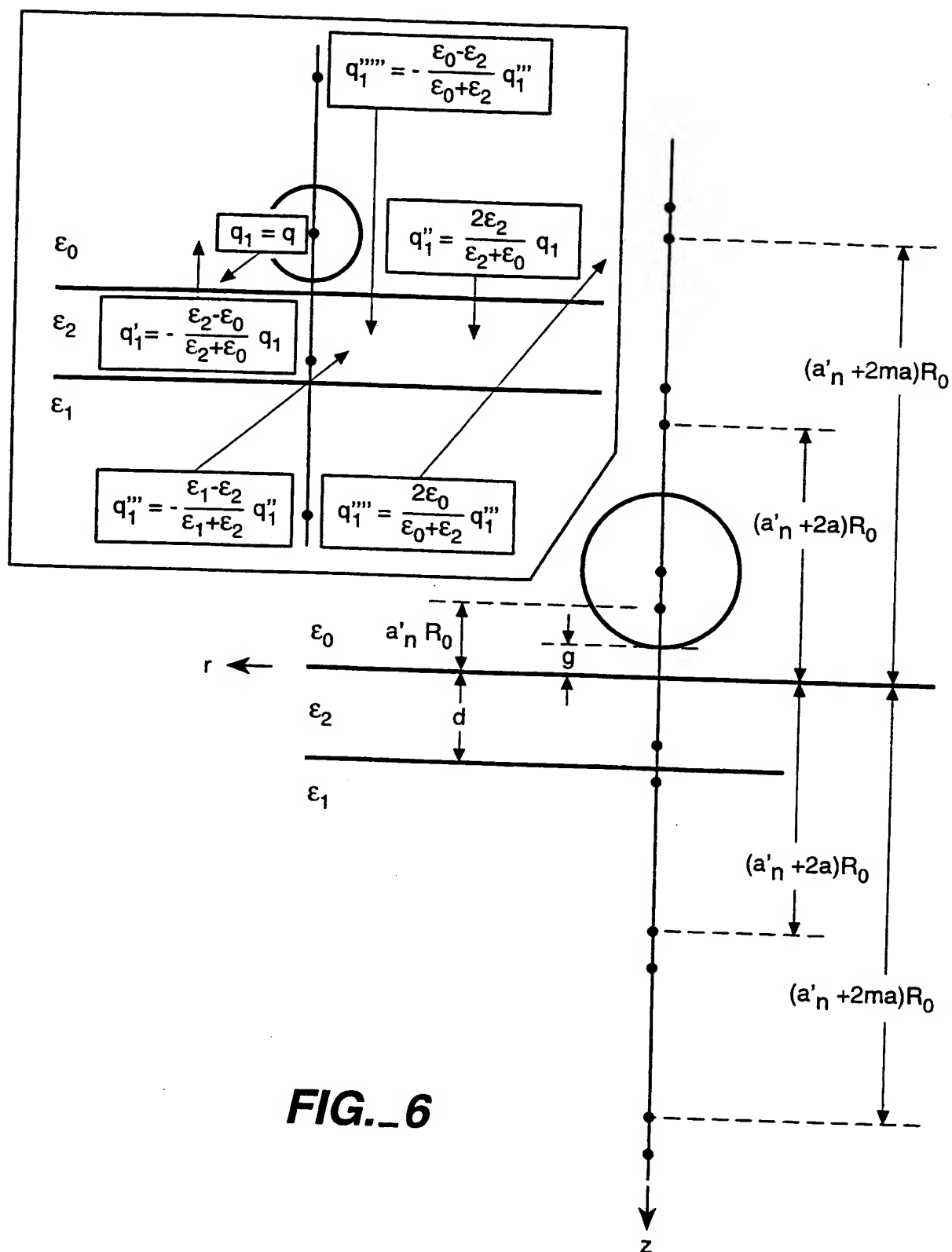
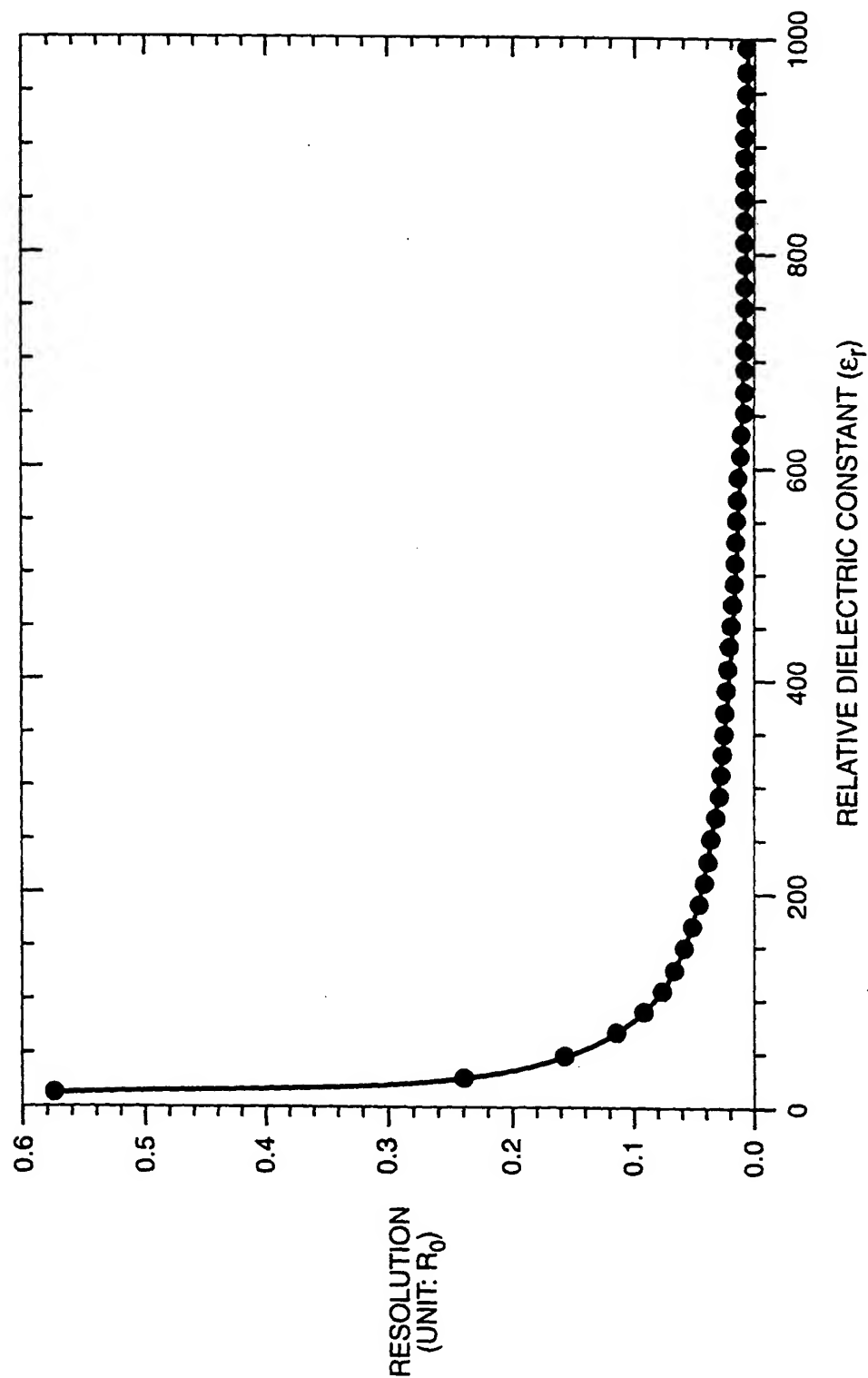
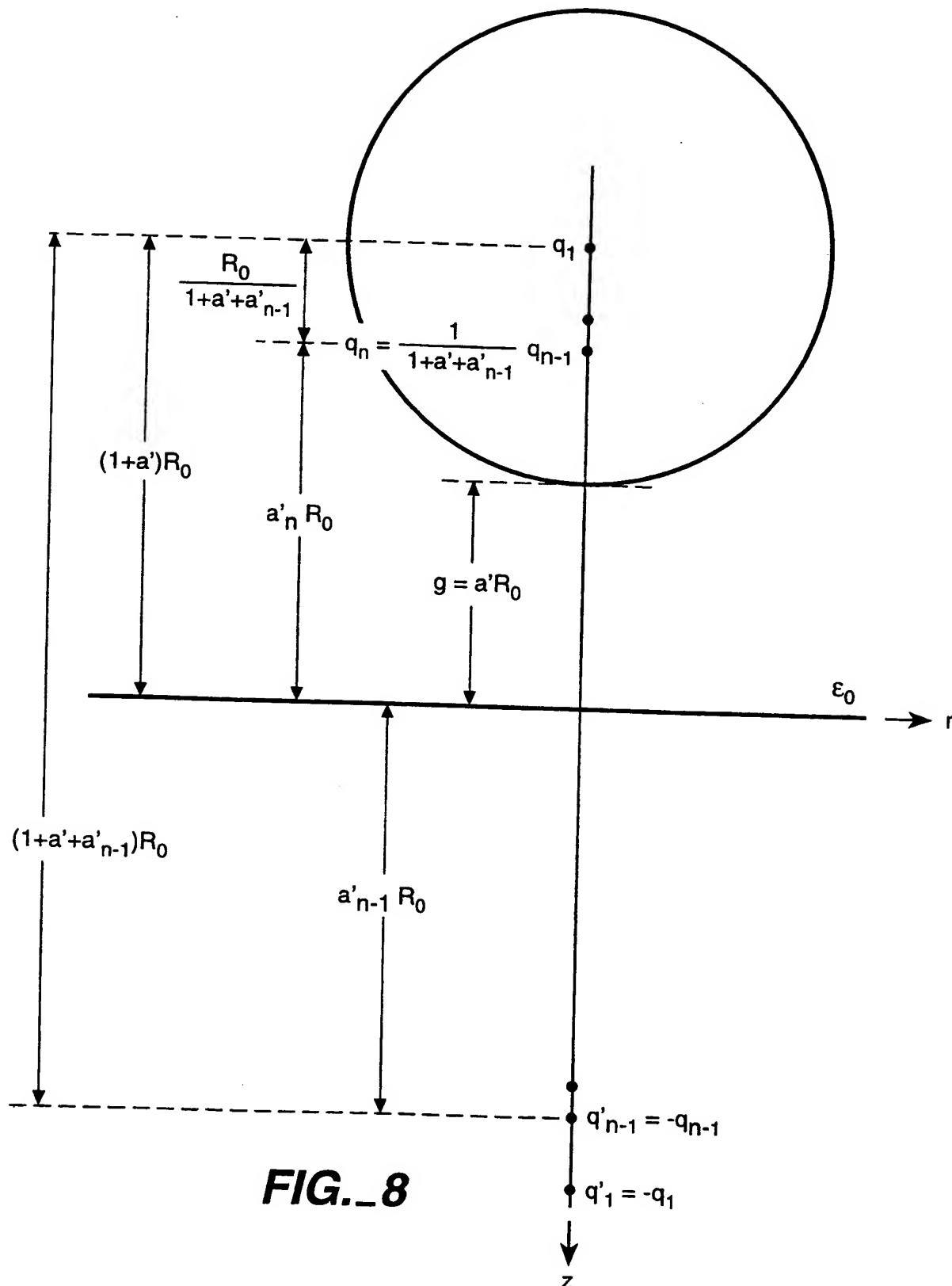


Figure 5

**FIG. 6**

**FIG.-7**

**FIG._8**

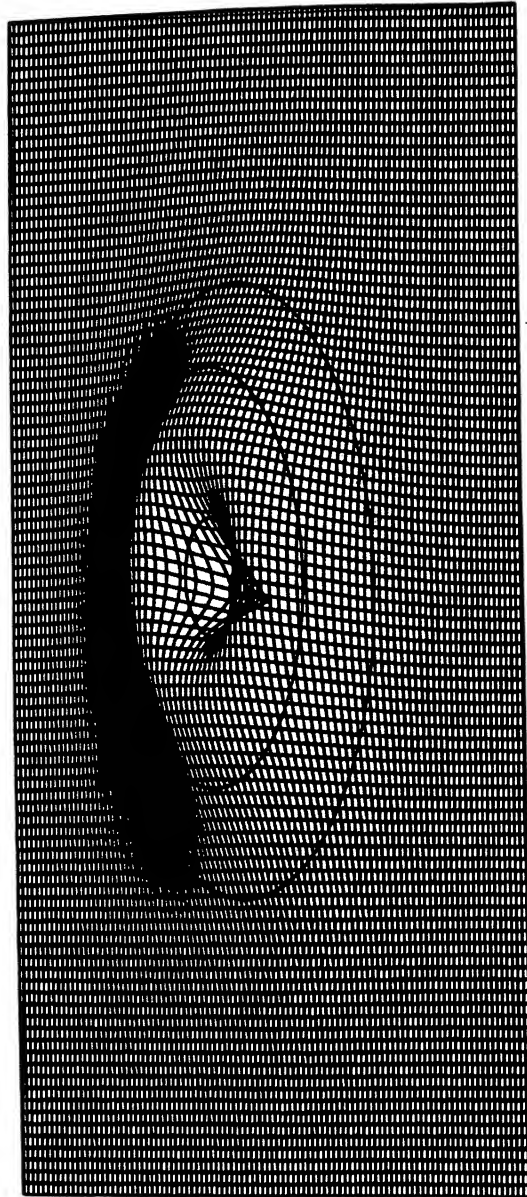
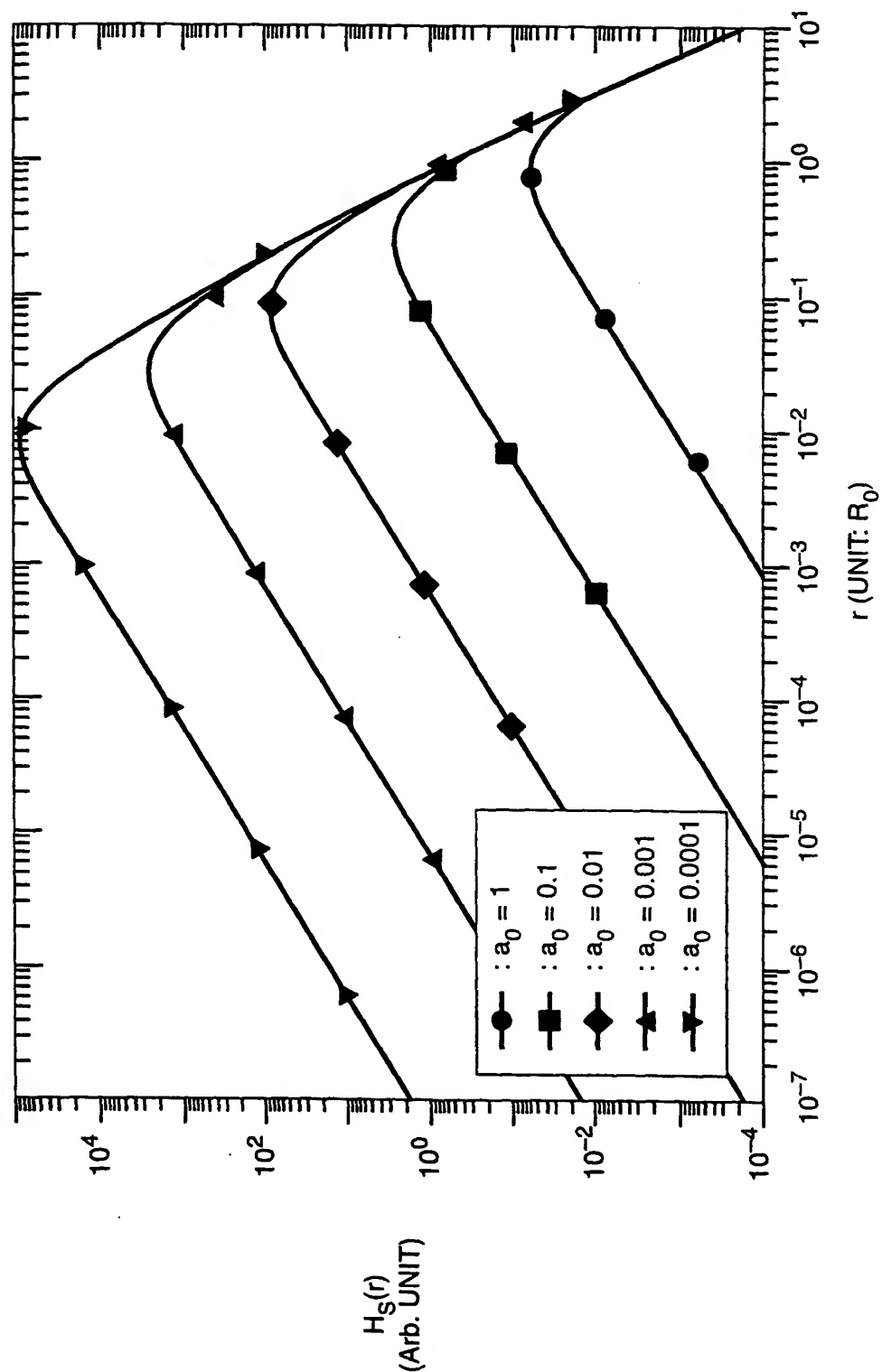


FIG. 9

WO 99/16102A1

**FIG. 10**

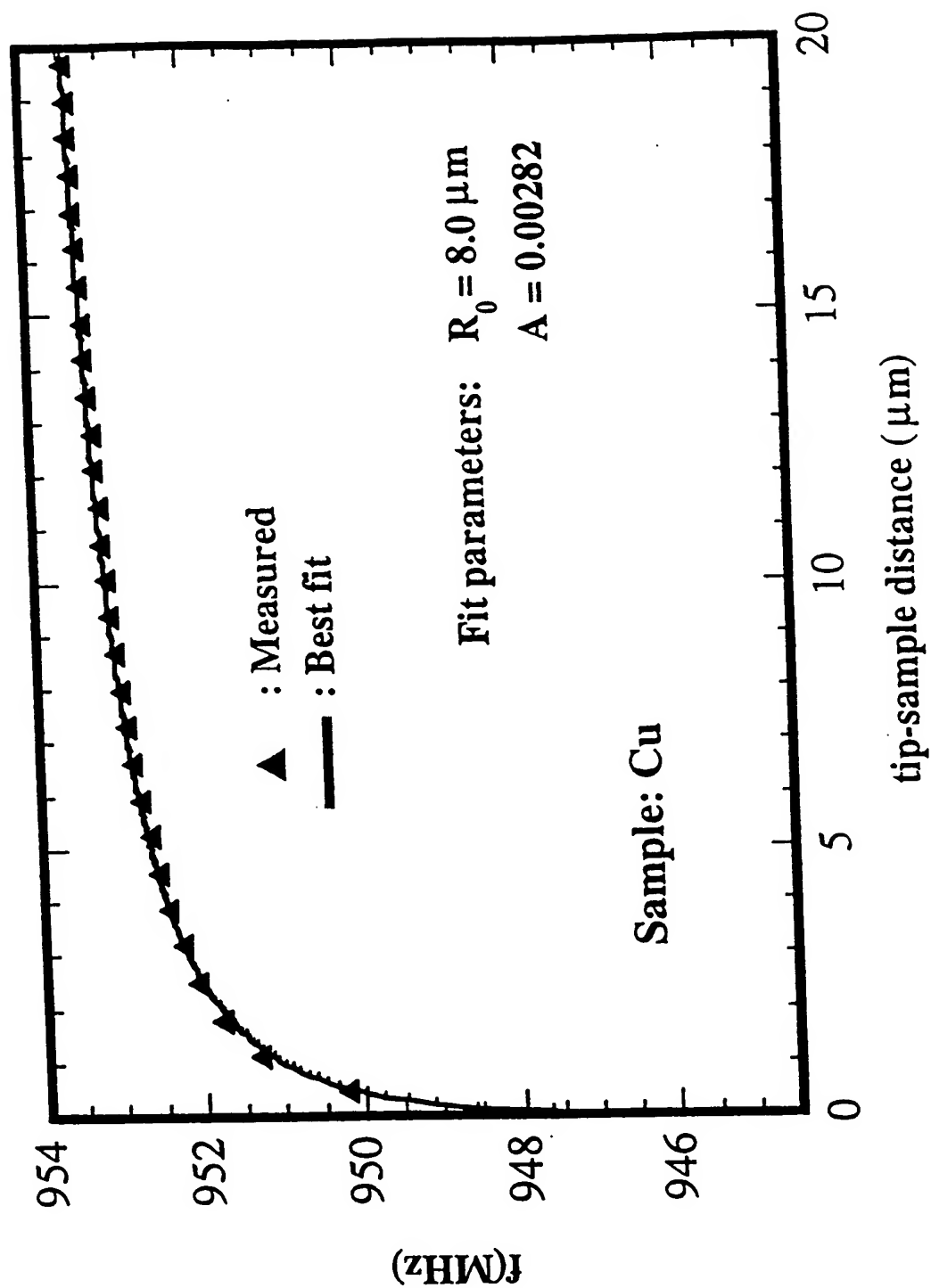


Fig. 11

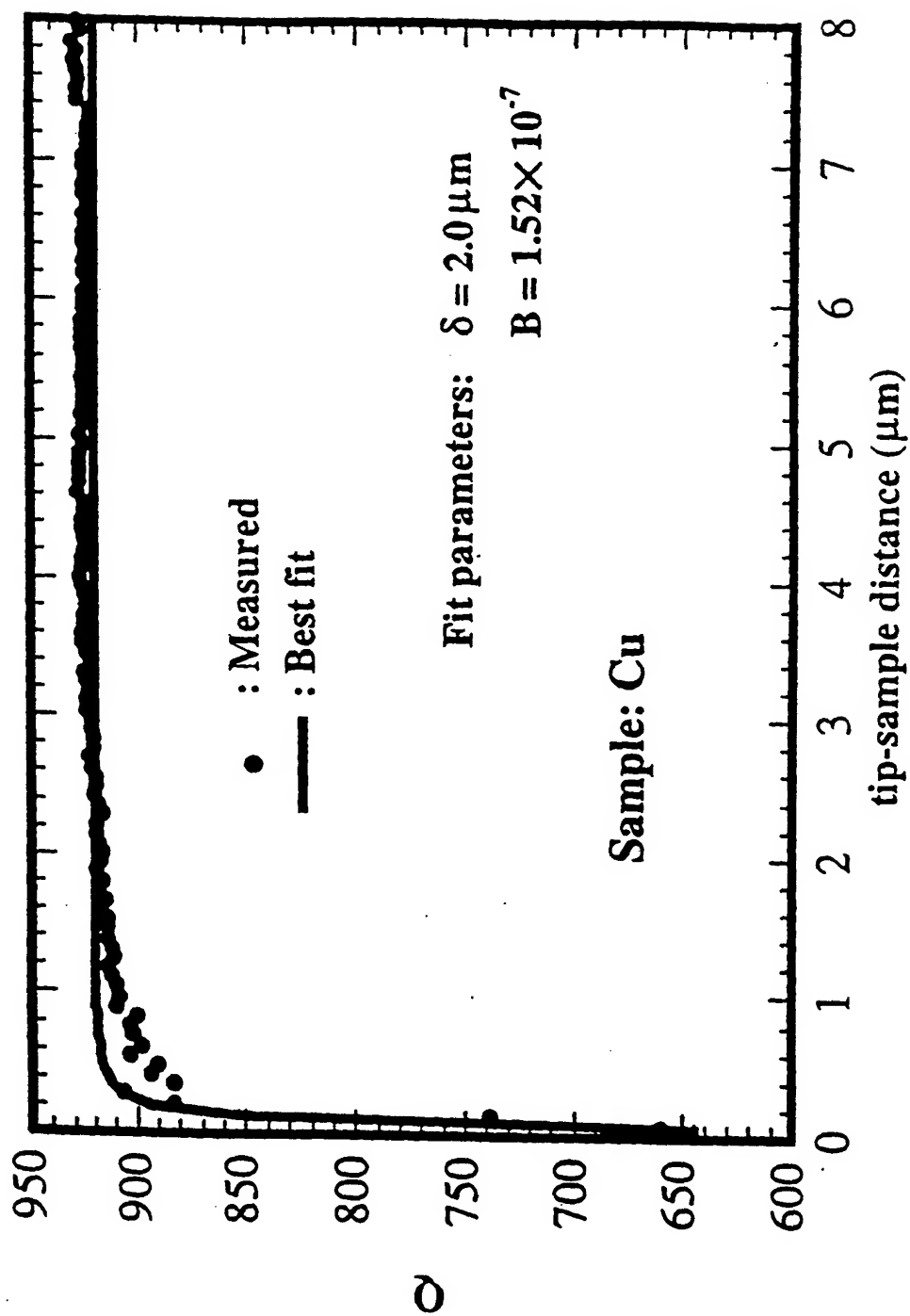
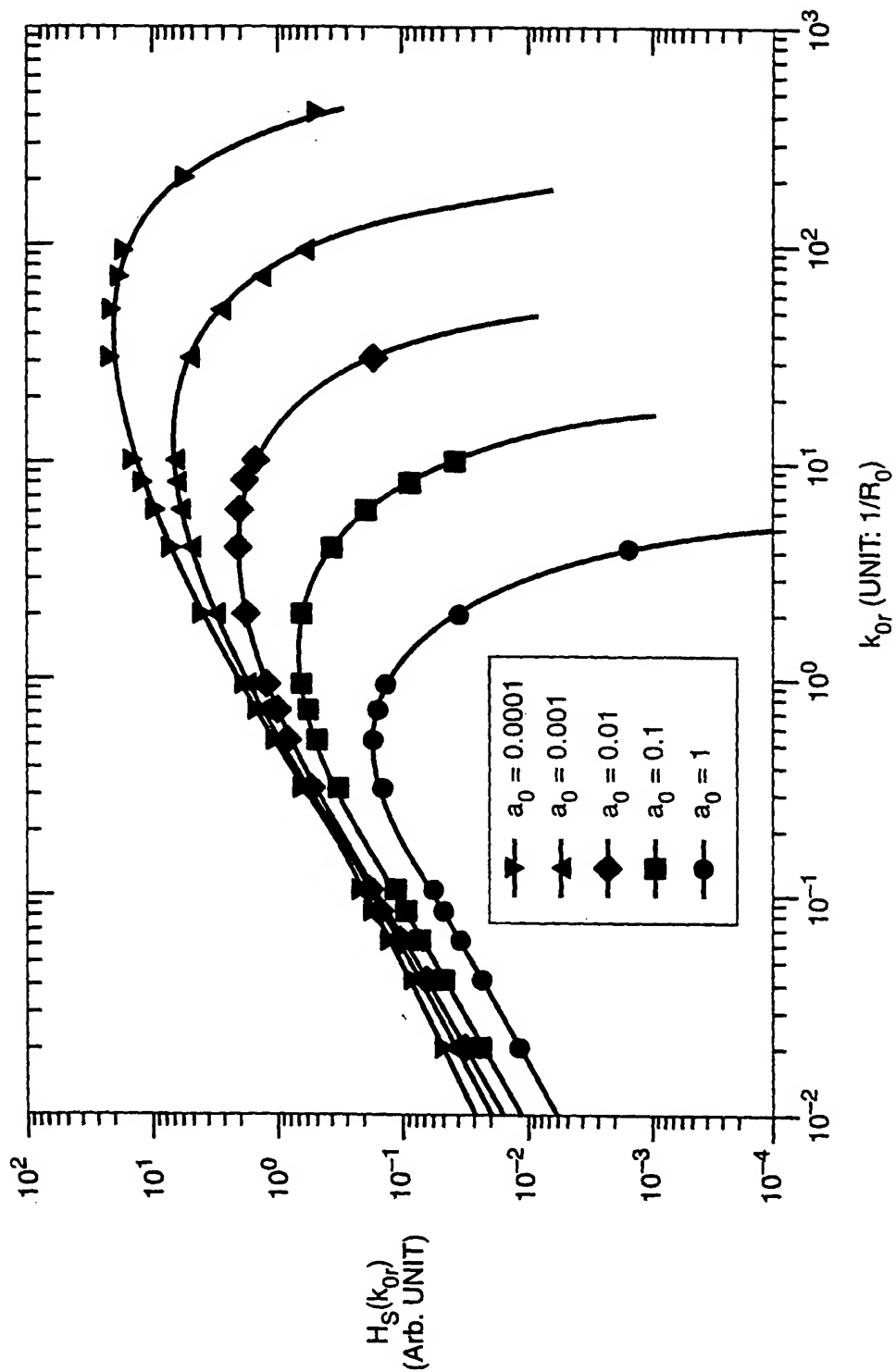


Fig. 12

**FIG. 13**

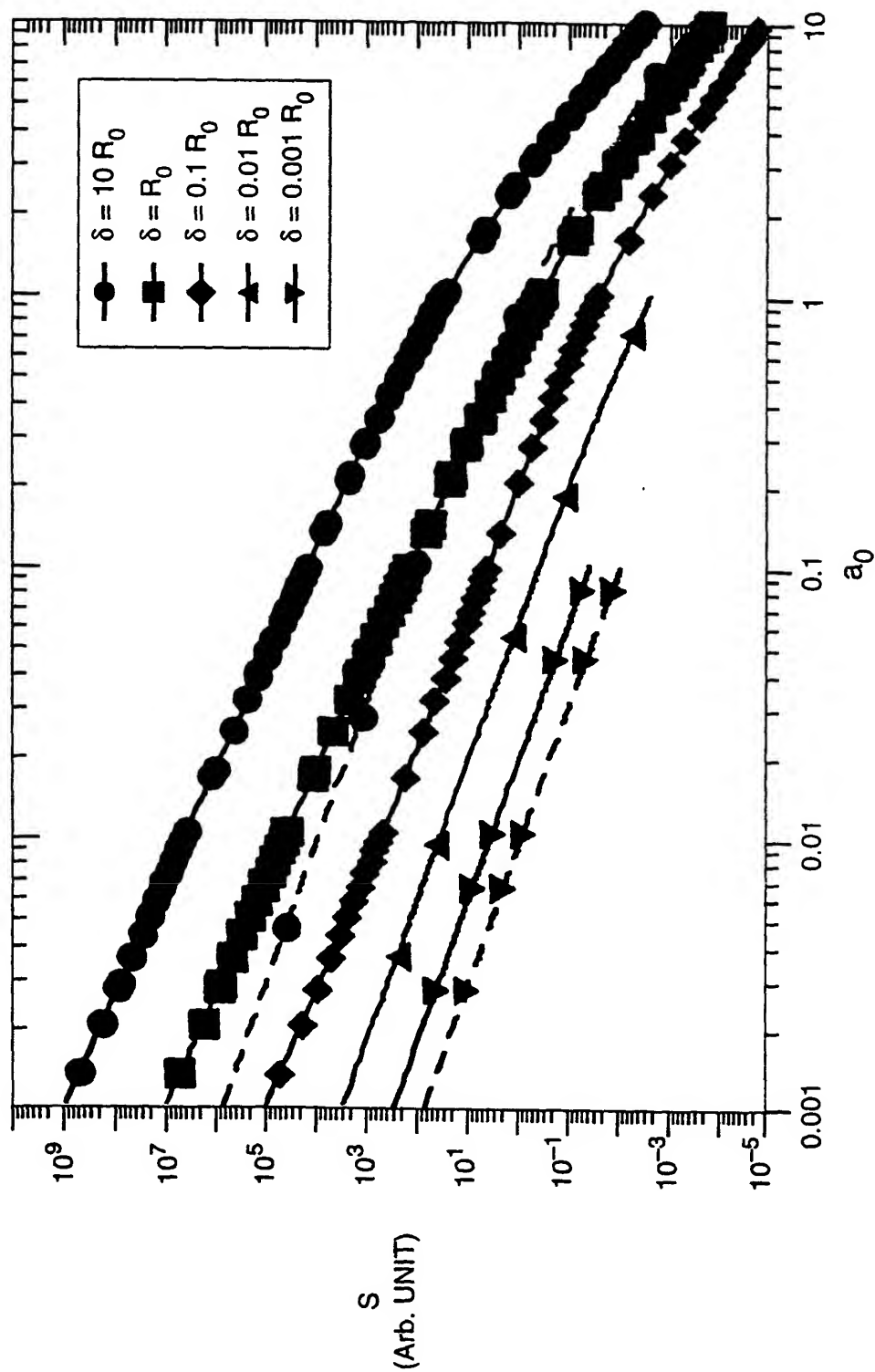
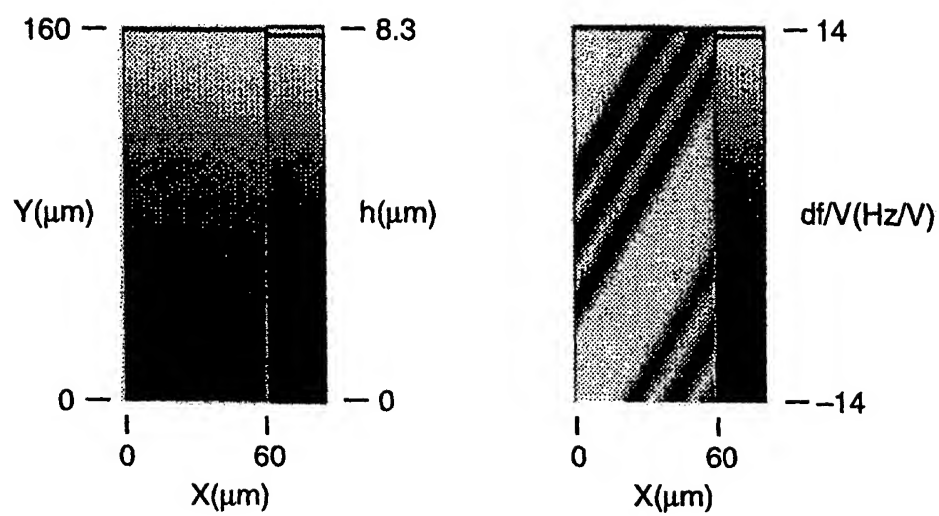


FIG. 14

**FIG. 15**

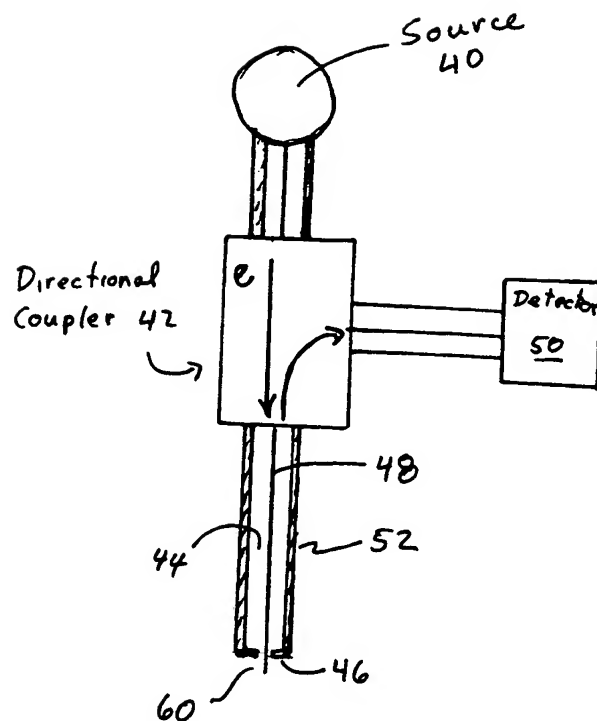


Figure 16
Coaxial Cable probe having end wall
shielding.

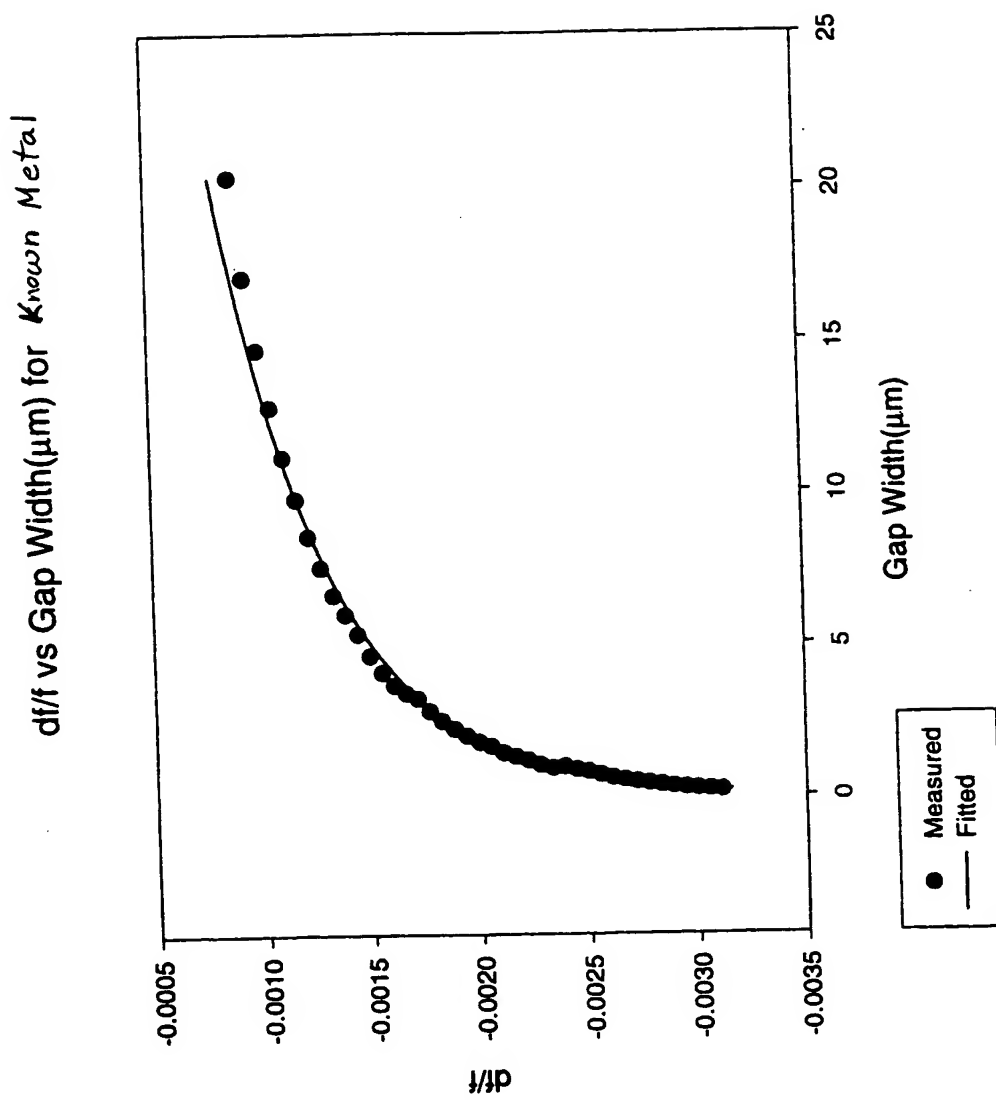


Figure 17

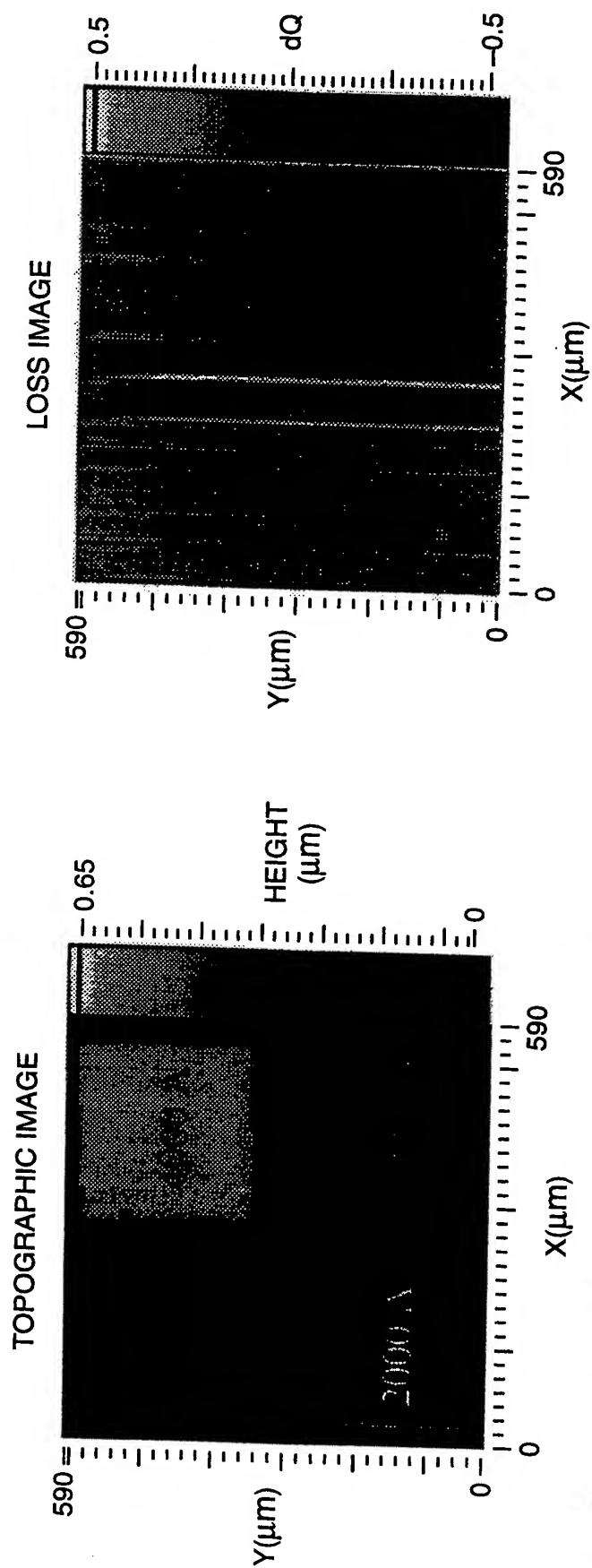


FIG. 18

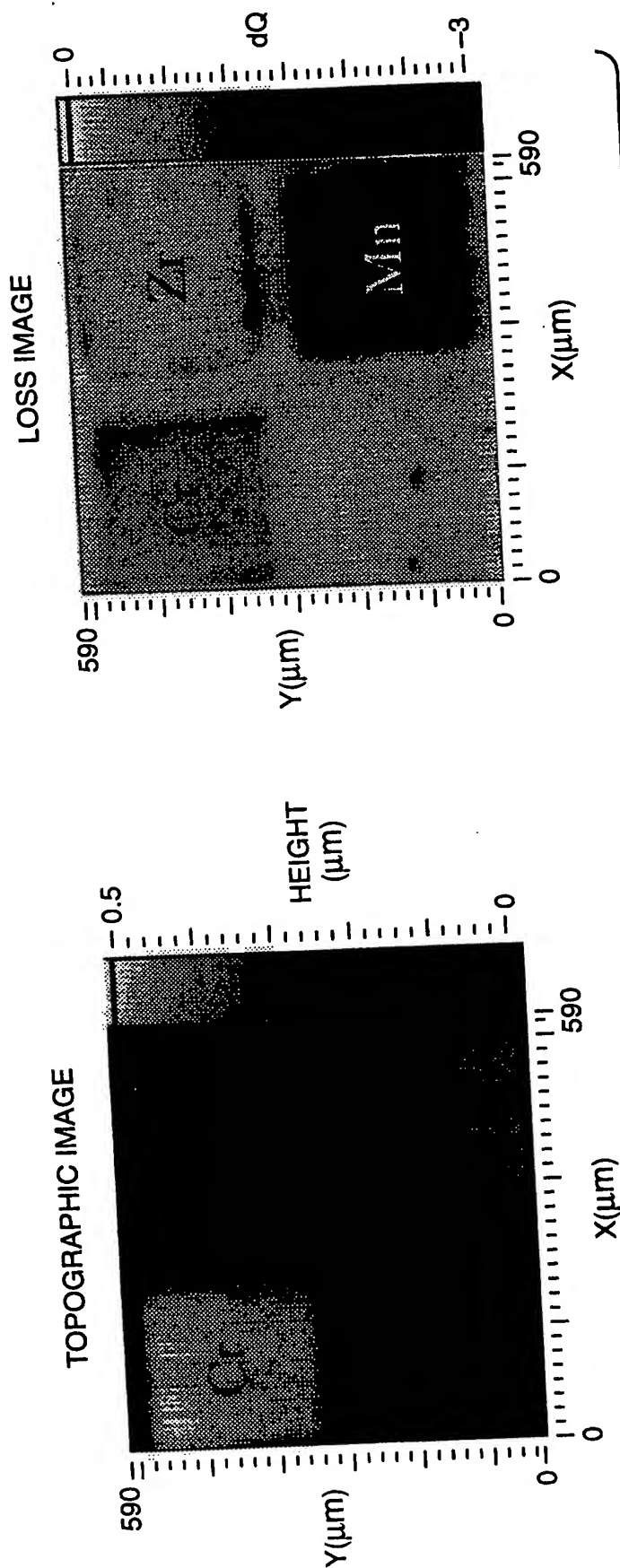


FIG. 19

INTERNATIONAL SEARCH REPORT

International application No.
PCT/US98/19764

A. CLASSIFICATION OF SUBJECT MATTER

IPC(6) : H01J 37/20; G01B 7/34

US CL : 73/105; 250/306, 307; 324/96

According to International Patent Classification (IPC) or to both national classification and IPC

B. FIELDS SEARCHED

Minimum documentation searched (classification system followed by classification symbols)

U.S. : 73/105; 250/306, 307; 324/96

Documentation searched other than minimum documentation to the extent that such documents are included in the fields searched
NONE

Electronic data base consulted during the international search (name of data base and, where practicable, search terms used)
NONE

C. DOCUMENTS CONSIDERED TO BE RELEVANT

Category*	Citation of document, with indication, where appropriate, of the relevant passages	Relevant to claim No.
X, E	US 5,821,410 A (XIANG et al.) 13 October 1998 (13.10.1998), whole document.	1-8
X	WEI, T. et al. Scanning Tip Microwave Near-Field Microscope, Appl. Phys. Lett. 10 June 1996, Vol. 68, No. 24. pages 1-3, specifically, Figure 1 and first full paragraph, left side of page 2.	3-5 and 7
X	TABIB-AZAR, M. et al., Non-Destructive Characterization of Materials By Evanescent Microwaves, Meas. Sci. Technology, 1993, Vol. 4. pages 583-590, specifically, Figures 1a and 4 and last paragraph right side of page 586 through and including first full paragraph on right side of page 587.	3-5, 7, and 8

☒ Further documents are listed in the continuation of Box C. ☐ See patent family annex.

* Special categories of cited documents:	"T" later document published after the international filing date or priority date and not in conflict with the application but cited to understand the principle or theory underlying the invention
"A" document defining the general state of the art which is not considered to be of particular relevance	"X" document of particular relevance; the claimed invention cannot be considered novel or cannot be considered to involve an inventive step when the document is taken alone
"E" earlier document published on or after the international filing date	"Y" document of particular relevance; the claimed invention cannot be considered to involve an inventive step when the document is combined with one or more other such documents, such combination being obvious to a person skilled in the art
"L" document which may throw doubts on priority claim(s) or which is cited to establish the publication date of another citation or other special reason (as specified)	"&" document member of the same patent family
"O" document referring to an oral disclosure, use, exhibition or other means	
"P" document published prior to the international filing date but later than the priority date claimed	

Date of the actual completion of the international search 12 FEBRUARY 1999	Date of mailing of the international search report 09 MAR 1999
Name and mailing address of the ISA/US Commissioner of Patents and Trademarks Box PCT Washington, D.C. 20231 Facsimile No. (703) 305-3230	Authorized officer DANIEL S. LARKIN Telephone No. (703) 308-6724

Form PCT/ISA/210 (sec nd sheet)(July 1992)*

INTERNATIONAL SEARCH REPORT

International application No.
PCT/US98/19764

C (Continuation). DOCUMENTS CONSIDERED TO BE RELEVANT

Category*	Citation of document, with indication, where appropriate, of the relevant passages	Relevant to claim No.
A	GUTMANN, R.J. et al., Microwave Scanning Microscopy for Planar Structure Diagnostics, IEEE MTT-S Digest, 1987, pages 281-284.	1-28



From the
INTERNATIONAL PRELIMINARY EXAMINING AUTHORITY

To:

SOKOHL,R
Sterne, Kessler, Goldstein & Fox
P.L.L.C.
Suite 600
1100 New York Avenue, N.W.
Washington, D.C. 20005-3934
ETATS-UNIS D'AMERIQUE

PCT

NOTIFICATION OF TRANSMITTAL OF *CCS 12/10/01*
THE INTERNATIONAL PRELIMINARY *KAC 12/12/01*
EXAMINATION REPORT *WBE 12/13/01*
(PCT Rule 71.1) *MB*

Date of mailing
(day/month/year) 05.12.2001

Applicant's or agent's file reference
1797.020PC02

IMPORTANT NOTIFICATION

International application No.
PCT/US00/08943

International filing date (day/month/year)
05/04/2000

Priority date (day/month/year)
10/09/1999

Applicant
UNIVERSITY OF MARYLAND et al.

1. The applicant is hereby notified that this International Preliminary Examining Authority transmits herewith the international preliminary examination report and its annexes, if any, established on the international application.
2. A copy of the report and its annexes, if any, is being transmitted to the International Bureau for communication to all the elected Offices.
3. Where required by any of the elected Offices, the International Bureau will prepare an English translation of the report (but not of any annexes) and will transmit such translation to those Offices.

4. REMINDER

The applicant must enter the national phase before each elected Office by performing certain acts (filing translations and paying national fees) within 30 months from the priority date (or later in some Offices) (Article 39(1)) (see also the reminder sent by the International Bureau with Form PCT/IB/301).

Where a translation of the international application must be furnished to an elected Office, that translation must contain a translation of any annexes to the international preliminary examination report. It is the applicant's responsibility to prepare and furnish such translation directly to each elected Office concerned.

For further details on the applicable time limits and requirements of the elected Offices, see Volume II of the PCT Applicant's Guide.

Chap II P.P. (3/10/02) 2/10/02

DOCKETED

Name and mailing address of the IPEA/

 European Patent Office
D-80298 Munich
Tel. +49 89 2399 - 0 Tx: 523656 epmu d
Fax: +49 89 2399 - 4465

Authorized officer

Baumann, H

Tel. +49 89 2399-2131







1234567890

PCT

INTERNATIONAL PRELIMINARY EXAMINATION REPORT

(PCT Article 36 and Rule 70)

Applicant's or agent's file reference 1797.020PC02		FOR FURTHER ACTION	See Notification of Transmittal of International Preliminary Examination Report (Form PCT/IPEA/416)
International application No. PCT/US00/08943	International filing date (day/month/year) 05/04/2000	Priority date (day/month/year) 10/09/1999	
International Patent Classification (IPC) or national classification and IPC G01R27/26			
Applicant UNIVERSITY OF MARYLAND et al.			
<p>1. This international preliminary examination report has been prepared by this International Preliminary Examining Authority and is transmitted to the applicant according to Article 36.</p> <p>2. This REPORT consists of a total of 6 sheets, including this cover sheet.</p> <p><input checked="" type="checkbox"/> This report is also accompanied by ANNEXES, i.e. sheets of the description, claims and/or drawings which have been amended and are the basis for this report and/or sheets containing rectifications made before this Authority (see Rule 70.16 and Section 607 of the Administrative Instructions under the PCT).</p> <p>These annexes consist of a total of 45 sheets.</p>			
<p>3. This report contains indications relating to the following items:</p> <p>I <input checked="" type="checkbox"/> Basis of the report</p> <p>II <input type="checkbox"/> Priority</p> <p>III <input checked="" type="checkbox"/> Non-establishment of opinion with regard to novelty, inventive step and industrial applicability</p> <p>IV <input checked="" type="checkbox"/> Lack of unity of invention</p> <p>V <input checked="" type="checkbox"/> Reasoned statement under Article 35(2) with regard to novelty, inventive step or industrial applicability; citations and explanations supporting such statement</p> <p>VI <input type="checkbox"/> Certain documents cited</p> <p>VII <input checked="" type="checkbox"/> Certain defects in the international application</p> <p>VIII <input type="checkbox"/> Certain observations on the international application</p>			
Date of submission of the demand 09/04/2001		Date of completion of this report 05.12.2001	
Name and mailing address of the international preliminary examining authority:  European Patent Office D-80298 Munich Tel. +49 89 2399 - 0 Tx: 523656 epmu d Fax: +49 89 2399 - 4465		Authorized officer Rath, R Telephone No. +49 89 2399 8950 	



**INTERNATIONAL PRELIMINARY
EXAMINATION REPORT**

International application No. PCT/US00/08943

I. Basis of the report

1. With regard to the **elements** of the international application (*Replacement sheets which have been furnished to the receiving Office in response to an invitation under Article 14 are referred to in this report as "originally filed" and are not annexed to this report since they do not contain amendments (Rules 70.16 and 70.17)*):

Description, pages:

1-30 as received on 12/11/2001 with letter of 09/11/2001

Claims, No.:

1-29 as received on 12/11/2001 with letter of 09/11/2001

Drawings, sheets:

1/19-19/19 as originally filed

2. With regard to the **language**, all the elements marked above were available or furnished to this Authority in the language in which the international application was filed, unless otherwise indicated under this item.

These elements were available or furnished to this Authority in the following language: , which is:

- ☐ the language of a translation furnished for the purposes of the international search (under Rule 23.1(b)).
☐ the language of publication of the international application (under Rule 48.3(b)).
☐ the language of a translation furnished for the purposes of international preliminary examination (under Rule 55.2 and/or 55.3).

3. With regard to any **nucleotide and/or amino acid sequence** disclosed in the international application, the international preliminary examination was carried out on the basis of the sequence listing:

- ☐ contained in the international application in written form.
☐ filed together with the international application in computer readable form.
☐ furnished subsequently to this Authority in written form.
☐ furnished subsequently to this Authority in computer readable form.
☐ The statement that the subsequently furnished written sequence listing does not go beyond the disclosure in the international application as filed has been furnished.
☐ The statement that the information recorded in computer readable form is identical to the written sequence listing has been furnished.

4. The amendments have resulted in the cancellation of:

- ☐ the description, pages:
☐ the claims, Nos.:



**INTERNATIONAL PRELIMINARY
EXAMINATION REPORT**

International application No. PCT/US00/08943

☐ the drawings, sheets:

5. ☐ This report has been established as if (some of) the amendments had not been made, since they have been considered to go beyond the disclosure as filed (Rule 70.2(c)):

(Any replacement sheet containing such amendments must be referred to under item 1 and annexed to this report.)

6. Additional observations, if necessary:

III. Non-establishment of opinion with regard to novelty, inventive step and industrial applicability

1. The questions whether the claimed invention appears to be novel, to involve an inventive step (to be non-obvious), or to be industrially applicable have not been examined in respect of:

☐ the entire international application.

☒ claims Nos. 19,21-25.

because:

☐ the said international application, or the said claims Nos. relate to the following subject matter which does not require an international preliminary examination (*specify*):

☐ the description, claims or drawings (*indicate particular elements below*) or said claims Nos. are so unclear that no meaningful opinion could be formed (*specify*):

☐ the claims, or said claims Nos. are so inadequately supported by the description that no meaningful opinion could be formed.

☒ no international search report has been established for the said claims Nos. 19,21-25.

2. A meaningful international preliminary examination cannot be carried out due to the failure of the nucleotide and/or amino acid sequence listing to comply with the standard provided for in Annex C of the Administrative Instructions:

☐ the written form has not been furnished or does not comply with the standard.

☐ the computer readable form has not been furnished or does not comply with the standard.

IV. Lack of unity of invention

1. In response to the invitation to restrict or pay additional fees the applicant has:

☐ restricted the claims.



**INTERNATIONAL PRELIMINARY
EXAMINATION REPORT**

International application No. PCT/US00/08943

- ☐ paid additional fees.
- ☐ paid additional fees under protest.
- ☒ neither restricted nor paid additional fees.
2. ☐ This Authority found that the requirement of unity of invention is not complied and chose, according to Rule 68.1, not to invite the applicant to restrict or pay additional fees.
3. This Authority considers that the requirement of unity of invention in accordance with Rules 13.1, 13.2 and 13.3 is
- ☐ complied with.
- ☒ not complied with for the following reasons:
see separate sheet
4. Consequently, the following parts of the international application were the subject of international preliminary examination in establishing this report:
- ☐ all parts.
- ☒ the parts relating to claims Nos. 1-18,26-29.

V. Reasoned statement under Article 35(2) with regard to novelty, inventive step or industrial applicability; citations and explanations supporting such statement

1. Statement

Novelty (N)	Yes:	Claims	1-18,20,26-29
	No:	Claims	
Inventive step (IS)	Yes:	Claims	2-17,27-29
	No:	Claims	1,20,26
Industrial applicability (IA)	Yes:	Claims	1-18,20,26-29
	No:	Claims	

2. Citations and explanations
see separate sheet

VII. Certain defects in the international application

The following defects in the form or contents of the international application have been noted:
see separate sheet



Re Item III

Non-establishment of opinion with regard to novelty, inventive step and industrial applicability

10/069996

JO Rec'd PCT/PTC 01 MAR 2002

- 1). As no required additional search fees were paid, no additional search was performed for claims 19 and 21-25.

Re Item V

Reasoned statement under Rule 66.2(a)(ii) with regard to novelty, inventive step or industrial applicability; citations and explanations supporting such statement

- 2). Reference is made to the following documents:

D1: WO 99 16102 A

D2: US-A-5 900 618 cited in the application

D3: C.GAO ET AL.: 'Quantitative microwave near-field microscopy of dielectric properties' REVIEW OF SCIENTIFIC INSTRUMENTS, vol. 69, no. 11, November 1998 (1998-11), pages 3846-3851, XP002144502 US

D4: TABIB-AZAR M ET AL: 'NOVEL PHYSICAL SENSORS USING EVANESCENT MICROWAVE PROBES' REVIEW OF SCIENTIFIC INSTRUMENTS,US,AMERICAN INSTITUTE OF PHYSICS. NEW YORK, vol. 70, no. 8, August 1999 (1999-08), pages 3381-3386, XP000870710
ISSN: 0034-6748

- 3). D1 and D2 describe near field microwave microscopes.

Document D1, which is considered to represent the most relevant state of the art, discloses an apparatus and method for contact-imaging (cf. Figs. 1 and 2) of the dielectric permittivity (see Table I), from which the subject-matter of claims 1, 20 and 26 differs only in minor details, which can be found in D2.

Claims 1,20 and 26 thus lack an inventive step.

- 4). The combination of the features of several dependent claims are neither known from, nor rendered obvious by, the available prior art. It has been suggested therefore that a new independent claim be drafted to include these features, bearing in mind that the features known in combination in D1 (or D2) should be placed in the preamble of such a claim in accordance with Rule 6.3(b) PCT.



Re Item VII

Certain defects in the international application

- 5). The features of the claims are not provided with reference signs placed in parentheses (Rule 6.2(b) PCT).
- 6). Contrary to the requirements of Rule 5.1(a)(ii) PCT, the relevant background art disclosed in the documents D1-D4 is not mentioned in the description, nor are these documents identified therein.

WO 01/20352 A1



For two-letter codes and other abbreviations, refer to the "Guidance Notes on Codes and Abbreviations" appearing at the beginning of each regular issue of the PCT Gazette.



Quantitative Imaging of Dielectric Permittivity and Tunability

Background of the Invention

Field of the Invention

The present invention relates generally to imaging, and more particularly to measuring dielectric properties using a near-field scanning microwave microscope.

Related Art

Dielectric thin film research has become increasingly important as the demand grows for smaller, faster, and more reliable electronics. For example, high permittivity thin films are under study in order to fabricate smaller capacitors while minimizing leakage. Low permittivity materials are being sought to allow smaller scale circuits while minimizing undesirable stray capacitance between wires. Nonlinear dielectrics, which have a dielectric permittivity which is a function of electric field, are being used in tunable devices, particularly at microwave frequencies. Finally, ferroelectric thin films are a solution for large-scale, non-volatile memories.

All of these dielectric thin film technologies demand high-quality, homogeneous films. However, this goal is often difficult to achieve because of the complicated fabrication process involved. Consequently, it is important to have a set of reliable techniques for evaluating thin film properties, such as permittivity and tunability. A number of different techniques are available. One standard low-frequency (≤ 1 MHz) method uses thin film capacitors to measure the normal and in-plane components of the permittivity tensor. Another uses reflection measurements from a Corbino probe. Still another method provides microwave measurements of permittivity by using transmission measurements through a



-2-

microstrip structure. However, these techniques average over large areas and involve depositing thin film electrodes which itself can alter the properties of the sample. Dielectric resonators have been used as well, but also have the problem of low spatial resolution. More recently, near-field microscopy techniques have
5 allowed quantitative measurements with spatial resolutions much less than the wavelength. These techniques use a resonator which is coupled to a localized region of the sample through a small probe and have the advantage of being non-destructive. However, it is still difficult to arrive at quantitative results and maintain high spatial resolution.

10 Therefore, what is needed is a non-destructive, non-invasive, system and method for imaging quantitative permittivity and tunability at high spatial resolution.

Summary of the Invention

The present invention meets the above-mentioned needs by providing a
15 system, apparatus, and method for quantitatively imaging the dielectric properties of bulk and thin film dielectric samples. Permittivity and dielectric tunability are two examples of dielectric properties capable of measurement by the present invention.

The system uses a near-field scanning microwave microscope (NSMM).
20 The NSMM is comprised of a coaxial transmission line resonator having one end coupled to a microwave signal source and the other end terminating with an open-ended coaxial probe. The probe, which has a sharp-tipped center conductor extending beyond the outer conductor, is held fixed while the sample is raster scanned beneath the probe tip. A spring-loaded cantilever sample holder gently
25 presses the sample against the probe tip with a force of about 50 μN (microNewtons). A feedback circuit keeps the microwave signal source locked onto a selected resonant frequency of the microscope resonator. Because the

-3-

electric fields generated by the microwave signal are concentrated at the probe tip, the resonant frequency and quality factor of the resonator are a function of the sample properties near the probe tip. Once the microwave signal has been applied to the sample through the probe tip, it is reflected back through the system. The feedback circuit is then able to receive the reflected microwave signal from the coaxial transmission line resonator and calculate a resonant frequency shift. The resonant frequency shift value is then stored in a computer. The computer also controls the scanning of the sample beneath the probe. To obtain quantitative results, the system uses calibration curves to exhibit the relationship between the calculated resonant frequency shift data values and the dielectric properties of a sample.

The invention described herein has the advantage of being able to provide quantitative results for samples on a length scale of about $1\mu\text{m}$ or less. This allows for the measuring of sample sizes relative to the actual environment in which they will be used.

The invention also has the advantage of providing more accurate quantitative results because the sharp protruding center conductor is represented as a cone during modeling.

Brief Description of the Figures

The features and advantages of the present invention will become more apparent from the detailed description set forth below and the following figures in which like reference numbers indicate identical or functionally similar elements. Additionally, the left-most digit of a reference number identifies the drawing in which the reference number first appears.

FIG. 1 illustrates the general structure and functionality of an embodiment of the present invention.

FIG. 2 illustrates the use of a spring-loaded cantilever sample support according to an embodiment of the present invention.

FIG. 3 is a diagram of a quantitative modeler used in an embodiment of the present invention.

5 FIG. 4 illustrates a resonant frequency shift detected by measurements taken when a sample was present versus when a sample was not present.

FIG. 5 shows a perturbation formula used in an embodiment of the present invention.

10 FIG. 6 is a diagram of the electric equipotential lines for a bulk sample according to a quantitative model of the present invention.

FIG. 7 is a diagram of the electric equipotential fields for a thin film sample according to a quantitative model of the present invention.

FIG. 8 is a diagram illustrating the modeling of the electric field near the microscope probe tip in an embodiment of the present invention.

15 FIG. 9 is a flow chart illustrating a method for determining dielectric properties according to the present invention.

FIG. 10 is a flow chart depicting an embodiment of a calibration routine of the present invention.

20 FIG. 11 is a flow chart depicting an embodiment of a scanning routine of the present invention.

FIG. 12 is a flow chart depicting an embodiment of a probe calibration curve generating routine.

FIG. 13 is a diagram representative of quantitative modeling curves generated in an embodiment of the present invention.

25 FIG. 14 is a diagram representative of a calibration curve generated in an embodiment of the present invention.

FIG. 15 illustrates the use of a modulating bias voltage to measure dielectric nonlinearity according to an embodiment of the present invention.

-5-

FIG. 16 illustrates a probe tip geometry descriptor according to an embodiment of the present invention.

FIG. 17 is a diagram representative of a calibration curve generated in an embodiment of the present invention.

5 FIG. 18 illustrates frequency shift measurements taken at different heights for several dielectric samples according to an embodiment of the present invention.

FIG. 19 is a diagram representative of calibration curves generated for frequency shift measurements taken at heights of 100 μm and 10 μm according to an embodiment of the present invention.

10 FIG. 20 illustrates the dielectric constant of a LaAlO_3 sample imaged at 100 μm and 9.08 GHz using a 480 μm diameter probe according to an embodiment of the present invention.

FIG. 21 is a chart displaying dielectric constant values taken from literature and the dielectric constant values obtained from experimental measurements taken according to a method of the present invention.

15 FIG. 22a illustrates a dielectric constant image of a test sample taken with a 480 μm probe at 9.08 GHz and 100 μm above the sample according to an embodiment of the present invention.

20 FIG. 22b illustrates the topography of a test sample found according to a method of the present invention.

Detailed Description of the Preferred Embodiments

25 The invention described herein is a system, apparatus, and method for displaying the dielectric properties of bulk and thin film samples. The invention uses a near-field scanning microwave microscope (NSMM).

Physical Design for the System of the Present Invention

An apparatus according to an embodiment of the present invention is illustrated in FIG. 1. System 100 shows a near-field scanning microwave microscope having an open-ended coaxial probe 130 with a sharp, protruding center conductor 185. A coaxial transmission line resonator 135 is used for producing a resonance between the probe tip 185 and the capacitive coupler 145. The microwave signal source 165 is responsible for generating a microwave signal. The feedback circuit 160 receives a reflected microwave signal from the coaxial transmission line resonator 135. Feedback circuit 160 also keeps the microwave signal source 165 locked onto a predetermined resonance. An additional function of the feedback circuit 160 is to calculate a value for at least one parameter related to a change in the resonance due to the dielectric properties of a sample 125. Two possible parameters measured are resonant frequency shift (Δf) and quality factor (Q). A stage-120 is used to support the sample 125 in contact with the sharp protruding center conductor 185. Alternatively, with respect to FIG. 2 described in more detail below, a further embodiment of the present invention has a spring-loaded cantilever sample holder 210 provided to hold the sample relative to the sharp protruding center conductor 185 and stage 120.

System 100 further includes motor controllers 115 for manipulating the sample 125 in contact with the sharp protruding center conductor 185 in a first, second, or third direction; for example, the sample can be moved and/or rotated along the x, y and z axes. A coupler 150 is attached between the microwave signal source 165 and the coaxial transmission line resonator 135. Coupler 150 could be a directional coupler, circulator, or other device for directing microwave signals known to one of ordinary skill in the art. The coupler initially directs the microwave signal towards the sample 125 and then directs the reflected microwave signal towards the feedback circuit 160.

-7-

A detector 155 is responsible for converting the reflected signal directed towards the feedback circuit 160 into a voltage signal representative of detected power. A computer 105 having both memory and a processor is also shown. The memory of computer 105 stores electric field configuration data files used for quantitative modeling. Computer 105 also stores calibration sample frequency shift values and test sample frequency shift values. The processor of computer 105 mathematically determines the functional relationship between at least one parameter related to a change in the resonant frequency shift and a known dielectric property value of a sample responsible for the change. An example of such a parameter is relative dielectric permittivity (ϵ_r). The processor of computer 105 is then able to receive from feedback circuit 160 resonant frequency shift values for a sample with unknown dielectric properties and determine the value of the unknown dielectric property based upon the model frequency shift-dielectric property relationship. Display device 110 is provided for displaying the value of the dielectric property once it has been determined by the processor 105.

FIG. 2 illustrates an alternative embodiment for the present invention where a spring-loaded sample support 200 is used to support the sample 125 beneath the probe tip 185. Sample support 200 uses a cantilever sample holder 210 having an angled end and a planar surface for supporting sample 125. A first bracing device 230 is fixed to the x-y stage and is joined to sample holder 210 by a spring 220. The spring 220 is positioned such that it is in close proximity to the pivot point created when the angled portion of sample holder 210 is brought into contact with a second bracing device 240 also attached to the x-y stage. This spring cantilever design allows the force applied by the probe tip 185 to remain substantially constant during scanning. Excessive wear of the probe tip during contact mode scanning is also reduced. The amount of force applied can be set by selecting an appropriate spring and adjusting the location of the spring and/or sample along the cantilever sample holder 210. In one example, a force of about 50 μN (microNewtons) is applied between the probe tip and sample 125.

System 100 also has a quantitative modeler described in FIG. 3 for determining the model frequency shift-dielectric property relationship.

Quantitative modeler 300 receives resonant frequency shift values for calibration samples with known dielectric properties and test samples with unknown dielectric properties from computer 105 memory. Quantitative modeler 300 provides the measured resonant frequency shift data to Model calibration curve generator 310 Probe calibration curve generator 320 and Test sample curve generator 330 in order to generate data (such as, tables, graphs, files or curves) showing the relationship between a measured resonant frequency shift and a particular dielectric property. In particular, Model calibration curve generator 310 generates model calibration curves at different values of a geometric descriptor that show the relationship between a measured resonant frequency shift (Δf) and a dielectric property (e.g. permittivity ϵ_r) for calibration reference samples. The operation of Model calibration curve generator 310 is further described with reference to figures 12 and 13. Probe calibration curve generator 320 and Test sample calibration curve generator 330 generate calibration curves drawn from the model calibration curves and a geometric descriptor value of the probe tip 185. The calibration curves show the relationship between a resonant frequency shift (Δf) measured during scanning and a dielectric property (e.g. permittivity ϵ_r) at a geometric descriptor value of the actual NSMM used in imaging. The calibration curve allows a dielectric property to be determined by finding the point on the curve corresponding to the resonant frequency shift measured during scanning. The operation of Probe calibration curve generator 320 and Test calibration curve generator 330 is further described with respect to figures 9, 12, 14 and 17.

It is helpful to begin with discussion of quantitative modeling according to the present invention with reference to figures 4 to 8, and 16. Operation of the present invention is then further described with respect to figures 9-15.

Quantitative Modeling

Calculating the Electric Field Near the Probe Tip

In order to arrive at quantitative results, the inventors developed a physical model for the system, starting with the simplest case of a uniform bulk sample. Because the probe tip length is much smaller than the free space wavelength of the microwaves (~ 4 cm), a static calculation of the microwave electric fields is performed. Cylindrical symmetry further simplifies the problem to two dimensions. Because of the complicated geometry of the probe tip in contact with a potentially multi-layered sample, a finite element model on a grid is used. Using relaxation potential Φ in the region represented by the grid and taking into account any changes in the permittivity ϵ_r , yields:

$$\nabla^2 \Phi + \frac{1}{\epsilon_r} (\nabla \Phi) \cdot (\nabla \epsilon_r) = 0 \quad (1)$$

Using a rectangular grid, the inventors represent the probe tip as a cone with a blunt end of radius r_0 , and perform the calculation in a spreadsheet program. From Eq. (1), if Φ_{ij} is the potential at the cell at column i and row j , Φ_{ij} is a weighted average of the values of the four adjacent cells:

$$\Phi_{ij} = \frac{\Phi_{i+1,j} \left(1 + \frac{\Delta r}{r} \right) + \Phi_{i-1,j} + \Phi_{i,j-1} + \Phi_{i,j+1}}{4 + \frac{\Delta r}{r}}, \quad (2)$$

where r is the radius from the cylindrical coordinate axis, referring to FIG. 16, Δr and Δz are the spacing between cells in the r and z directions, respectively, and



-10-

$\Delta r = \Delta z$. Equation (2) is the simplest case; in practice, the equation is more complicated, such as at the interface between the dielectric sample ($\epsilon_r > 1$) and the air ($\epsilon_r = 1$). Near the probe tip where the electric field is the strongest, and hence, the most critical, the grid spacings Δr and Δz are small and uniform. Inside this
 5 box, $\Delta z = \Delta z_{in} = 0.1 \mu\text{m}$, is fixed while the value of $\Delta r = \Delta r_{in}$ is uniform, but adjustable ($0.5 \mu\text{m} \leq \Delta r_{in} \leq 1.0 \mu\text{m}$), to allow for probe tips with different sharpness. In FIG. 16, the geometry descriptor of a probe tip's sharpness is represented with an aspect ratio parameter $\alpha \equiv \Delta z_{in}/\Delta r_{in}$.

The boundaries of the grid should be sufficiently far away in order to
 10 minimize the effect of the chosen boundary conditions on the electric field near the probe tip. To accomplish this, outside a region close to the probe tip, the values of Δr and Δz continuously increase with distance away from the probe tip, allowing the outer radius of the grid to be at least 4 mm, and the height of the grid to be 2 mm. The resulting grid consists of 84×117 cells, which is small enough
 15 to be a manageable calculation with a modern personal computer. The top and outer boundary conditions are $d\phi/dn = 0$ where n is the coordinate normal to the edge. At the bottom of the grid, which represents the bottom side of the $500 \mu\text{m}$ thick sample, $\phi = 0$ is used for the boundary condition. To match this condition, the sample is placed on top of a metallic layer for scanning; this has the added
 20 benefit of shielding the microscope from the effects of whatever is beneath the sample, which could be difficult to model.

Two possible fitting parameters for the model are the geometry descriptor, i.e., aspect ratio α , and the radius r_0 of the blunt probe end. The inventors found that a satisfactory fit with data could be obtained by fixing $r_0 = (0.6 \mu\text{m})/\alpha$. This
 25 leaves α as a single fitting parameter to represent all probes; the inventors have found that typically $1 < \alpha < 2$. When α is small, for example less than 1.5, the probe tip is considered to be blunt. When α is large, for example greater than 1.5, the probe tip is considered to be sharp.



Calculating the Frequency Shift of the Microscope

Using perturbation theory, the frequency shift of the microscope is calculated as a function of the fields near the probe tip. FIG. 4 illustrates the frequency shift during an unperturbed state, i.e., no sample present and a perturbed state, i.e., sample present beneath the probe. The width of the minima change with respect to the changes in quality factor (Q). With reference to FIG. 5, ϵ_{r1} and ϵ_{r2} are defined as the permittivities of two model samples, the subscripts 1 and 2 indicating the unperturbed and perturbed system. If \vec{E}_1 and \vec{E}_2 are the calculated electric fields inside the two model samples, where $\vec{E} = -\nabla\Phi$, the frequency shift of the microscope upon going from sample 1 to sample 2 is

$$\frac{\Delta f}{f} \approx \frac{\epsilon_0}{4W} \int_{V_s} (\epsilon_{r2} - \epsilon_{r1}) \vec{E}_1 \cdot \vec{E}_2 dV \quad (3)$$

where $\epsilon_0 = 8.85 \times 10^{-12}$ F/m is the permittivity of free space, W is the energy stored in the resonator, and the integral is over the volume V_s of the sample. An approximate W is calculated using the equation for the loaded Q of the resonator, $Q_L = \omega_0 W / P_l$, where ω_0 is the resonant frequency, and P_l is the power loss in the resonator. In one example, a bare 500 μm thick LaAlO_3 (LAO) substrate is used for the unperturbed system because its properties are well-characterized ($\epsilon_r = 24$) and it is a common substrate for oxide dielectric thin films.

FIG. 6 illustrates the electric fields present when a bulk sample is scanned beneath probe tip.



Modeling of Dielectric Thin Films

FIG. 7 illustrates the modeling of thin films. To provide for imaging of thin films, the finite element model is extended to include a thin film 710 on top of a dielectric substrate 715 having the same thickness as the model samples. As long as the thin film 710 is on a substrate having the same thickness as the model sample, the only perturbation is the thin film (the change in total thickness of the sample is negligible compared to the thick substrate). The electric field 705 in the thin film sample is calculated using the finite element model of the present invention and Eq. (3) to calculate Δf , integrating only over the volume of the thin film. Once a probe's α parameter is found using the process described above for bulk samples, the thin film model is used to obtain a functional relationship between Δf and ϵ_r of the thin film.

In producing the quantitative models discussed above, samples are chosen so as to cover a range of permittivity values in which the dielectric permittivity of an unknown sample is expected to fall within. The known values ϵ_r and t (thickness of the thin film 710) and the calculated values α and Φ are all stored in electric field configuration data files respective to each sample. In FIG. 8 for example, quantitative modeling data has been generated using samples with dielectric permittivity values of 10 to 200 and probe tip geometry of $\alpha=1$ and $\alpha=2$. Accordingly, the electric field configuration data files are usable in cases where the dielectric permittivity for an unknown sample can be expected to be between 10 and 200.

The following articles are related to quantitative modeling according to the present invention and are incorporated by reference herein in their entirety:

"Imaging of microwave permittivity, tunability, and damage recovery in (Ba, Sr) TiO₃ thin films", D.E. Steinhauer, C.P. Vlahacos, F.C. Wellstood, Steven M. Anlage, C. Canedy, R. Ramesh, A. Stanishevsky, and J. Melngailis, *Applied Physics Letters*, Volume 75, Number 20, p. 3180 (1999); and

"Non-Contact Imaging of Dielectric Constant with a Near-Field Scanning Microwave Microscope", C.P. Vlahacos, D. E. Steinhauer, Steven M. Anlage, F.C. Wellstood, Sudeep K. Dutta, and Johan B. Feenstra, *The Americas Microscopy and Analysis*, p. 5, January 2000.

5 ***Method of the Present Invention***

Dielectric Permittivity Imaging

A method for an embodiment of the present invention is illustrated by flowchart 900 of FIG. 9. The method begins with a step 905. In a step 910, system 100 is calibrated according to the probe calibration routine described in
10 FIG. 10 to obtain calibration sample frequency shift values ($\Delta f_{\text{sampleC}}$), a probe tip geometry descriptor, and sample geometry.

Test Sample Scanning

In a step 915, a test sample 125 with unknown dielectric properties is scanned according to the routine described in FIG. 11 to obtain test sample
15 resonant frequency shift measurements ($\Delta f_{\text{sampleT}}$). These measurements can also include determining quality factor (Q), and/or tunability information. If the test sample is a thin film then it contains both a dielectric thin film and substrate. Step 915 will now be described with reference to the steps provided in FIG. 11. The method begins with a step 1105. In a step 1110 a resonant frequency of the near-
20 field scanning microwave microscope is selected. In a step 1115 a test sample is placed on the microscope stage. In a step 1120 the probe tip is moved into contact with the test sample. In a step 1125 raster scanning begins. In a step 1130 a position value corresponding to the initial point of contact with the test sample is stored in computer 105 memory as the next scanning point.

-14-

In a step 1135 the probe is moved to a predetermined background measurement position where the calibration sample no longer perturbs the resonator. For example, the predetermined background measurement position can be a height 1.5 times greater than the diameter of the microscope transmission line 135, or a height at least approximately 3 millimeters above the calibration sample. In a step 1140 a background resonant frequency shift measurement is taken from the background measurement position. In a step 1145 the probe tip is moved back into contact with the test sample at the next scanning point. In a step 1150 the contact resonant frequency shift at the scanning point is measured. In a step 1155 the difference between the contact resonant frequency shift at the scanning point and the background resonant frequency shift is calculated. In a step 1160 the calculated difference is saved in computer 105 memory as the test sample resonant frequency shift value.

In a step 1165 the microscope probe tip is moved to the next scanning position. In a step 1170 computer 105 determines if the next scanning position is the end of a scan line. If the end of a scan line has not been reached then steps 1150 through 1165 are repeated. Next, at a step 1175 computer 105 determines if the next scanning position is the end of a scan area. If it is not then steps 1135 through 1170 are repeated until the end of a scan area has been reached. At the conclusion of step 915 a set of test sample resonant frequency values have been recorded or stored in computer 105 memory.

In a step 920, the calibration sample resonant frequency shift values obtained from step 910 are used to generate a probe calibration curve according to the routine described in FIG. 12. In a step 925, a determination of whether the test sample is a thin film is made. In a step 930, a determination of whether all of the calibration samples have the same thickness as the test sample is made. If the test sample is not a thin film, and all of the calibration samples have the same thickness as the test sample, then in a step 945, one is able to determine an unknown dielectric property for a sample by first retrieving a test sample resonant

-15-

frequency shift value ($\Delta f_{\text{sampleT}}$) obtained in step 915 and then locating the corresponding Δf value on the probe calibration curve resulting from step 920. The dielectric property of the test sample is equal to the dielectric property corresponding to the Δf value on the probe calibration curve resulting from step 920. If the test sample is a thin film, or if only one calibration sample has the same thickness as the test sample, then in a step 935 a test sample calibration curve is generated. In a step 940 one is able to determine an unknown dielectric property for a test sample by first retrieving a test sample resonant frequency shift value ($\Delta f_{\text{sampleT}}$) obtained in step 915 and then locating the corresponding Δf value on the test sample calibration curve resulting from step 940. The dielectric property of the test sample is equal to the dielectric property corresponding to the Δf value on the test sample calibration curve. The process concludes with a step 950.

In an alternative embodiment, step 920 can be performed prior to step 915. In a further embodiment, step 910 can be performed after step 915 but before step 920. Furthermore, steps 1135, 1140, and 1145 could alternatively be measured at each point on the sample, any desired number of times during the scan, before the scan, or after the scan.

Calibration

To measure the unknown dielectric permittivity (ϵ_r) of a dielectric sample, the NSMM is calibrated to determine the parameter α using at least two samples with known permittivity (ϵ_r) and thickness (t). The thickness of a bulk dielectric test sample or a thin film test sample on top of a dielectric substrate, is referred to as the first determined thickness. For thin film dielectric test samples the thickness of the thin film is referred to as the second determined thickness.

The process of calibrating system 100 is illustrated by flowchart 1000 of FIG. 10. The process starts at a step 1010. At a step 1015, at least two



-16-

calibration samples that have known dielectric properties are selected. At least two of the calibration samples have the same approximate thickness with one another. In addition, at least one of the calibration samples has the same approximate thickness as the test sample with first determined thickness and unknown dielectric properties. If the test sample contains a thin film, an additional requirement is that the at least one calibration sample with approximate thickness equal to the test sample first determined thickness have the same permittivity as the substrate of the test sample.

Calibration Sample Scanning

In a step 1020, each selected calibration sample is scanned according to the scanning routine described in FIG. 11 to determine respective sets of resonant frequency shift information for samples with known dielectric permittivity values. The method begins with a step 1105. In a step 1110 a resonant frequency of the near-field scanning microwave microscope is selected. In a step 1115 a calibration sample is placed on the microscope stage. In a step 1120 the probe tip is moved into contact with the calibration sample. In a step 1125 raster scanning begins. In a step 1130 a position value corresponding to the initial point of contact with the calibration sample is stored in computer 105 memory as the next scanning point. In a step 1135 the probe is moved to a predetermined background measurement position where the calibration sample no longer perturbs the resonator. For example, the predetermined background measurement position can be a height 1.5 times greater than the diameter of the microscope transmission line 135, or a height at least approximately 3 millimeters above the calibration sample. In a step 1140 a background resonant frequency shift measurement is taken from the background measurement position. In a step 1145 the probe tip is moved back into contact with the calibration sample at the next scanning point. In a step 1150 the contact resonant frequency shift at the scanning point is measured. In a step

1155 the difference between the contact resonant frequency shift at the scanning point and the background resonant frequency shift is calculated. In a step 1160 the calculated difference is saved in computer 105 memory as the calibration sample resonant frequency shift value. In a step 1165 the microscope probe tip
5 is moved to the next scanning position. In a step 1170 computer 105 determines if the next scanning position is the end of a scan line. If the end of a scan line has not been reached then steps 1150 through 1165 are repeated. Next, at a step 1175 computer 105 determines if the next scanning position is the end of a scan area. If it is not then steps 1135 through 1170 are repeated until the end of a scan area
10 has been reached. Step 1020 is repeated for each calibration sample.

At a step 1025, a geometry descriptor of the probe tip is determined. The geometry descriptor can be input by a user or calculated by System 100. A geometry descriptor can be any descriptor representative of the geometry of the probe tip. Accordingly, in one embodiment of the present invention, a geometry
15 descriptor is referred to as a first probe tip geometry descriptor value and a second probe tip geometry descriptor value. In another embodiment, an aspect ratio $\alpha = \Delta z / \Delta r$ is used where, Δz is a distance along a z-direction parallel to a length of the resonator and the probe tip and Δr is a radius distance extending from the central axis of the probe tip 185 to its outermost surface.

20 At a step 1030, sample geometry data is input. For example, with bulk samples, sample geometry data includes the thickness of the sample. For thin film samples on a bulk substrate, the thickness of the thin film is provided as well.

Calibration Curve Generation

FIG 12 describes the routine for generating a calibration curve. The routine begins at a step 1205. At a step 1210 electric field configuration data is stored as described in FIG 8. The stored files contain data for model samples having approximately the same thickness as the calibration sample scanned in step 1020. At least one file for each value of α has the same permittivity value as one of the calibration samples scanned in step 1020. This permittivity is defined to give the unperturbed system, with $\Delta f=0$.

At a step 1215 model calibration curves are generated by reading from at least two of the previously stored electric field configuration data files, electric field values and permittivity values for at least two respective probe tip geometry descriptor values. FIG. 13 provides an example of model calibration curves for $\alpha=1$ and $\alpha=2$. To generate the model calibration curve where $\alpha=1$, a first previously stored electric field value (E_1) and a first permittivity value (ϵ_{r1}) is chosen to represent the zero point ($\Delta f=0$). A second electric field configuration data file where $\alpha=1$ is then read to obtain a second previously stored electrical field value (E_2) and a second permittivity value (ϵ_{r2}). A point on the first model calibration curve is then generated by solving the equation

$$\frac{\Delta f}{f} \approx \frac{\epsilon_0}{4W} \int_{V_s} (\epsilon_{r2} - \epsilon_{r1}) \vec{E}_1 \cdot \vec{E}_2 dV$$

Multiple points on the first model calibration curve can be generated by repeating step 1215 for different values of ϵ_{r2} and E_2 . The second model calibration curve for $\alpha=2$ is generated as described above except that electric field configuration data files where α equals two are used instead.

At a step 1220, a calibration curve is generated using the model calibration curves from step 1215 and the calibration sample frequency shift values



from step 1020. A point on the calibration curve is generated by first calculating the difference between two calibration sample frequency shift values. One of the calibration frequency shift values used in the calculation should correspond to zero point permittivity value from step 1215. Once the difference value has been
5 determined it can be plotted with respect to the Δf axis of the model calibration curve. FIG. 14 provides an example where four calibration points have been plotted with respect to the model calibration curve of FIG. 13 to produce a calibration curve for $\alpha=1.5$. The value for α for the probe is determined by observing the position of the curve C_p relative to the curves C_{m2} and C_{m1} .

10

Test Sample Calibration Curve Generation

If the test sample is a thin film sample, or if only one calibration sample has the same thickness as the first determined thickness of the test sample, then a separate test sample calibration curve must be generated, in step 935.

15

An example test sample calibration curve C_{ts} is shown in FIG. 17. The curve C_{ts} is used in step 940 to convert the frequency shift values obtained in step 915 to the values of the permittivity of the test sample. The curve C_{ts} can be calculated using one of two methods. For the first method, the calculation is done for the specific value of α determined in step 920 (such as $\alpha = 1.5$, as shown in FIG. 17). For the second method, the calculation is done for two or more values
20 of α , shown in FIG. 17 as the curves C_{ts1} and C_{ts2} . Then, the curve C_{ts} is calculated for the value of α determined in step 920 by interpolating between the curves C_{ts1} and C_{ts2} . The advantage of the second method is that generating the curves C_{ts1} and C_{ts2} can be done in advance just once, requiring less calculation for each scan.

20

25

For the case where the test sample is a bulk sample, and only one calibration sample has the same thickness as the test sample, the curves in FIG 17 are calculated using the same method as was performed in the previous section with the probe calibration curve. The difference is that a new set of files



(represented in FIG. 8) are used, which represent a sample thickness equal to the test sample thickness. The frequency shift measured with the NSMM for the calibration sample having the same thickness as the test sample (done in step 910) is defined as $\Delta f=0$ for the test sample calibration curves in FIG. 17.

5 For the case of a thin film test sample, the curves C_{ts1} and C_{ts2} in FIG. 17 are calculated according to the routine described in FIG. 12. However, a different set of files represented in FIG. 8 is now used. In this new set, the files represent a thin film having a thickness equal to the second determined thickness of the thin film in the test sample. The volume V_s is the volume of the thin film, rather than
10 the volume of the entire sample. The frequency shift measured with the NSMM for the calibration sample which has the same thickness as the test sample, and the sample permittivity as the test sample substrate, is defined as $\Delta f=0$ for the curves in FIG. 17.

Nonlinear Dielectric Imaging

15 FIG. 15 illustrates how electric field-dependent imaging can be accomplished by applying a voltage bias (V_b) 1505 to the probe tip via a bias tee 180 in the resonator according to a further feature of the present invention. A metallic layer 1520 beneath the thin film 1510 acts as a grounded
counterelectrode.

20 As shown in FIG 15, a sample 125 can be a dielectric thin film 1510. The dielectric thin film 1510 is disposed on a grounded counterelectrode 1520. The grounded counterelectrode 1520 is provided on a substrate 1530. In order to prevent the counterelectrode 1520 from dominating the microwave measurement (modeling of the system has shown this to be a potential problem), the inventors
25 use a high-sheet-resistance counterelectrode, making it virtually invisible to the microwave fields. As a result, the presence of the thin-film counterelectrode 1520 can be safely ignored in the finite element model described above. Because the



-21-

counterelectrode 1520 is immediately beneath the dielectric thin film, the applied electric field is primarily in the vertical direction, unlike the microwave electric field, which is mainly in the horizontal direction for thin films with large permittivities. Also, by simulating the applied field using a finite element model similar to that presented above, the inventors find that the applied electric field beneath the probe tip is approximately uniform and equal to $E_b = V_b/t_f$ where t_f is the thickness of the dielectric thin film.

By modulating the bias voltage 1505 applied to the probe tip, nonlinear terms in the permittivity can be extracted. Expanding the electric displacement D in powers of the electric field E, and keeping only the nonzero terms yields

$$D_1(E) = \epsilon_{11}E_1 + \frac{1}{2}\epsilon_{113}E_1E_3 + \frac{1}{6}\epsilon_{1133}E_1E_3^2 + \dots \quad (4)$$

where E_1 is the rf electric field in the r direction, and $E_3 = E_b$ is the applied bias electric field in the z direction.

Adding a low-frequency oscillatory component ($\omega_b = 1$ kHz, with an amplitude of $\tilde{V}_b = 1$ V, for example) to the bias voltage, the applied electric field is $E_b = E_b^{dc} + \tilde{E}_b \cos \omega_b t$. The effective rf permittivity is then

$$\begin{aligned} \epsilon_{rf} = & \epsilon_{11} + \epsilon_{113}E_b^{dc} + \epsilon_{1133}\left(\frac{(E_b^{dc})^2}{2} + \frac{\tilde{E}_b}{4}\right) \\ & + (\epsilon_{113} + \epsilon_{1133}E_b^{dc})\tilde{E}_b \cos(\omega_b t) \\ & + \frac{1}{4}\epsilon_{1133}\tilde{E}_b^2 \cos(2\omega_b t) + \dots \end{aligned} \quad (5)$$



-22-

Note that the components of ϵ_{rf} at ω_b and $2\omega_b$ are approximately proportional to ϵ_{113} and ϵ_{1133} , respectively. Expanding the resonant frequency of the microscope as a Taylor series about $f_0(\epsilon_{rf} = \epsilon_{11})$, yields

$$f_0[\epsilon_{rf}(t)] = f_0(\epsilon_{11}) + \left. \frac{df_0}{d\epsilon_{rf}} \right|_{\epsilon_{rf}=\epsilon_{11}} [\epsilon_{rf}(t) - \epsilon_{11}] + \dots \quad (6)$$

5 Substituting Eq. 5 into Eq. 6, and keeping only the larger terms,

$$\begin{aligned} f_0(t) \approx & \text{constant} + \epsilon_{113} \tilde{E}_b \left. \frac{df_0}{d\epsilon_{rf}} \right|_{\epsilon_{11}} \cos(\omega t) \\ & + \frac{1}{4} \epsilon_{1133} \tilde{E}_b^2 \left. \frac{df_0}{d\epsilon_{rf}} \right|_{\epsilon_{11}} \cos(2\omega t). \end{aligned} \quad (7)$$

Thus, the components of the frequency shift signal at ω_b and $2\omega_b$ can be extracted to determine the nonlinear permittivity terms ϵ_{113} and ϵ_{1133} . These nonlinear terms can be measured simultaneously with the linear permittivity (ϵ_{11}) while scanning.

10 As an alternative, the electric field E_b could be applied in the horizontal direction using thin film electrodes deposited on top of the dielectric thin film. The advantage here is that diagonal nonlinear permittivity tensor terms could be measured, such as ϵ_{111} and ϵ_{1111} ; the disadvantage in this case is that imaging is limited to the small gap between the electrodes.



Simultaneously Measuring Sample Topography

Using a spring-loaded sample holder such as that shown in FIG. 2, one can also measure sample topography. This is accomplished by measuring the deflection of the sample holder during a scan. Because the probe tip is held fixed, the sample holder will deflect depending on the topography of the sample. For example, if the sample has a bump on top of it, the sample holder will deflect downward. One can record this deflection during a scan, and obtain a topographical image corresponding to the same region as the microwave image(s).

The measurement of the deflection of the sample holder could be accomplished using one of many techniques, including an optical sensor, a capacitive sensor, an interferometer, etc.

Overview

The microwave microscope, as covered in patent 5,900,618, consists of a resonator contained in a microwave transmission line. One end of the resonator is an open-ended coaxial probe, which is held close to the sample, and the other end is coupled to a microwave source with a coupling capacitor. A sample is scanned beneath the probe. Because of the concentration of the microwave fields at the probe center conductor, the resonant frequency and quality factor Q of the resonator are perturbed depending on the properties of the sample near the probe center conductor. One quantity recorded while scanning is the resonant frequency shift (Δf) of the resonator.

Two modes of operation are non-contact mode and contact mode. In non-contact mode, the preferred embodiment is with the probe center conductor flush with the face of the probe, so that the end of the center conductor is in the same plane as the end of the outer conductor. A sample is scanned beneath the probe with a small gap of 10-100 μm between the probe and the sample. In contact

-24-

mode imaging, the center conductor extends beyond the outer conductor, and has a sharp point. The sample holder gently presses the sample against the probe tip with a small force.

5 The invention involves calibration using dielectric samples with known permittivity. In the case of non-contact mode, the calibration data is interpolated, allowing one to scan dielectric samples with the same thickness as the calibration samples, and to convert the microscope frequency shift into the local permittivity of the sample. In the case of contact-mode imaging, a physical model is used to generate the relationship between the frequency shift of the microscope and the
10 local permittivity of the sample. Because of the use of the model with contact-mode imaging, quantitative imaging in this case is not limited to samples which have the same thickness as the calibration samples. The contact-mode imaging can be used for both bulk and thin-film samples.

15 In contact mode, a low-frequency electric field can also be applied to the sample, so that permittivity can be measured as a function of the applied electric field. Thus, dielectric nonlinearity can be measured as well as the linear permittivity.

When scanning in contact mode, an optical sensor can be used to measure the deflection of the sample holder, and hence, the sample, as the sample is
20 scanned in contact with the probe tip. The deflection is exactly equal to the topographic changes in the sample. Thus, by recording this reflection at the same time that Δf is measured, the sample topography can be imaged simultaneously with the permittivity.

25 In one embodiment of non-contact mode imaging, the local dielectric constant of a material is determined by measuring the frequency shift of the microscope as a function of height above the sample. Areas as small as 100 μm in diameter can be measured.

-25-

An unknown sample is scanned and a dielectric constant is measured as a function of position as long as the height of the probe above the sample is accurately known.

5 The technique can be performed quickly and at many locations on a bulk dielectric material.

The techniques can be done over a very broad range of frequencies simply by choosing other resonant modes of the microscope. In principle one can measure between about 100 MHz and 50 GHz.

10 The technique can be applied over a broad range of temperatures, from 1.2K to well above room temperature, possibly as high as 1000°C.

Non-Contact Imaging of Dielectric Constant with a Near-Field Scanning Microwave Microscope

15 In another embodiment of the present invention, a non-contact technique for imaging dielectric constant using a resonant near-field scanning microwave microscope is provided. By measuring the shift in the system's resonant frequency during a scan over an insulating sample, one can obtain quantitative images of dielectric variations. In one example, the inventors scanned seven samples with dielectric constants ϵ_r ranging from 1 to 230, using a 480 μm diameter probe at
20 a height of 100 μm and a frequency of 9.08 GHz. The technique achieves an accuracy of about 25% for $\epsilon_r=230$ and less than 2% for $\epsilon_r=2.1$, limited mainly by variations in the probe-sample separation.

This approach offers a fast, simple, broadband method to image dielectrics using readily available microwave components.

25 In one embodiment, resonant near-field scanning microwave microscope consists of a 1m long coaxial transmission line which is capacitatively coupled to a microwave source at one end and terminated by an open-ended coaxial probe at the other end. This arrangement creates a resonant circuit in which the resonant frequency f_0 and quality factor Q are modified when a sample approaches the open

end of the probe (see inset in Fig. 18). By using a frequency-following feedback circuit the invention keeps the microscope source locked on resonance. The shift of the system's resonant frequency Δf as the sample under the probe is scanned. The variations in Δf are directly related to spatial variations in dielectric constant in the sample. In addition, however, topographic changes will also give rise to changes in Δf .

Calibration Example

To calibrate the system, the inventors constructed a test sample by placing six pieces of different dielectric material into the bottom of a square plastic mould and pouring epoxy into the mould. In addition, silicone adhesive was used to hold each piece down. After the epoxy cured, the test sample was removed from the mould, polished, and positioned on the XY table. The materials embedded in the epoxy were silicon, glass microscope slide, SrTiO_3 , Teflon, sapphire, and LaAlO_3 . All six pieces were approximately 500 μm thick and about 6 mm x 8 mm in size. The overall thickness of the test sample was 6 mm.

The frequency shift Δf versus height h above the six pieces having dielectric constants ranging from 2.1 to about 230 is measured. The inventors also tested the epoxy which has an unknown dielectric constant. Each piece, as well as the probe, was flat and smooth on the scale of 5 μm as judged by an optical microscope. For these measurements, a probe with a 480 μm center conductor diameter and a source frequency of 9.08 GHz was used in one example of implementation. For each scan, the probe was first brought in contact with a dielectric sample and the frequency shift Δf was recorded as the height was systematically increased. The results are plotted in Fig. 18. Samples with the largest dielectric constant produced the largest frequency shift, as expected. The largest shift observed was -26.2 MHz, when the probe was in contact with a SrTiO_3 sample with $\epsilon_r=230$. The smallest shift found was -1.2 MHz when the



probe was in contact with a Teflon sample with $\epsilon_r=2.1$. As can be seen from Fig. 18, the frequency shift is essentially zero above 1 mm and saturates when the probe-sample distance is smaller than a few microns.

5 The inventors used the above information to construct an empirical calibration curve that directly relates the frequency shift to the dielectric constant ϵ_r . In order to construct the calibration curve the inventors took the difference between the frequency shift at two different heights h_1 and h_2 , i.e., $f_d=\Delta f(h_2)-\Delta f(h_1)$, where h_2 is far away ($h_2>1000\text{ }\mu\text{m}$). By taking the difference, the effect of drift in the microwave source frequency is eliminated. As shown in Fig. 19, two
10 calibration curves of f_d versus ϵ_r can be constructed, one curve for $h_1=10\text{ }\mu\text{m}$ and $h_2=1.1\text{ mm}$ and the other for $h_1=100\text{ }\mu\text{m}$ and $h_2=1.1\text{ }\mu\text{m}$. The parameters in each calibration curve are set with an empirical function (solid lines in Fig. 19), allowing us to easily transform any measured frequency shift to a dielectric constant. From these curves one can see that one can enhance the sensitivity to
15 the dielectric constant considerably by using a small probe height. On the other hand, at closer probe-sample separations the influence of topographic features will be enhanced.

Imaging Results

To test the dielectric imaging capabilities of our system, the inventors next
20 scanned a single sample of LaAlO_3 which had an 8 x 5 mm triangular shape and a thickness of 510 μm . The inventors placed the sample directly on the metal scanning table and recorded the frequency shift as a function of position. The data was taken at 9.08 GHz using the 480 μm probe at heights of 100 μm and 1.1 mm. The two data sets are subtracted and a 100 μm calibration curve is used to
25 transform the resulting frequency shift image into a dielectric constant image. Figure 20 shows the resulting contour image of dielectric constant versus position. The dielectric constant varies from about 20 to 25 over the sample and equals 1

when the probe is away from the sample. For comparison, the reported value of relative permittivity for LaAlO_3 at room temperature is $\epsilon_r=23.9$ at 18 GHz. In this image, the main variation in ϵ_r over the sample is due to a slight tilt in the sample surface of about 20 μm . The edges of the sample show a smaller value of ϵ_r due to averaging over the inner conductor of the probe. The width of the affected region is in good agreement with the expected spatial resolution of about 500 μm .

The inventors next recorded a frequency shift image of the six-piece test sample using a probe-sample separation of 100 μm and the 480 μm diameter probe at 9.08 GHz. As before, using the $\epsilon_r(f_d)$ calibration, the frequency shift image is transformed into a dielectric constant image (see Fig. 22a). The darker regions in Fig. 22a indicate a higher dielectric constant (larger frequency shift) and the lighter regions indicate a smaller dielectric constant (smaller frequency shift). Figure 22b shows the corresponding surface plot representation. Note that the z-axis in Fig. 22b uses a logarithmic scale to allow us to show the large range of dielectric constants present in the sample. As expected, the largest dielectric constant materials (SrTiO_3 and LaAlO_3) are the highest surfaces and the smallest dielectric constant materials (Teflon and vacuum) are the lowest. Further, notice that the Teflon sample forms a depression in Fig. 22b, indicating that the dielectric constant of Teflon is lower than the surrounding epoxy. Note that voids in the epoxy can easily be seen as irregularly shaped low-dielectric regions (white regions in Fig. 22a) in the epoxy. Fig. 21 summarizes the dielectric constants for the six test materials and provides comparative data taken from literary sources.

From Fig. 22b, it is apparent that there is some noise in our images of dielectric constant. In our system, the predominant sources of random errors are noise in our recording electronics and fluctuations in the source frequency. To establish the precision to which ϵ_r can be determined, we determined the standard deviation in ϵ_r over a small region near the center of the LaAlO_3 sample in Fig. 20; we found $\Delta \epsilon_r=0.06$ for a sampling time of 30 ms. Similarly, over the Teflon in Fig. 22a, the standard deviation in ϵ_r was 7×10^{-4} for a sampling time of 30 ms.

From Fig. 22 we can also estimate the absolute accuracy of our technique. For $\epsilon_r=230$ (SrTiO_3) the accuracy is about 25% while for $\epsilon_r=2.1$ (Teflon) the accuracy is better than 2%. The main source of these errors is topographic variations. In our test sample, even after polishing, there are small height variations of about 30 μm (e.g. between the sapphire and SrTiO_3 in Fig. 22) between the different dielectrics. Such height variations cause an additional frequency shift, resulting in an error in the measured dielectric constant. In this regard, an accurate measurement of the dielectric constant of a single flat dielectric sample is considerably easier. However, the image of the composite sample clearly demonstrates the strength and sensitivity of this non-contact technique to measure variations in ϵ_r .

Conclusion

While various embodiments of the present invention have been described above, it should be understood that they have been presented by way of example, and not limitation. It will be apparent to persons skilled in the relevant art(s) that various changes in form and detail can be made therein without departing from the spirit and scope of the invention. Thus the present invention should not be limited by any of the above-described exemplary embodiments, but should be defined only in accordance with the following claims and their equivalents.

What Is Claimed Is:

1. A method for contact imaging of dielectric permittivity using a near-field scanning microwave microscope having a resonator with a probe tip comprising the steps of:
 - 5 (a) calibrating the near-field scanning microwave microscope to determine a geometry descriptor of the probe tip;
 - (b) generating calibration curves;
 - (c) scanning a test sample in contact with the probe tip at scanning locations and generating at least one test sample frequency shift value at each scanning location; and
 - 10 (d) determining the dielectric permittivity of the test sample at the sample locations based on the respective generated test sample frequency shift values and the generated calibration curves.
- 15 2. The method of claim 1, wherein said calibrating step (a) includes the steps of:
 - (i) selecting a resonant frequency of the near-field scanning microwave microscope;
 - (ii) scanning each of said at least two calibration samples, where for each scan the probe tip is first
 - 20 brought into contact with each of said at least two calibration samples;
 - (iii) moving the microscope probe to a predetermined background measurement position;
 - 25 (iv) measuring a background resonant frequency at said predetermined background measurement position;

-31-

- 5 (v) moving the probe tip into contact with said one of
said at least two calibration samples at a scanning
position;
- (vi) measuring a contact resonant frequency at said
scanning position;
- 10 (vii) calculating the difference between said contact
resonant frequency and said background resonant
frequency;
- (viii) storing in memory said calculated difference as a
calibration sample resonant frequency shift value;
- (ix) moving the sample to the next scanning position;
- (x) determining if said next scanning position is the
end of a scan line;
- 15 (xi) repeating steps (vi) through (x) until said end of a
scan line has been reached;
- (xii) moving the sample to the next scan line;
- (xiii) determining if said next scan line is the end of a
scan area;
- 20 (xiv) repeating steps (iii) through (xiii) for each of said
at least two calibration samples until said end of a
scan area has been reached.

3. The method of claim 2, wherein the resonator includes a
microscope transmission line, and wherein said step (iii) comprises
moving the microscope probe to a height 1.5 times greater than
25 the diameter of the microscope transmission line.

-32-

4. The method of claim 2, wherein said step (iii) comprises moving the microscope probe to a height where the calibration sample no longer perturbs the resonator.
5. The method of claim 2, wherein said step (iii) comprises moving the microscope probe to a height at least approximately 3 millimeters above the calibration sample.
6. The method of claim 1, wherein the geometry descriptor comprises an aspect ratio of the probe tip, and the calibration step (a) further includes calculating the aspect ratio of the microscope probe tip as $\Delta z/\Delta r$, where Δz is a distance along a z-direction parallel to a length of the resonator and the probe tip and Δr is a radius distance extending from the central axis of the probe tip to its outermost surface.
7. The method of claim 1, wherein the scanning step (c) includes the steps of:
- (i) selecting a resonant frequency of the near-field scanning microwave microscope;
 - (ii) placing said test sample on the microscope stage;
 - (iii) moving the probe tip into contact with said test sample;
 - (iv) storing a position value corresponding to the point of contact with said test sample;
 - (v) moving the probe to a predetermined background measurement position;
 - (vi) measuring a background resonant frequency at said background measurement position;

-33-

- (vii) moving the probe tip into contact with said test sample at the scanning position;
- (viii) measuring the contact resonant frequency at said scanning position;
- 5 (ix) calculating the difference between said contact resonant frequency and said background resonant frequency;
- (x) storing in memory said calculated difference as a test sample resonant frequency shift value;
- 10 (xi) moving the sample to the next scanning position;
- (xii) determining if said next scanning position is the end of a scan line;
- (xiii) repeating steps (viii) through (xii) until said end of a scan line has been reached;
- 15 (xiv) moving the sample to the next scan line;
- (xv) determining if said next scan line is the end of a scan area;
- (xvi) repeating steps (v) through (xv) until said end of a scan area has been reached.
- 20 8. The method of claim 7, wherein the resonator includes a microscope transmission line, and wherein said step (v) comprises moving the microscope probe to a height that is at least approximately 1.5 times greater than the diameter of the microscope transmission line.
- 25 9. The method of claim 7, wherein said step (v) comprises moving the probe to a height where the test sample no longer perturbs the resonator.



1

2

-34-

10. The method of claim 7, wherein said step (v) comprises moving the probe to a height at least approximately 3 millimeters above the test sample.
- 5 11. The method of claim 1, wherein the scanning step (c) includes placing a bulk test sample on the microscope stage.
12. The method of claim 11, wherein the generating a calibration curve step (b) includes the steps of:
- 10 (i) storing electric field configuration data files, wherein the data corresponds to a model sample having approximately the same first thickness and further having approximately the same permittivity as one of said at least two calibration samples with known dielectric properties; and wherein the data stored is representative of electric field values at
- 15 respective ϵ_r and α over a predetermined range of ϵ_r and α , where ϵ_r is a dielectric permittivity value and α is the probe tip geometry descriptor;
- (ii) generating a first model calibration curve using said stored electric field configuration data;
- 20 (iii) generating a second model calibration curve using said stored electric field configuration data;
- (iv) generating a probe calibration curve using said first and second generated model calibration curves and said generated calibration sample frequency shift values; and
- 25 (v) determining the geometry descriptor of the probe tip at the time of scanning of the test sample based

-35-

upon the positioning of said generated probe calibration curve in relation to said first and second generated model calibration curves.

13. The method of claim 12 wherein the generating a first model calibration curve using said previously stored electric field configuration data (ii) includes the steps of:

(1) reading from a first electric field configuration data file where α = a first probe tip geometry descriptor value, a first previously stored electric field value (E_1) and a first permittivity value (ϵ_{r1});

(2) reading from a second electric field configuration data file where α = a first probe tip geometry descriptor value, a second previously stored electrical field value (E_2);

(3) calculating a point on the first model calibration curve by solving the equation

$$\frac{\Delta f}{f} \approx \frac{\epsilon_0}{4W} \int_{V_s} (\epsilon_{r2} - \epsilon_{r1}) \vec{E}_1 \cdot \vec{E}_2 dV; \text{ and}$$

(4) repeating steps (1) through (3) until a predetermined number of points on the first model calibration curve have been generated.

-36-

14. The method of claim 12 wherein the generating a second model calibration curve using said previously stored electric field configuration data files step (iii) includes the steps of:

5 (1) reading from a first previously stored electric field configuration data file where α =a second probe tip geometry descriptor value, a first previously stored electric field value (E_1) and a first permittivity value (ϵ_{r1});

10 (2) reading from a second previously stored electric field configuration data file where α =a second probe tip geometry descriptor value, a second previously stored electric field value (E_2) and a second permittivity value (ϵ_{r2});

15 (3) calculating a point on the second model calibration curve by solving the equation

$$\frac{\Delta f}{f} \approx \frac{\epsilon_0}{4W} \int_{V_s} (\epsilon_{r2} - \epsilon_{r1}) \vec{E}_1 \cdot \vec{E}_2 dV ; \text{ and}$$

20 (4) repeating steps (1) through (3) until a predetermined number of points on the second model calibration curve have been generated.

- 25 15. The method of claim 1, wherein the scanning step (c) includes arranging a thin film test sample on top of a dielectric substrate having approximately the same first determined thickness and the same permittivity as at least one of said calibration samples and then placing said arrangement on the microscope stage.

-37-

16. The method of claim 15, wherein the generating a calibration curve includes the steps of:

- 5 (i) storing electric field configuration data files wherein the data corresponds to a model sample having a thin film of approximately the same second determined thickness and a known dielectric permittivity value arranged on top of said dielectric substrate having approximately the same first determined thickness and the same permittivity as at least one of said calibration samples with known dielectric properties; wherein the stored data files are representative of electric field values at respective ϵ_r and α over a predetermined range of ϵ_r and α , wherein ϵ_r is a dielectric permittivity value for the model sample thin film and α is representative of a probe tip geometry descriptor;
- 10 (ii) generating a first test sample calibration curve using said stored electric field configuration data files;
- 15 (iii) generating a second test sample calibration curve using said stored electric field configuration data files;
- 20 (iv) generating an additional test sample calibration curve using said first and second test sample calibration curves and said generated test sample frequency shift values;
- 25

17. The method of claim 16 wherein the generating a first test sample calibration curve using said previously stored electric field configuration data files step (ii) includes the steps of:

- 5 (1) reading from a first electric field configuration data file where $\alpha =$ a first probe tip geometry descriptor value, a first previously stored electric field value (E_1) and a first permittivity value (ϵ_{r1}) where ϵ_{r1} is the permittivity of said thin film having approximately the same second determined thickness and known dielectric permittivity;
- 10 (2) reading from a second electric field configuration data file where $\alpha =$ a first probe tip geometry descriptor value, a second previously stored electric field value (E_2) and a second permittivity value (ϵ_{r2}) where ϵ_{r2} is the permittivity of said thin film having approximately the same second determined thickness and known dielectric permittivity;
- 15 (3) calculating a point on the first test sample calibration curve by solving the equation

$$\frac{\Delta f}{f} \approx \frac{\epsilon_0}{4W} \int_{V_s} (\epsilon_{r2} - \epsilon_{r1}) \vec{E}_1 \cdot \vec{E}_2 dV; \text{ and}$$
- 20 (4) repeating steps (1) through (3) until a predetermined number of points on the first test sample calibration curve have been generated.
- 25

18. The method of claim 16 wherein the generating a second test sample calibration curve using said previously stored electric field configuration data files step (iii) includes the steps of:

(1) reading from a first previously stored electric field configuration data file where α = a second probe tip geometry descriptor value, a first previously stored electric field value (E_1) and a first permittivity value (ϵ_{r1}) where ϵ_{r1} is the permittivity of said thin film having approximately the same second determined thickness and known dielectric permittivity;

(2) reading from a second previously stored electric field configuration data file where α = a second probe tip geometry descriptor value, a second previously stored electric field value (E_2) and a second permittivity value (ϵ_{r2}) where ϵ_{r2} is the permittivity of said thin film having approximately the same second determined thickness and known dielectric permittivity;

(3) calculating a point on the second test sample calibration curve by solving the equation

$$\frac{\Delta f}{f} \approx \frac{\epsilon_0}{4W} \int_{V_s} (\epsilon_{r2} - \epsilon_{r1}) \vec{E}_1 \cdot \vec{E}_2 dV ; \text{and}$$

(4) repeating steps (1) through (3) until a predetermined number of points on the

-40-

second test sample calibration curve have
been generated.

19. An apparatus for displaying dielectric properties comprising:
- 5 (a) a near-field scanning microwave microscope having an open-ended coaxial probe with a sharp, protruding center conductor;
 - (b) a coaxial transmission line resonator that has a resonant frequency;
 - 10 (c) a microwave source coupled to said coaxial transmission line resonator through a capacitive coupler for generating said voltage;
 - (d) a spring-loaded cantilever for supporting said sample in contact with said sharp protruding center conductor;
 - 15 (e) a bias tee coupled to said coaxial transmission line resonator for applying a local electric field to said sample in contact with said sharp protruding center conductor;
 - (f) a first motor controller for manipulating said sample in contact with said sharp protruding center conductor in a first direction;
 - 20 (g) a second motor controller for manipulating said sample in contact with said sharp protruding center conductor in a second direction;
 - (h) a third motor controller for manipulating said sample in contact with said sharp protruding center conductor in a third direction;
 - 25 (i) a coupler joined to said microwave source and said coaxial transmission line resonator;

-41-

- (j) a detector for converting the microwave signal from said coupler into an output signal;
- (k) a feedback circuit receives the output signal from said detector and measures a shift change in resonance frequency, wherein said feedback circuit keeps said microwave source locked onto a predetermined resonant frequency;
- (l) a processor for determining between at least one parameter related to a change in said resonant frequency and a known dielectric property value of a sample responsible for said change; wherein the processor is further able to receive from said feedback circuit said value for at least one parameter related to a change in said resonant frequency due to an unknown dielectric property of said sample and determine the value of said unknown dielectric property; and
- (m) a display device for imaging the value of said unknown dielectric property once said value is determined by said processor.
20. A system for quantitatively modeling and imaging of dielectric properties, comprising:
- (a) a memory device that stores
- (i) files of electric field values, ϵ_r , and α over a predetermined range of ϵ_r and α , where ϵ_r is a dielectric permittivity value and α is representative of said probe tip geometry descriptor;
- (ii) calibration sample resonant frequency shift values;
- (iii) test sample resonant frequency shift values;

-42-

- 5 (b) a model calibration curve generator that generates two model calibration curves using the stored files in said memory;
- (c) a probe calibration curve generator that generates a probe calibration curve using said generated model calibration curves and said calibration sample frequency shift values.
- 10 (d) a test sample calibration curve generator that generates a test sample calibration curve using additional model calibration curves and additional calibration sample frequency shift values;
21. A spring-loaded sample holder comprising:
- 15 (a) a sample support having an angled end and a planar surface for supporting a sample;
- (b) a first bracing device in contact with the angled end of said sample support so as to create a pivot point;
- (c) a spring mounted to the sample support; and
- (d) a second bracing device in contact with said spring for holding the spring in place.
22. The method of claim 21, wherein a probe is held fixed and in contact with the sample.
- 20 23. The method of claim 22, wherein the sample holder and sample are scanned horizontally.
24. The method of claim 23, wherein a sensor measures the vertical displacement of the sample holder, such that this displacement is a function of the topography of the sample.
- 25

-43-

25. An apparatus for imaging a sample using a near-field scanning microwave microscope, comprising:
- 5 a bias tee in a coaxial transmission line resonator for applying a low-frequency bias voltage to a microscope probe tip and wherein the low-frequency bias voltage is independent of a microwave signal, whereby a local electric field can be applied to a sample to allow for nonlinearity and tunability measuring.
26. A method for non-contact imaging of dielectric permittivity using a near-field scanning microwave microscope having a resonator with a probe tip comprising the steps of:
- 10 (a) calibrating the near-field scanning microwave microscope using at least three dielectric samples with known dielectric properties;
- (b) generating calibration curves;
- 15 (c) scanning a test sample with the probe at a predetermined scanning height and generating at least one test sample frequency shift value at said predetermined scanning height; and
- (d) determining the dielectric permittivity of the test sample based on the generated test sample resonant frequency shift value and the generated calibration curves.
- 20 27. The method of claim 26, wherein said calibrating step (a) includes the steps of:
- (i) selecting a resonant frequency of the near-field scanning microwave microscope;
- 25 (ii) placing one of said at least three calibration samples beneath the probe;

-44-

- 5 (iii) positioning the probe at a first predetermined height;
- (iv) measuring a resonant frequency at said first predetermined height;
- 10 (v) moving the probe to a second predetermined height;
- (vi) measuring the resonant frequency at said second predetermined height;
- (vii) calculating the difference between said resonant frequency at said first predetermined height and said resonant frequency at said second predetermined height;
- 15 (viii) storing in memory said calculated difference as a calibration sample resonant frequency shift value;
- (ix) repeating steps (ii) through (viii) for each of said at least two calibration samples.

28. The method of claim 26, wherein said generating calibration curves step (b) includes the step of plotting said calibration frequency shift values as a function of dielectric constant (ϵ_r) and frequency shift.

- 20 29. The method of claim 26, wherein said scanning a test sample step (c) includes the steps of:
- (i) selecting a resonant frequency of the near-field scanning microwave microscope;
- (ii) placing said test sample beneath the probe;
- 25 (iii) positioning the probe at a first predetermined height;

-45-

- (iv) measuring a resonant frequency at said first predetermined height;
- (v) moving the probe to a second predetermined height;
- 5 (vi) measuring the resonant frequency at said second predetermined height;
- (vii) calculating the difference between said resonant frequency at said first predetermined height and said resonant frequency at said second predetermined height;
- 10 (viii) storing in memory said calculated difference as a test sample resonant frequency shift value.

1/19

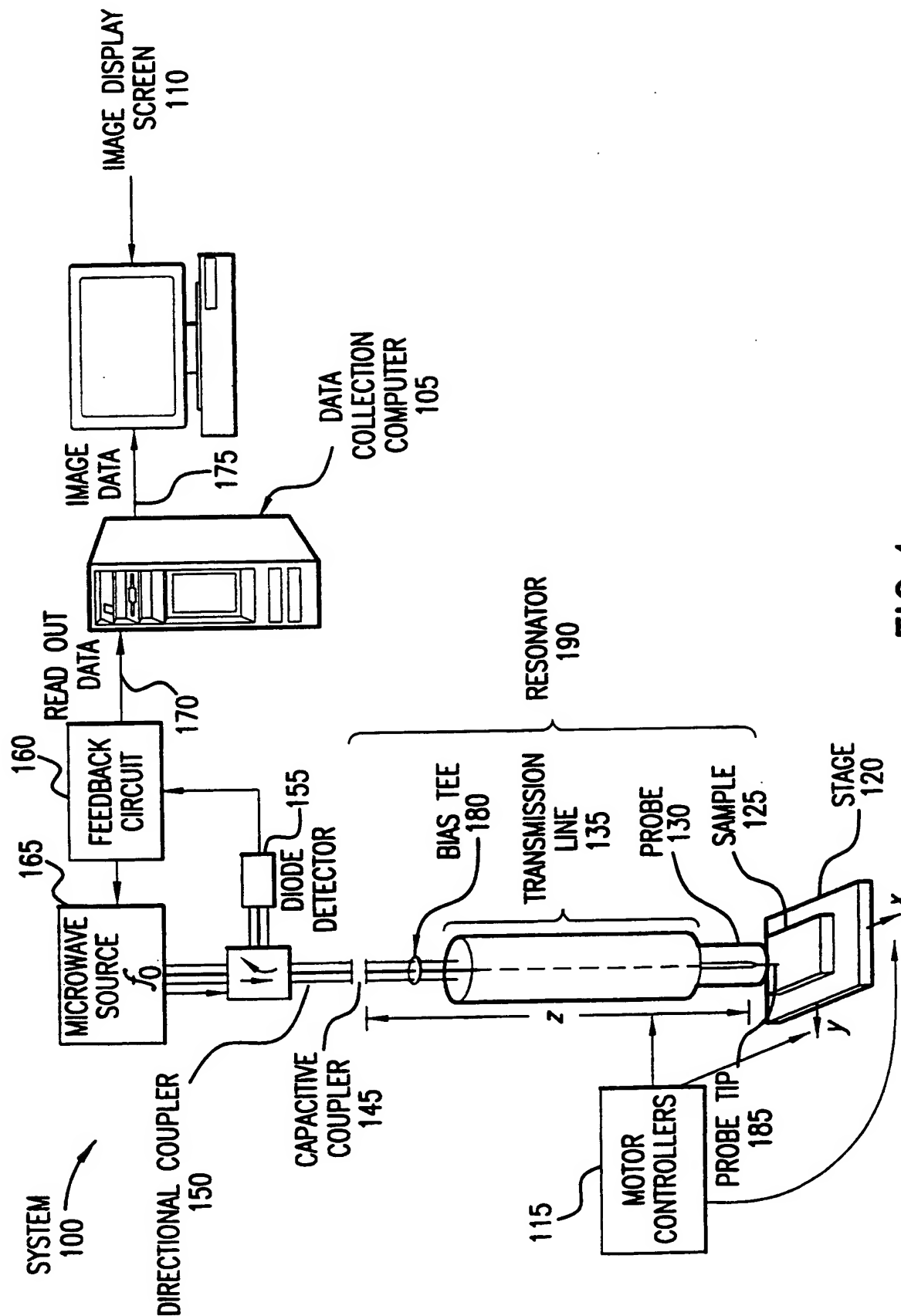


FIG.1

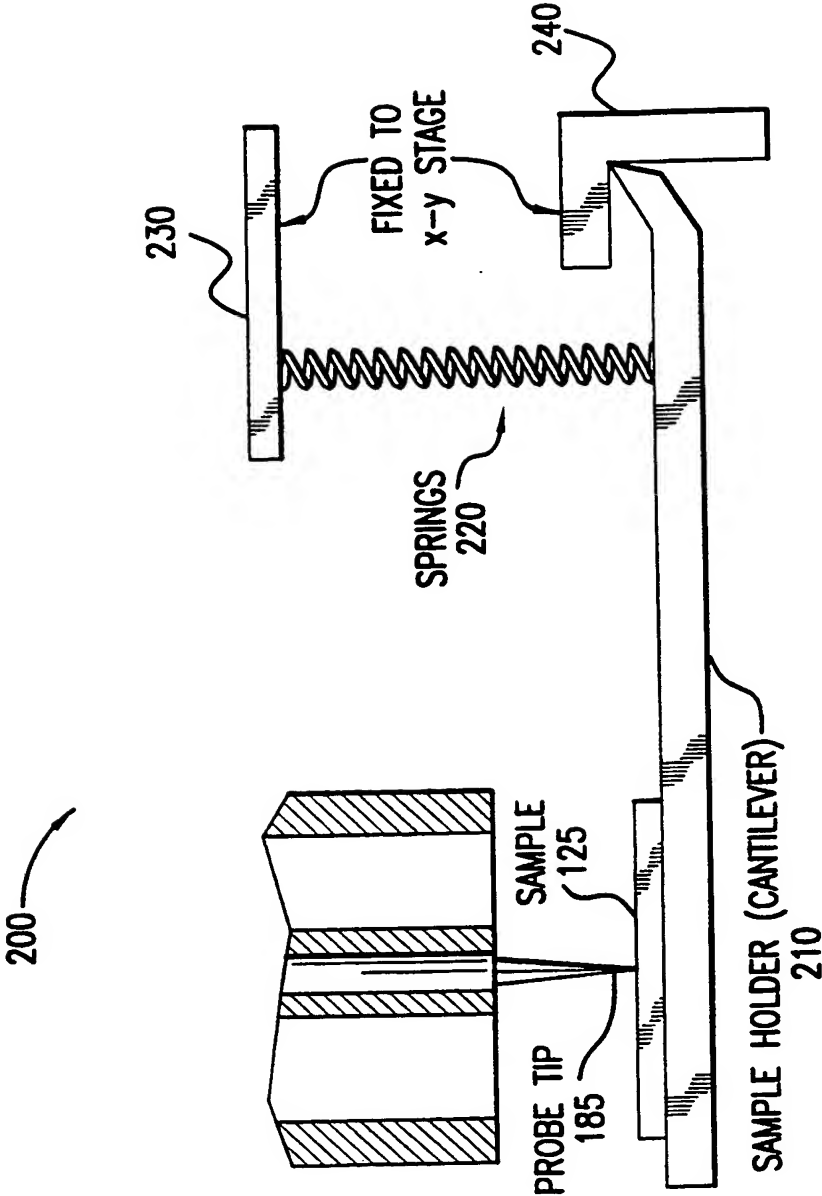


FIG.2

3/19

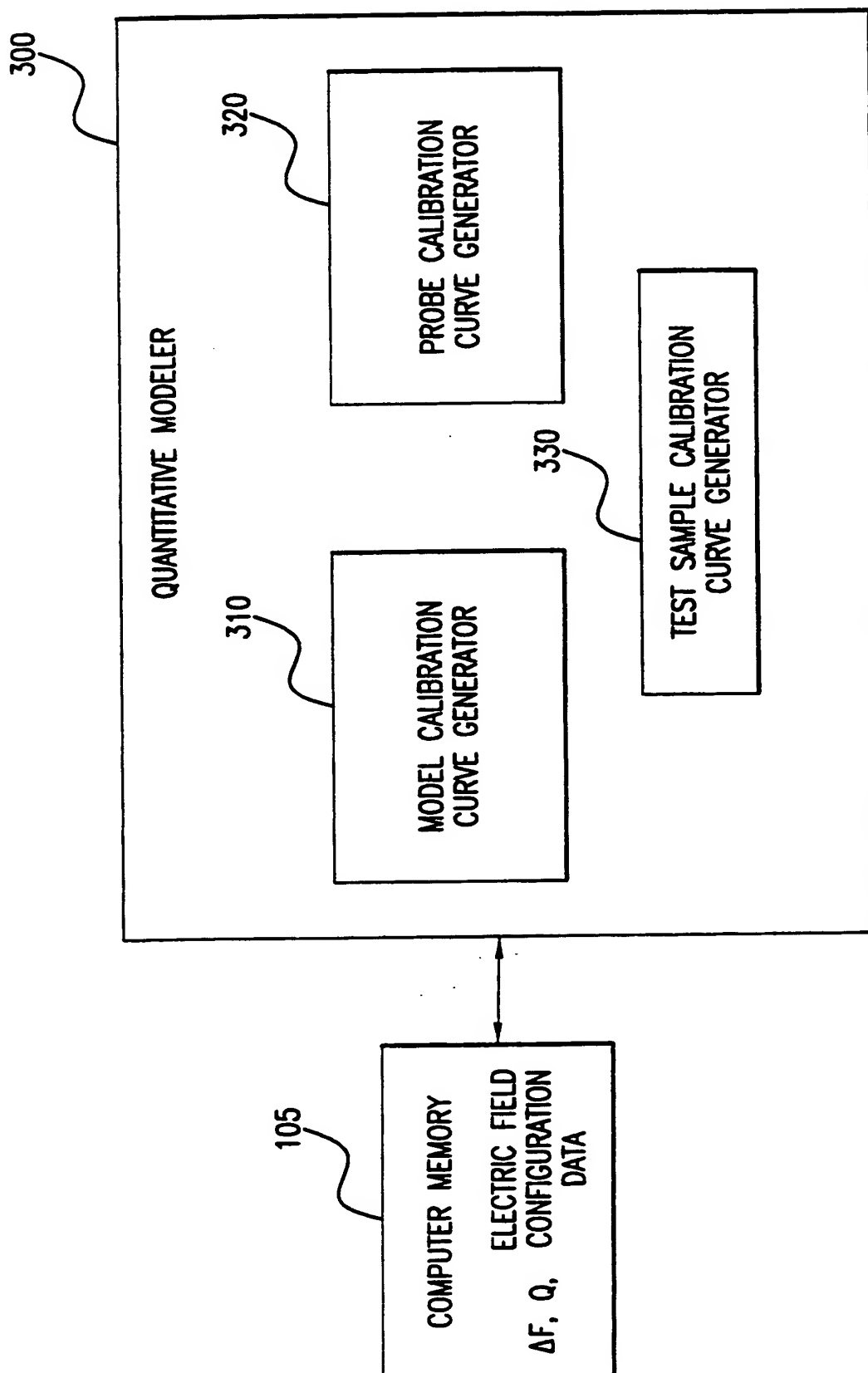


FIG.3

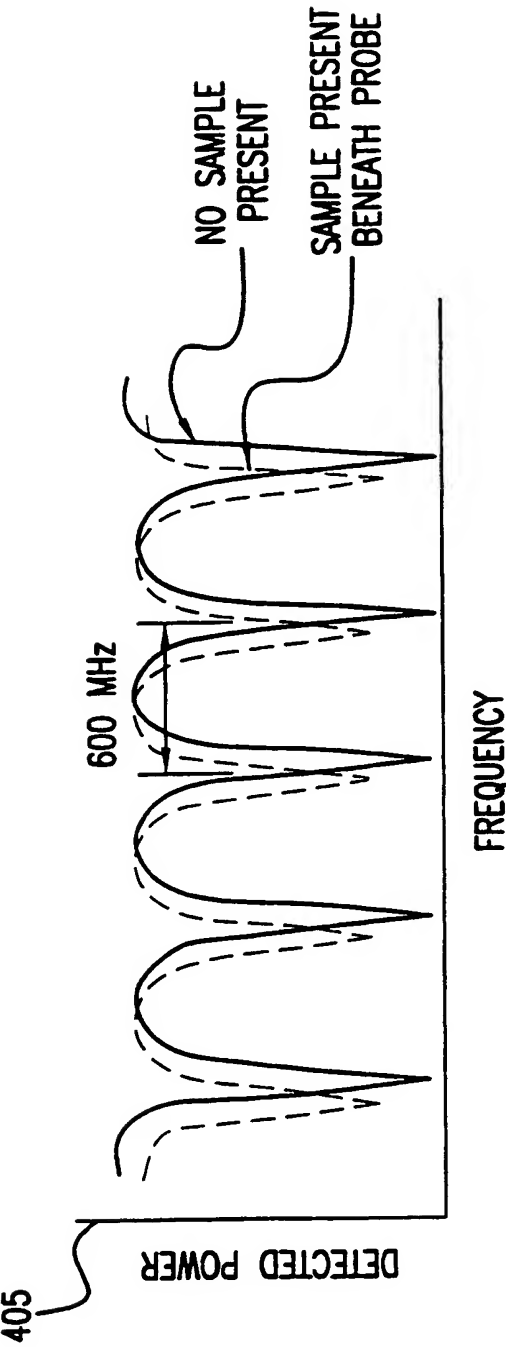


FIG.4

PERTURBATION FORMULA

$$\frac{\Delta f}{f} \approx \left(\frac{\epsilon_{r1} - \epsilon_{r2}}{4W} \right) \int_{V_S} \vec{E}_1 \cdot \vec{E}_2 \, dV$$
$$\Delta f = f(\epsilon_{r1}, \epsilon_{r2})$$

FIG.5



5/19

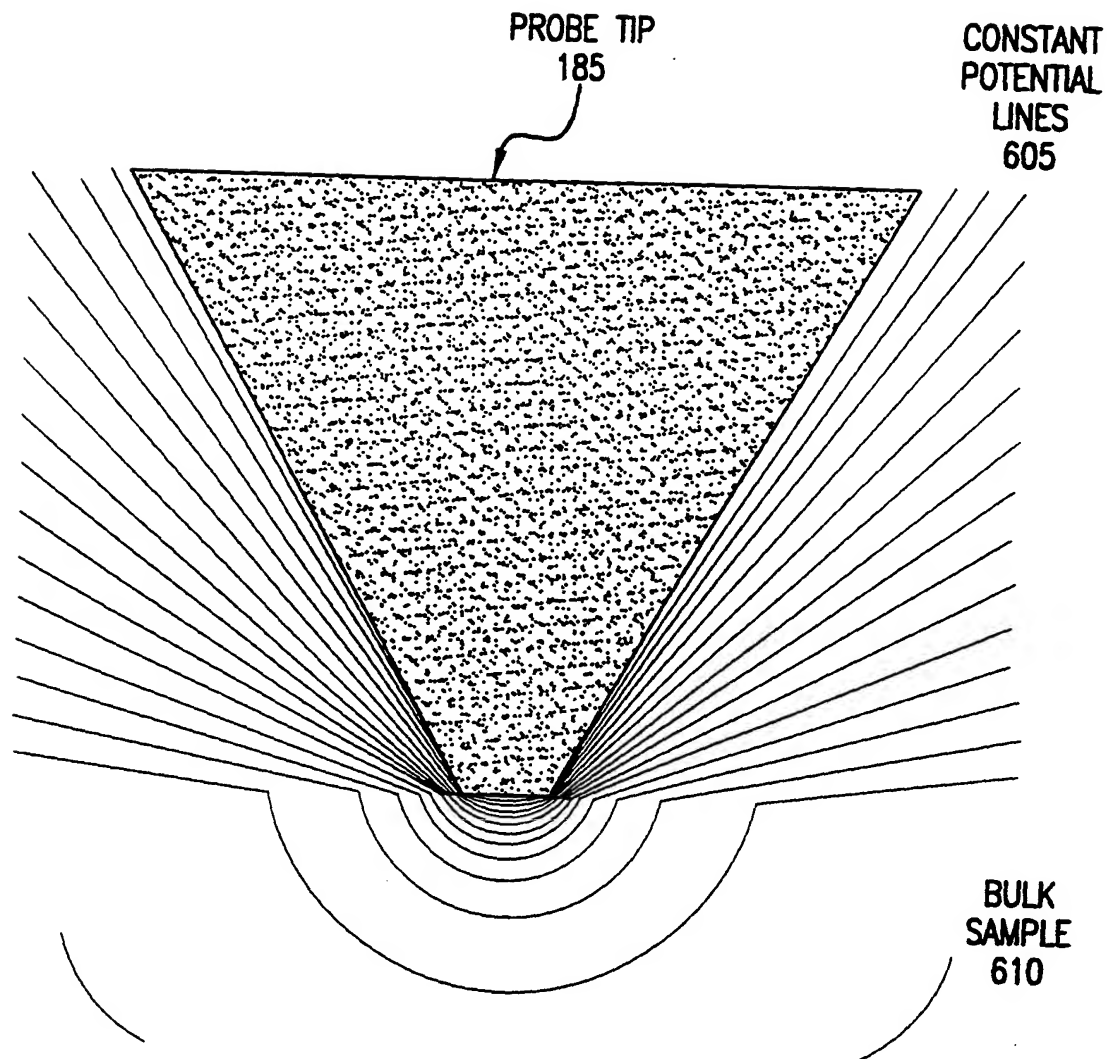


FIG.6

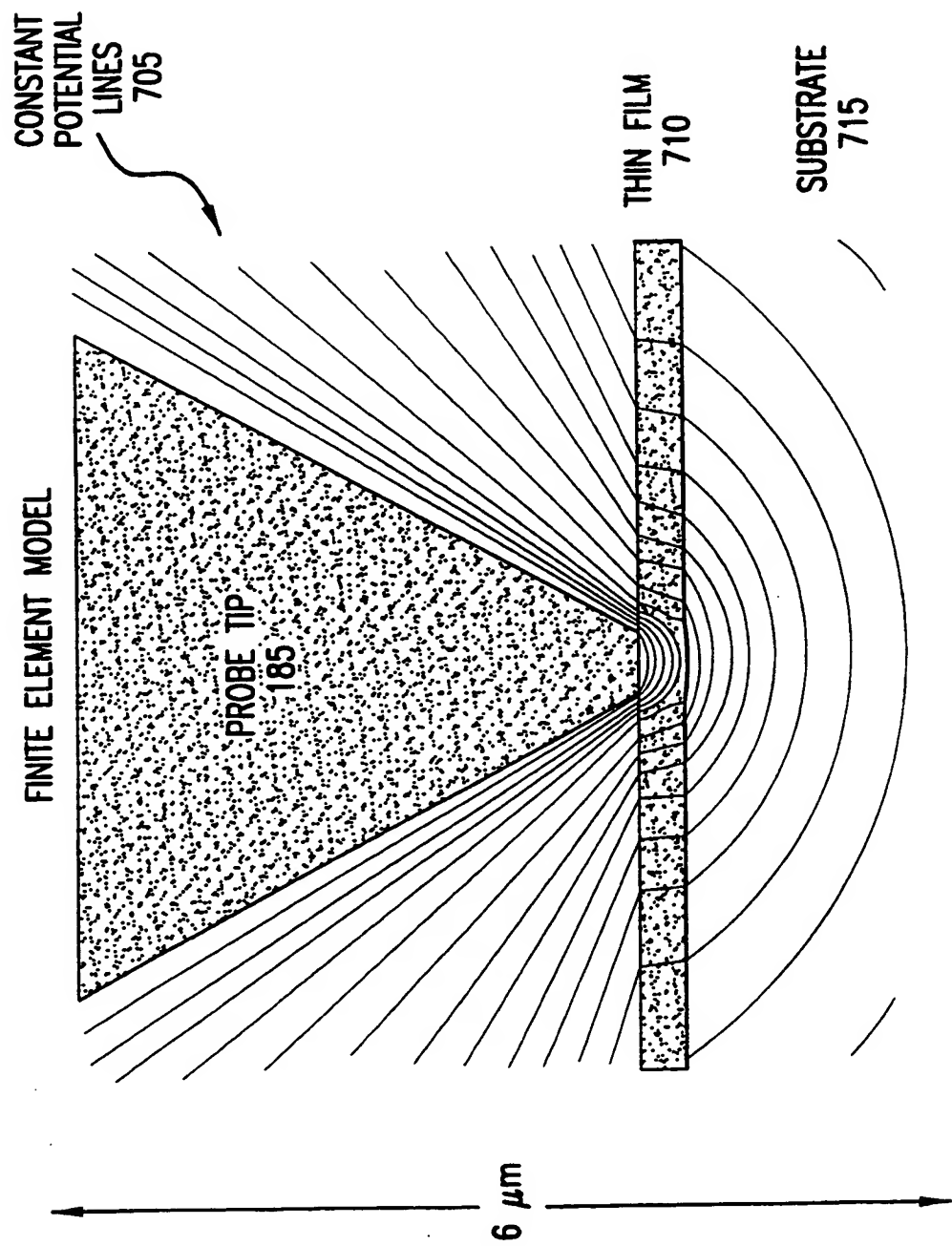


FIG.7

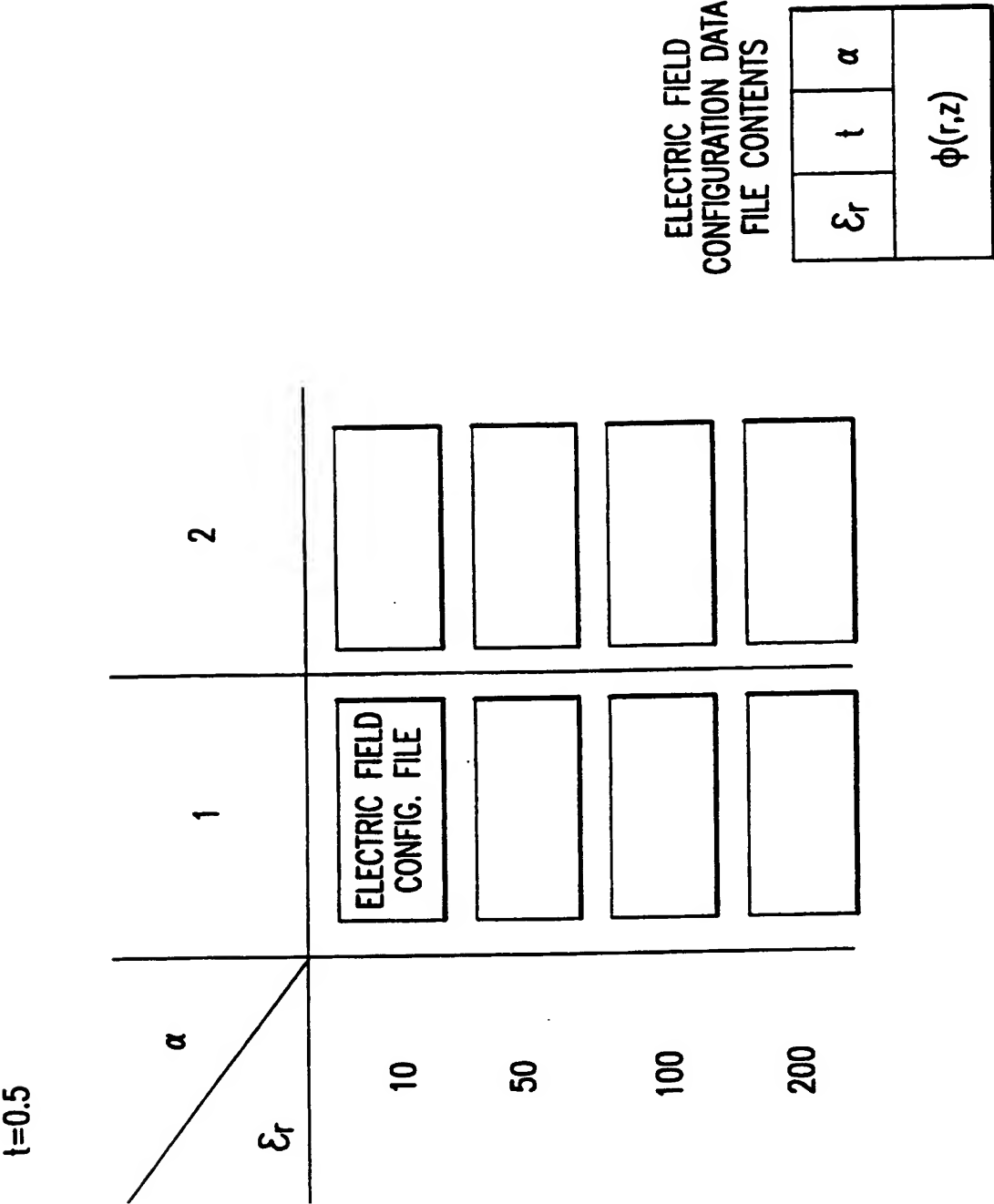
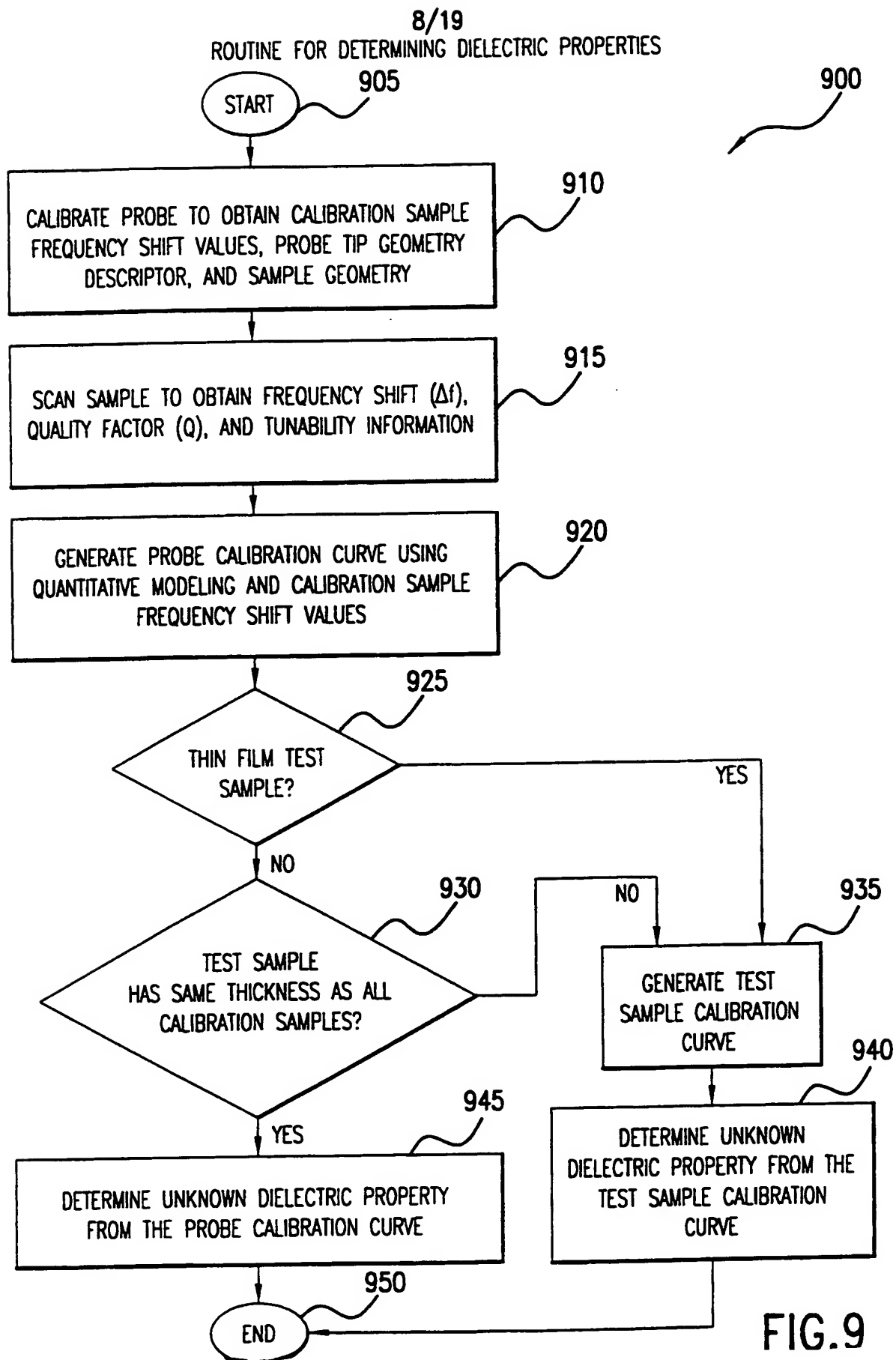


FIG.8



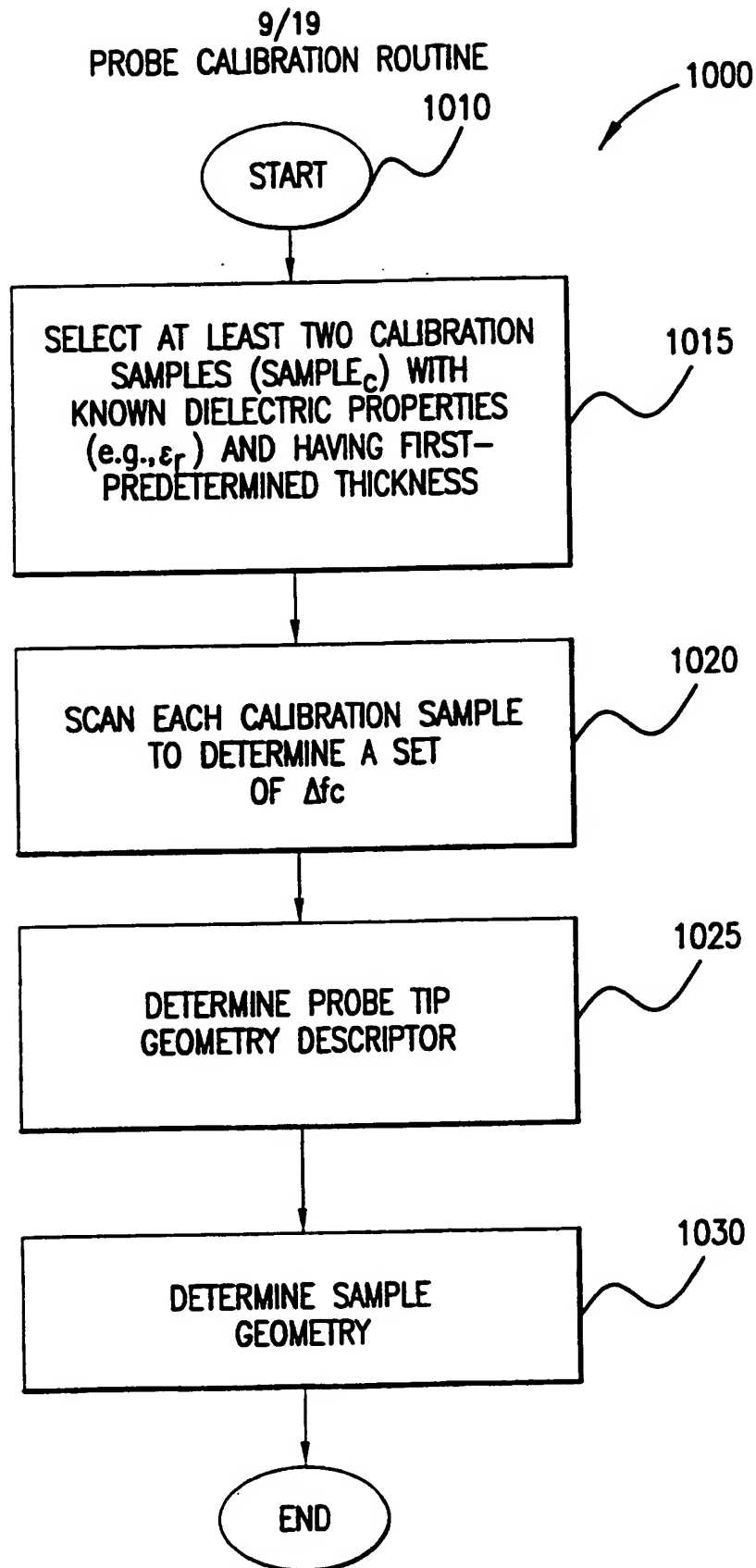


FIG.10

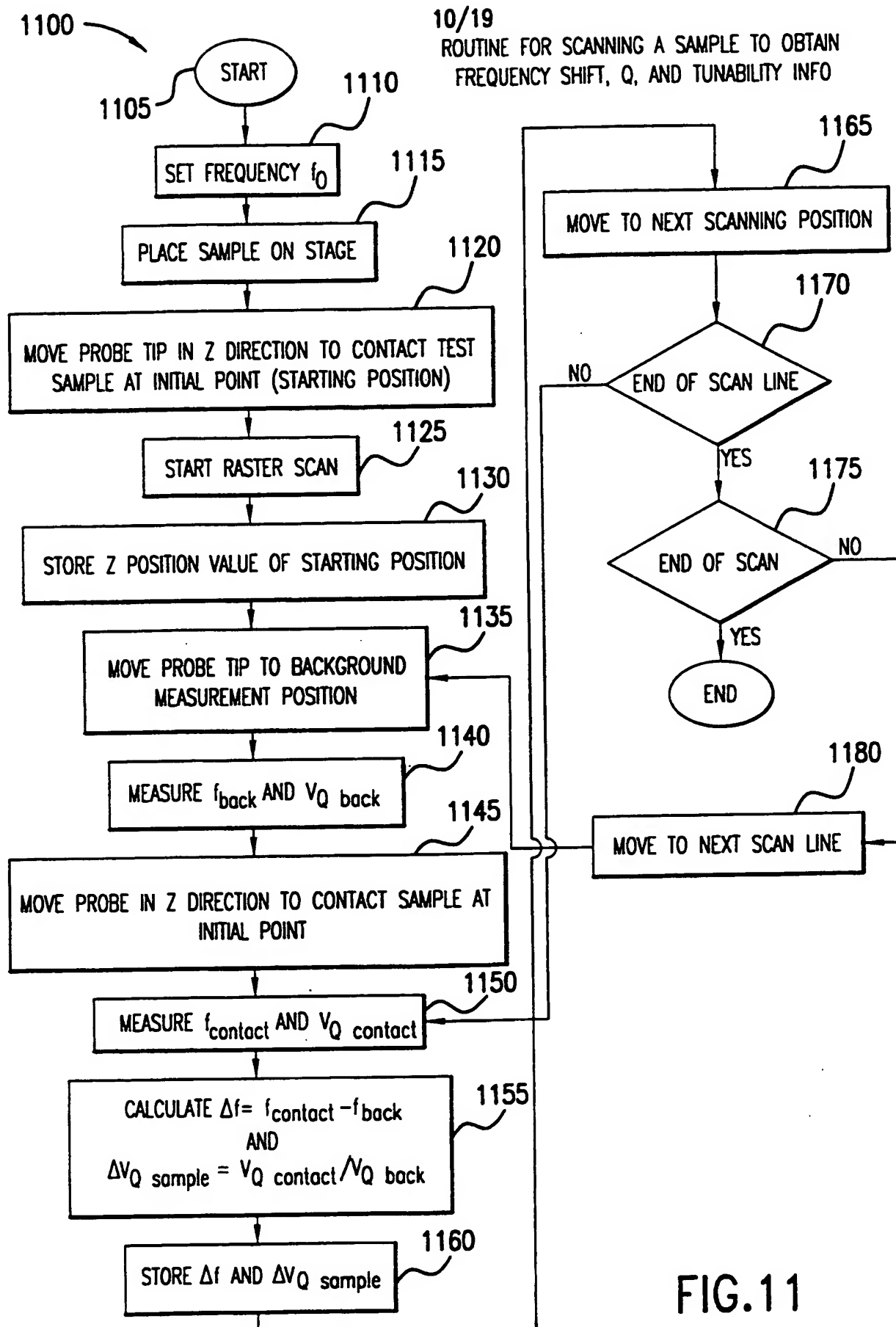


FIG.11

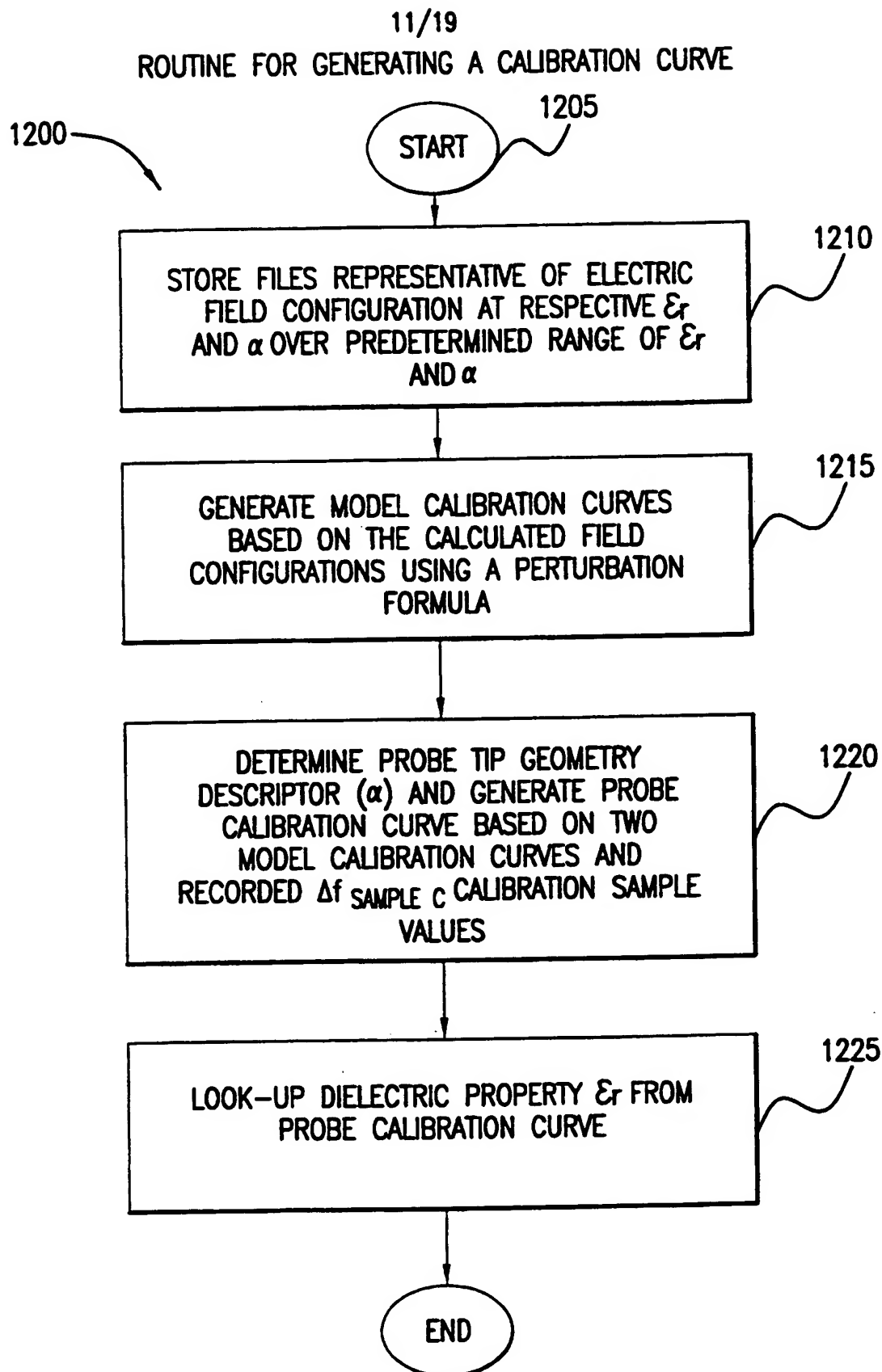


FIG.12

12/19

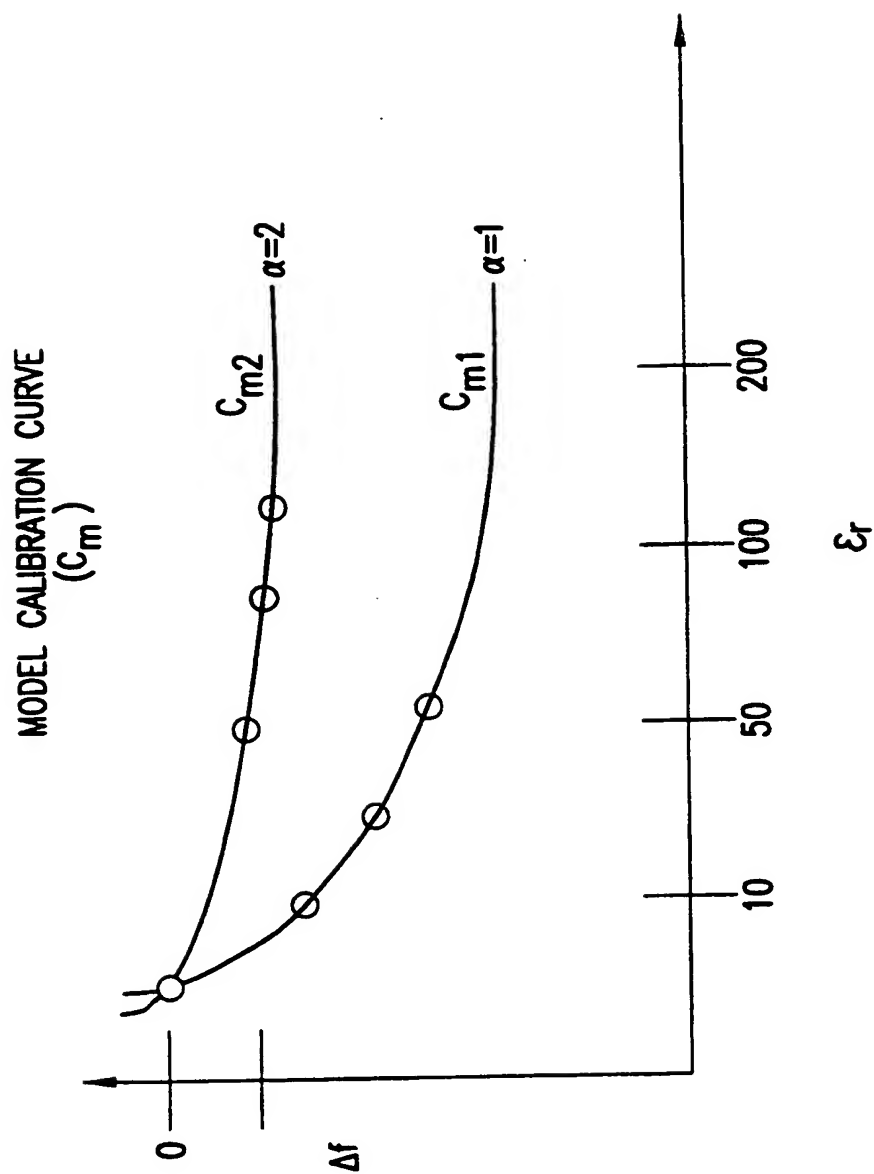
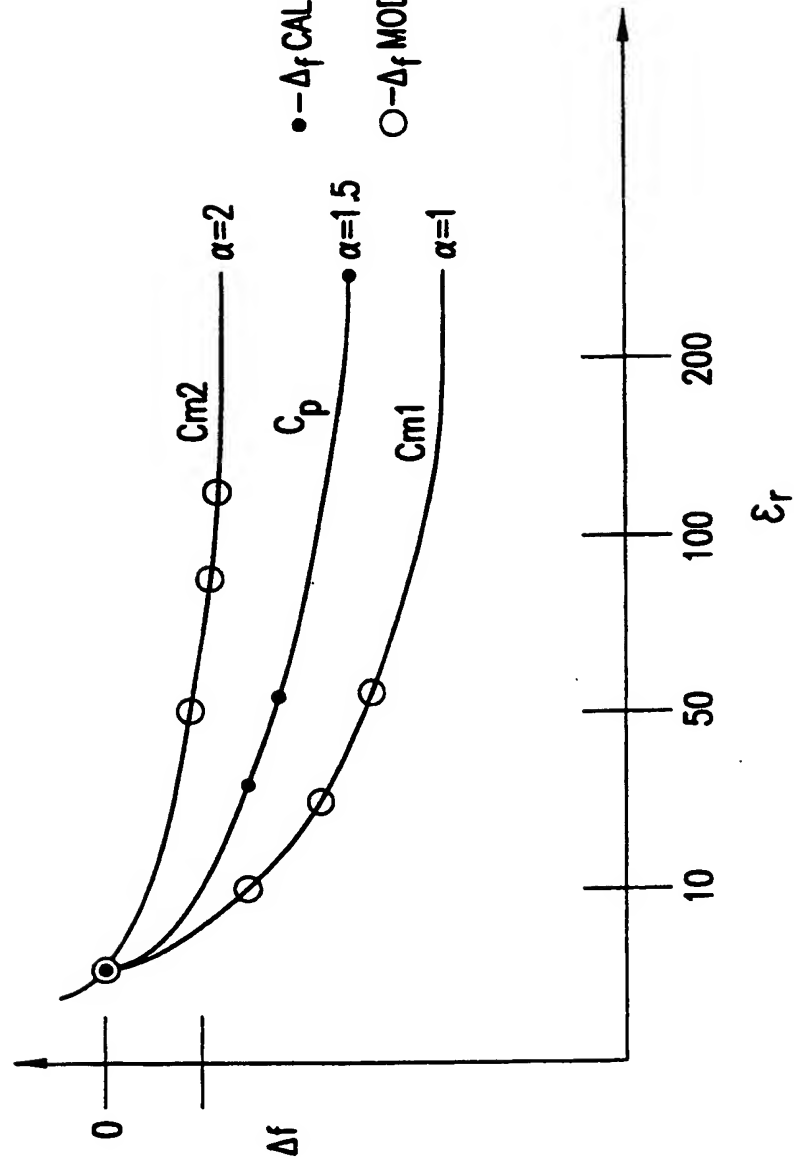


FIG.13



PROBE CALIBRATION CURVE
(C_p)



• -- Δf CALIBRATION SAMPLE VALUES

○ -- Δf MODEL SAMPLE VALUES

13/19

FIG.14



14/19

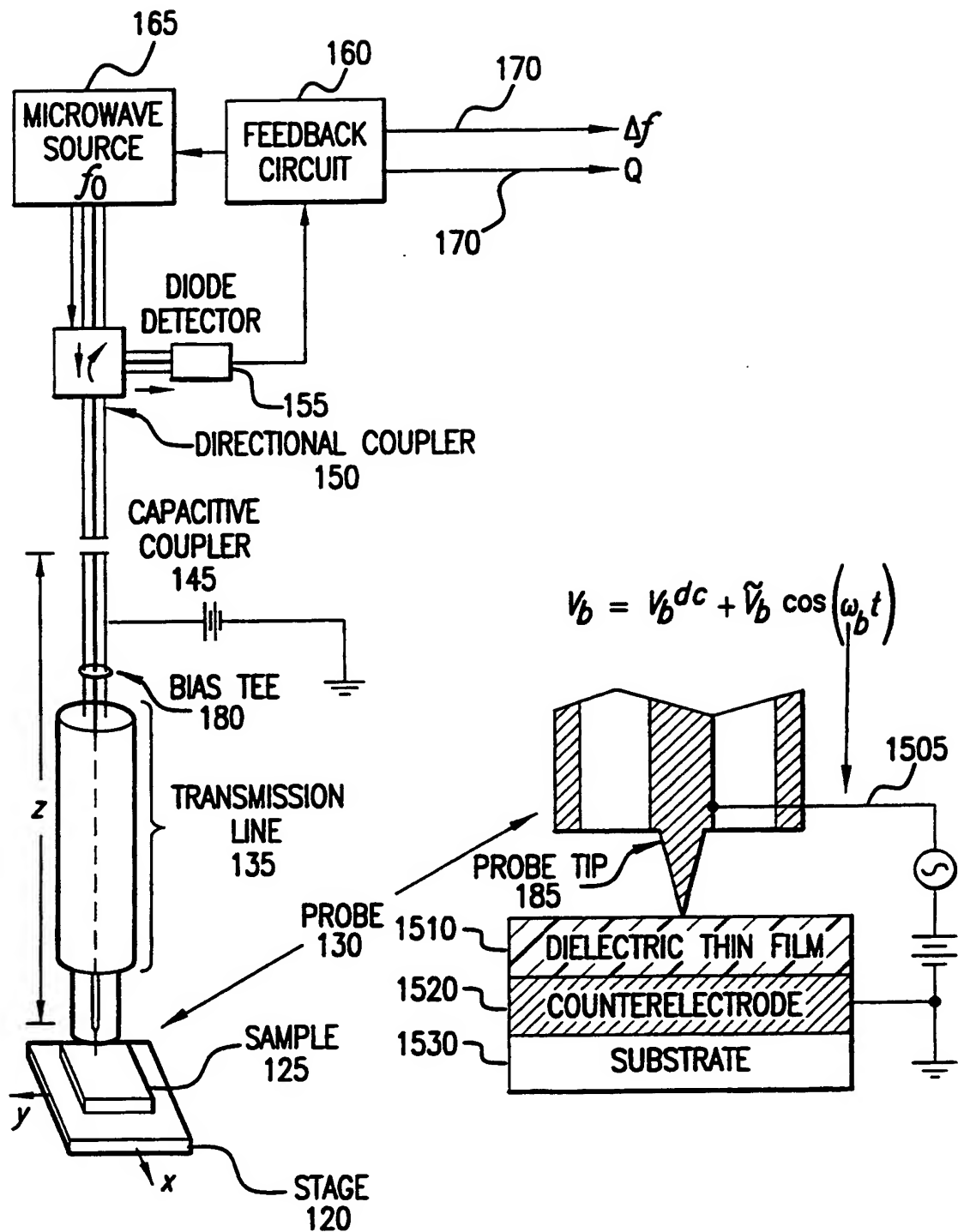
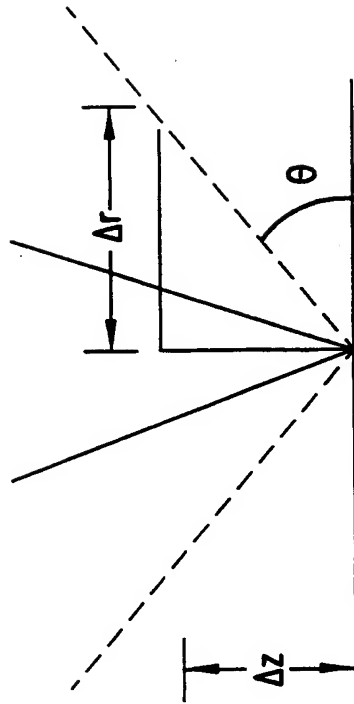


FIG.15

15/19



SMALL ASPECT RATIO = BLUNT TIP

$$\text{ASPECT RATIO} \equiv \alpha = \frac{\Delta z}{\Delta r} = \tan \theta$$

HIGH ASPECT RATIO = SHARP TIP

FIG.16

TEST SAMPLE CALIBRATION CURVE

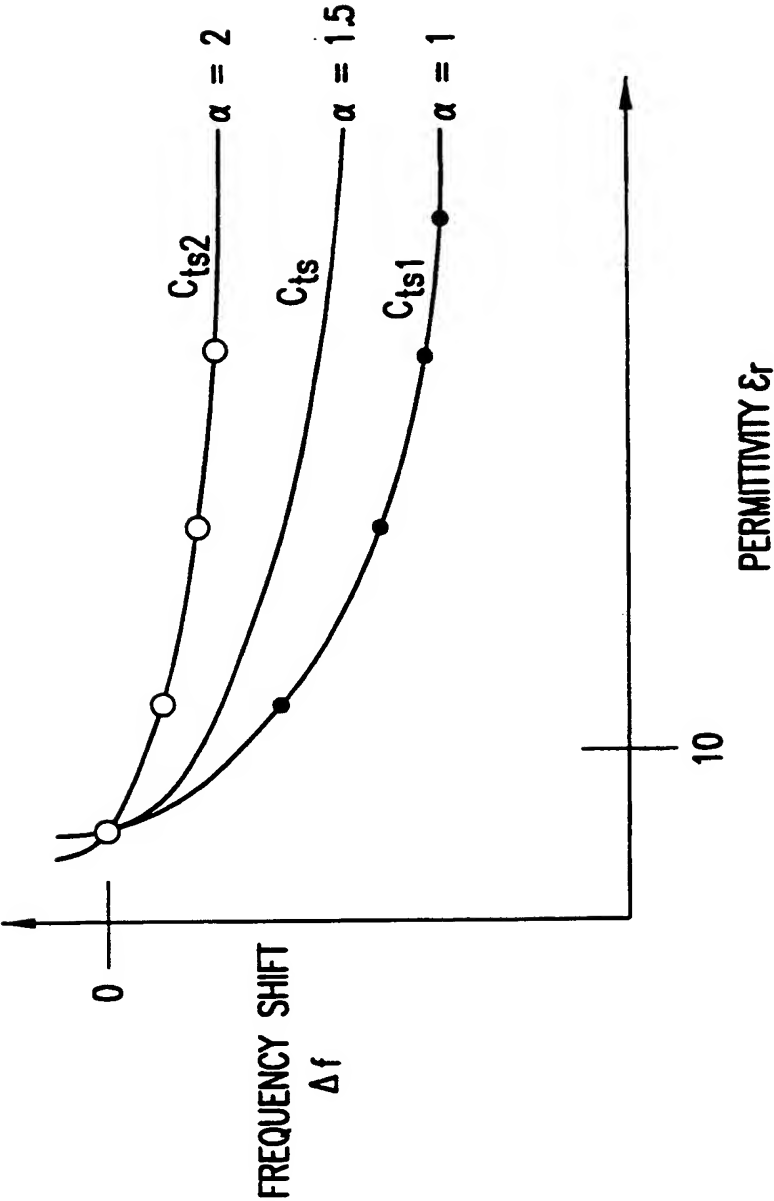


FIG.17

17/19

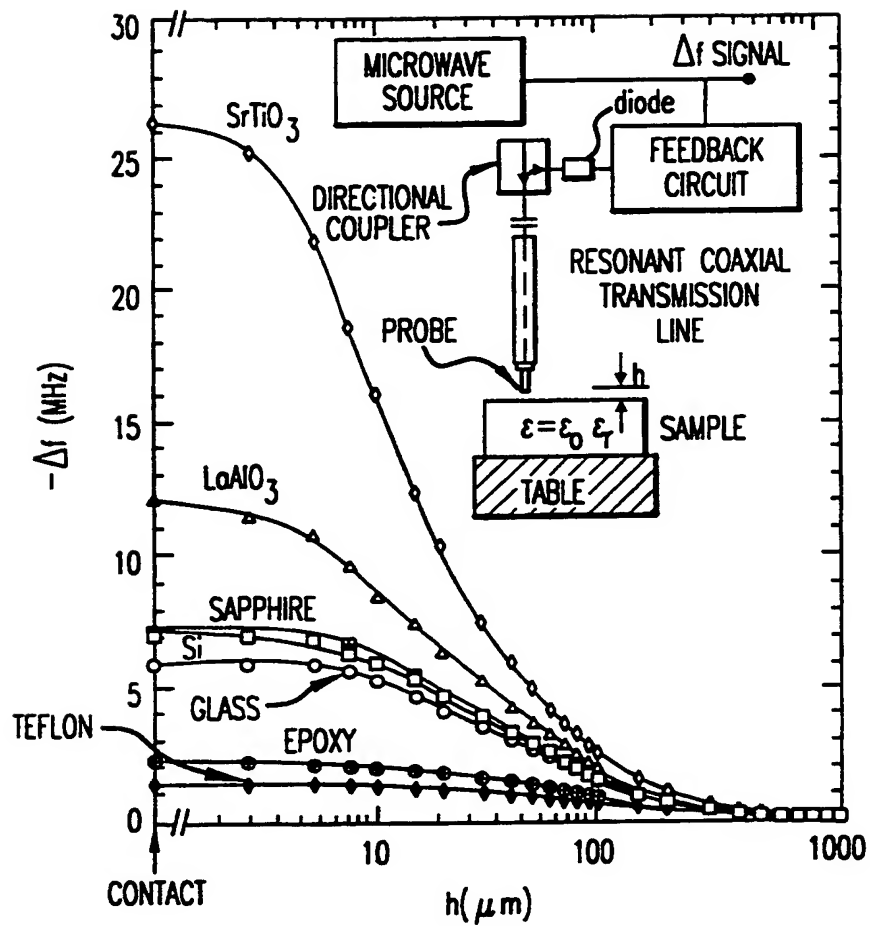


FIG. 18

18/19

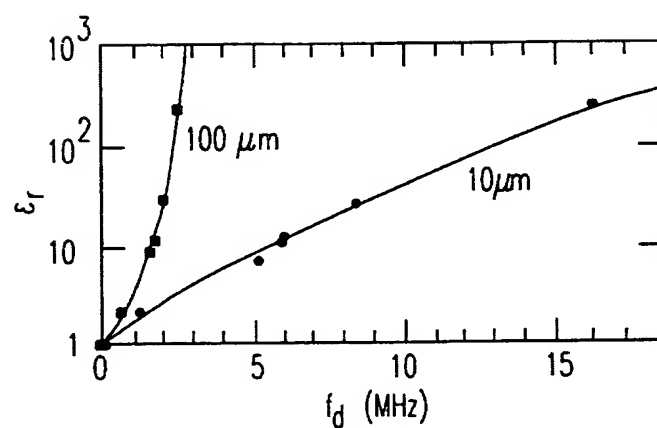


FIG.19

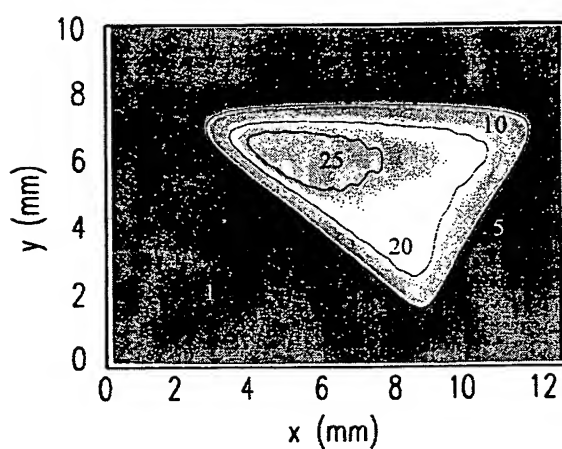


FIG.20

MATERIAL	EXPERIMENTAL VALUE	LITERATURE VALUE	FREQUENCY (GHz)	REFERENCES
SILICON	12	11.7	100	11
GLASS	12	6.7	10^{-3}	12
SrTiO ₃	180	230	0.1	9
LaAlO ₃	20	23.9	18	10
SAPPHIRE (CERAMIC)	20	10.0	100	11
TEFLON	2.1	2.1	10	9

FIG.21

19/19

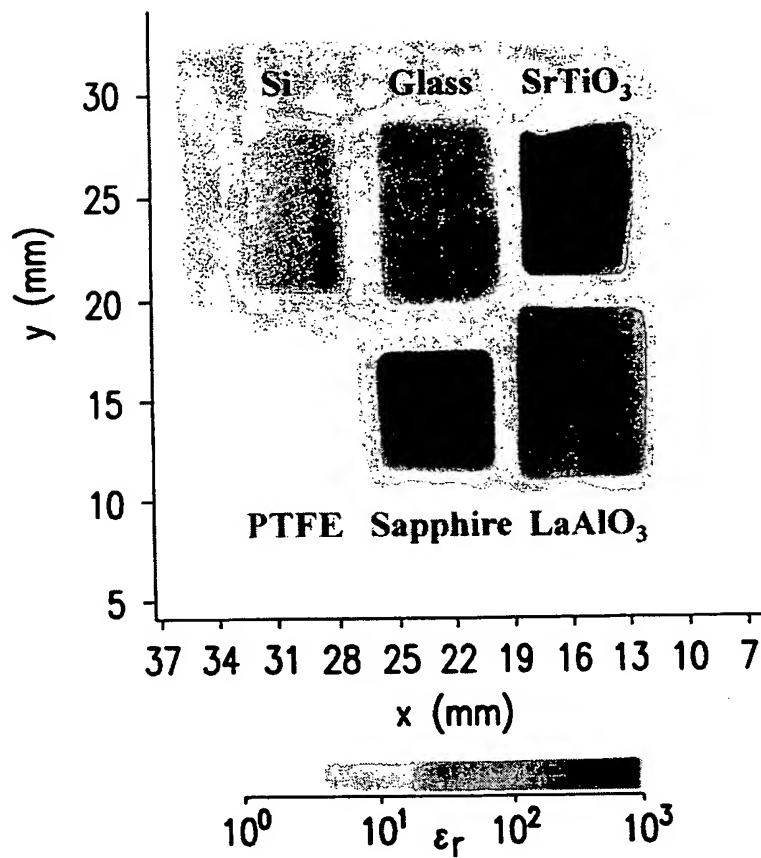


FIG.22A

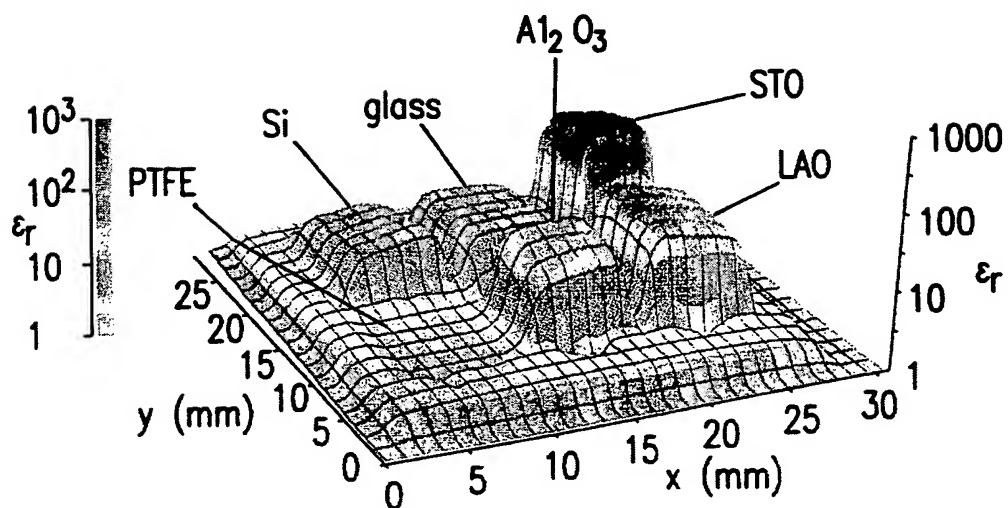


FIG.22B

Statement Concerning Non-Prejudicial Disclosure or Exception to Lack of Novelty

Due to possible disclosure not earlier than April 5, 1999, the applicant respectfully requests that the subject international application be granted the respective provisions under national laws concerning Exceptions to Lack of Novelty in each of the designated countries. This is not an admission that the subject invention is not novel. Exception to Lack of Novelty is hereby requested for purposes of disclosure and precautionary measures.

INTERNATIONAL SEARCH REPORT

International Application No
PCT/US 00/08943

A. CLASSIFICATION OF SUBJECT MATTER
IPC 7 G01R27/26

According to International Patent Classification (IPC) or to both national classification and IPC

B. FIELDS SEARCHED

Minimum documentation searched (classification system followed by classification symbols)
IPC 7 G01R G01N

Documentation searched other than minimum documentation to the extent that such documents are included in the fields searched

Electronic data base consulted during the international search (name of data base and, where practical, search terms used)

C. DOCUMENTS CONSIDERED TO BE RELEVANT

Category *	Citation of document, with indication, where appropriate, of the relevant passages	Relevant to claim No.
Y	<p>WO 99 16102 A (UNIV CALIFORNIA) 1 April 1999 (1999-04-01) abstract; claims 10,24; figures 2,16 page 2, line 15 -page 4, line 7 page 8, line 20 -page 9, line 9 page 13, line 8 - line 29 page 15, line 7 -page 16, line 20 page 19, line 2 - line 8 page 20, line 3 - line 5 page 21, line 16 -page 22, line 9 page 43, line 7 - line 10 --- -/-</p>	1,20,26

☒ Further documents are listed in the continuation of box C.

☒ Patent family members are listed in annex.

* Special categories of cited documents :

- *A* document defining the general state of the art which is not considered to be of particular relevance
- *E* earlier document but published on or after the international filing date
- *L* document which may throw doubts on priority claim(s) or which is cited to establish the publication date of another citation or other special reason (as specified)
- *O* document referring to an oral disclosure, use, exhibition or other means
- *P* document published prior to the international filing date but later than the priority date claimed

- *T* later document published after the international filing date or priority date and not in conflict with the application but cited to understand the principle or theory underlying the invention
- *X* document of particular relevance; the claimed invention cannot be considered novel or cannot be considered to involve an inventive step when the document is taken alone
- *Y* document of particular relevance; the claimed invention cannot be considered to involve an inventive step when the document is combined with one or more other such documents, such combination being obvious to a person skilled in the art.
- *Z* document member of the same patent family

Date of the actual completion of the international search

8 August 2000

Date of mailing of the international search report

30 Oct 2000

Name and mailing address of the ISA

European Patent Office, P.B. 5818 Patentlaan 2
NL - 2280 HV Rijswijk
Tel. (+31-70) 340-2040, Tx. 31 651 epo nl,
Fax: (+31-70) 340-3016

Authorized officer

FRITZ, S



INTERNATIONAL SEARCH REPORT

International Application No
PCT/US 00/08943

C.(Continuation) DOCUMENTS CONSIDERED TO BE RELEVANT

Category *	Citation of document, with indication, where appropriate, of the relevant passages	Relevant to claim No.
A	C.GAO ET AL.: "Quantitative microwave near-field microscopy of dielectric properties" REVIEW OF SCIENTIFIC INSTRUMENTS, vol. 69, no. 11, November 1998 (1998-11), pages 3846-3851, XP002144502 US abstract; figure 1 ---	1,20,26
Y	US 5 900 618 A (S.M.ANLAGE ET AL.) 4 May 1999 (1999-05-04) cited in the application abstract; claim 17; figures 1A,6-9 column 1, line 47 -column 2, line 15 column 7, line 66 -column 8, line 24 column 8, line 45 - line 47 ---	1,20,26
A	TABIB-AZAR M ET AL: "NOVEL PHYSICAL SENSORS USING EVANESCENT MICROWAVE PROBES" REVIEW OF SCIENTIFIC INSTRUMENTS,US,AMERICAN INSTITUTE OF PHYSICS. NEW YORK, vol. 70, no. 8, August 1999 (1999-08), pages 3381-3386, XP000870710 ISSN: 0034-6748 abstract; figures 1-3 -----	1,20,26



2

3

4

5

INTERNATIONAL SEARCH REPORT

International application No.
PCT/US 00/08943

Box I Observations where certain claims were found unsearchable (Continuation of item 1 of first sheet)

This International Search Report has not been established in respect of certain claims under Article 17(2)(a) for the following reasons:

1. ☐ Claims Nos.:
because they relate to subject matter not required to be searched by this Authority, namely:
2. ☐ Claims Nos.:
because they relate to parts of the International Application that do not comply with the prescribed requirements to such an extent that no meaningful International Search can be carried out, specifically:
3. ☐ Claims Nos.:
because they are dependent claims and are not drafted in accordance with the second and third sentences of Rule 6.4(a).

Box II Observations where unity of invention is lacking (Continuation of item 2 of first sheet)

This International Searching Authority found multiple inventions in this international application, as follows:

1. ☐ As all required additional search fees were timely paid by the applicant, this International Search Report covers all searchable claims.
2. ☐ As all searchable claims could be searched without effort justifying an additional fee, this Authority did not invite payment of any additional fee.
3. ☐ As only some of the required additional search fees were timely paid by the applicant, this International Search Report covers only those claims for which fees were paid, specifically claims Nos.:
4. ☒ No required additional search fees were timely paid by the applicant. Consequently, this International Search Report is restricted to the invention first mentioned in the claims; it is covered by claims Nos.:

1-18,20,26-29

Remark on Protest

- ☐ The additional search fees were accompanied by the applicant's protest.
- ☐ No protest accompanied the payment of additional search fees.

INTERNATIONAL SEARCH REPORT

International Application No. PCT/US 00/08943

FURTHER INFORMATION CONTINUED FROM PCT/ISA/ 210

1. Claims: 1-18,20,26-29

Quantitative imaging dielectric permittivity

2. Claims: 19(partially), 21-24

Spring loaded sample holder

3. Claims: 19(partially), 25

Bias tee

